CHAPTER 1: INTRODUCTION

TABLE OF CONTENTS

		Page
1	INTRODUCTION	1-1
1.1	BACKGROUND	1-1
1.2	OBJECTIVE OF THE STUDY	1-4
1.3	SCOPE OF THE STUDY	1-4
1.4	METHODOLOGY	1-5
1.5	ORGANISATION OF THE THESIS	1-6

LIST OF FIGURES

Figure 1.1: Concrete pavements in South Africa 1-1

1 INTRODUCTION

1.1 BACKGROUND

Prior to 1968 concrete pavements were used only in exceptional cases in the Republic of South Africa. They were constructed using hand methods and rudimentary plant, which did not produce the longitudinal profile needed for modern traffic. As a result, the utilisation of concrete pavements was discontinued during the 1950's and 1960's. However, the results of the AASHO road test and studies and observations of modern concrete pavement performance, notably in the USA, stimulated interest in modern concrete pavements as a means of accommodating the rapidly growing traffic loading on South African highways. The high traffic densities not only made it expensive to rehabilitate existing national routes, but also dangerous, and the need for a relatively maintenance free pavement surface arose. Construction of modern concrete pavements in the RSA, therefore, commenced in 1968, where both jointed un-reinforced and continuously reinforced concrete pavements were constructed on a few selected routes for new construction and for rehabilitation purposes. Amongst others, the following routes were provided with concrete pavements (see Figure 1.1):

N2 from Cape Town to Somerset West (1968)
N4 between Witbank and Middelburg (1971)
N1 from the Vaal River to Johannesburg (1979)
N3 between Estcourt and Frere (1978)
R22 between Witbank and Springs (Experimental, 1973)
N1 between Johannesburg and Pretoria (1987/8)

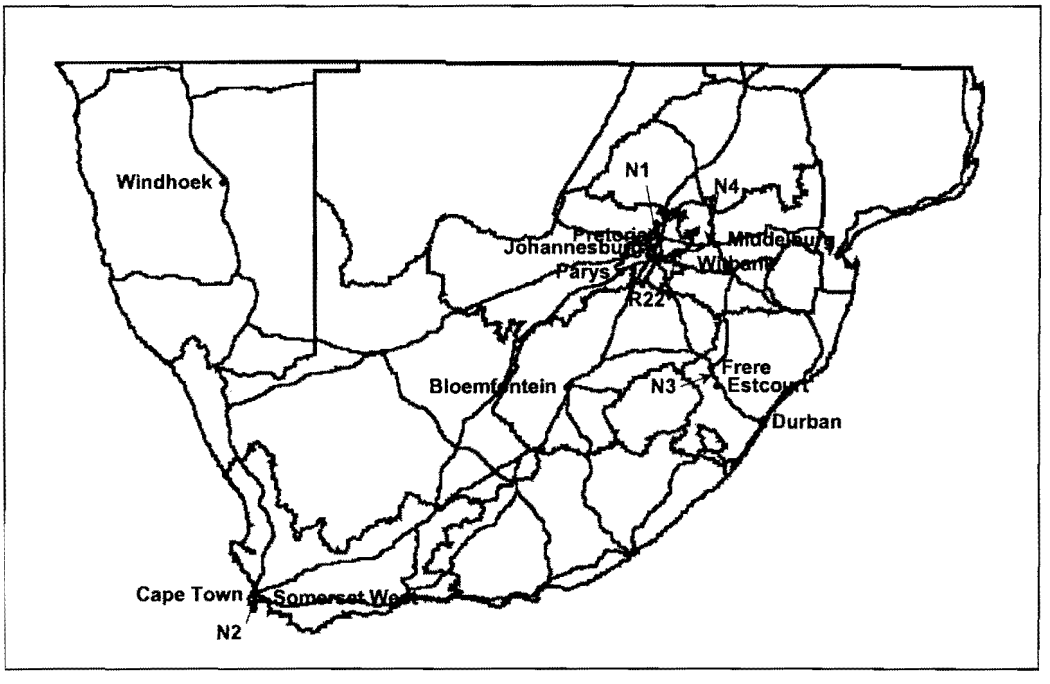

Figure 1.1 Concrete pavements in South Africa

The technology previously applied in South Africa was initially based on empirical methods developed from observations during the AASHO road test, the Alconbury Hill Experiment in the UK and also local Heavy Vehicle Simulator (HVS) tests (Du Plessis and Freeme, 1989). This was followed by designers using procedures developed by the US Portland Cement Association, Road Note 29 (Developed by the UK Transport and Road Research Laboratory), the US Army Corps of Engineers method and also procedures developed by the California State Highway Department (Mitchell et al, 1988). Local application of these design methods resulted in the construction of mostly jointed concrete pavements, without dowels at the joints, relying on aggregate interlock load transfer. Slab thicknesses of between 200 and 235 mm with 100 mm thick cement stabilised subbases were typically used to decrease the risk of subbase erosion, pumping and subsequent differential settlement or faulting at joints.

In most industrialised countries, road authorities specify that certain proportions of their highway networks be constructed in concrete. In England and Wales, for example, at least 20 percent of the major highways are required to be concrete pavement. In the USA, more than 50 percent of interstate highways and 15 percent of arterial roads are constructed of concrete. Yet, concrete pavements have in the past, (and still today according to many road engineers) been regarded as a pavement solution which is out of the ordinary and which requires greater attention than the more common asphalt pavement types. This myth, as well as resistance to the high initial construction costs has to some extent been prejudicial to the more extensive use of concrete pavements in South Africa. Less than 400 km (0,75 %) of the surfaced national road network is built as concrete pavements (Du Plessis and Freeme, 1989).

In Europe, jointed concrete pavements (JCPs) with doweled joints are commonly used. In the USA a variety of concrete pavement types are used, which include JCPs, jointed reinforced concrete pavements (JRCPs), continuously reinforced concrete pavements (CRCPs) and even pre-stressed (experimentally only) pavements.

In an attempt to introduce a degree of rationality into the design process, the South African Department of Transport issued a publication during 1980 in which the economics of the pavement type selection process for major roads was analysed, and all relevant factors were considered. This document, prepared by the Committee on Pavement Type Selection for the National Transport Commission, held that for pavements carrying 12 to 50 million equivalent standard axles over its design life: ".. there is no significant difference in present worth of cost between bituminous and concrete pavements based on 1978/79 unit costs. The cheapest alternative will depend on the local factors prevailing at the time." (Mitchell, 1988).

In 1985 the situation changed, due to a better understanding of road-user delay costs. It was shown that for heavy-duty pavements to carry up to 75 million equivalent axle loads over a 30-year analysis

period, a concrete pavement is more economical than a bituminous pavement on a present worth of cost basis (Mitchell, 1988).

The Department of Transport commissioned a research project aimed at providing a manual for the design and construction of concrete pavements in South Africa, during 1986. This study covered subjects such as the performance of existing concrete pavements, simulation of pavement response under laboratory conditions, mathematical analysis, mechanistic design and construction. At the initial stages of this study (which resulted in the Concrete Pavement Design and Construction, Manual M10, 1995) it was found that the performance of concrete pavements is influenced to a large extent by quality control during the construction phase. But, even more important, it was stated that the *behaviour of* joints was found to be significant in pavement behaviour as a whole. The *load transfer efficiency of the joint* not only influences the stresses in the pavement, but also has more importantly a direct effect on the possible erosion of the subbase material (Malan et al, 1988).

During the upgrading of the South African Concrete Pavement Design and Construction Manual M10 (Manual M10, 1995), to a concrete pavement design manual based on mechanistic design principles, a re-evaluation of factors affecting riding quality, structural service life, maintenance and rehabilitation needs re-confirmed the prominent effect of joint performance. It was identified that the current relationship modelling the mechanism of concrete joints in shear (aggregate interlock) was not accurate, especially for the smaller sized coarse aggregates used in the construction of concrete. Further research was therefore needed, which prompted the study presented in this thesis.

It has already been stated that most of the concrete pavements constructed in South Africa are JCPs, without dowels at the joints, relying on aggregate interlock load transfer. There are three primary types of joints in JCPs: contraction, isolation, and construction. Contraction joints are usually spaced every 3-5 m on average to permit contraction of the slabs, to control cracking in the concrete and to limit curling and warping stresses in the slab. They are typically formed by saw-cutting $^1/_4$ to $^1/_3$ the pavement thickness after curing, forcing a crack to occur at the joint through the pavement thickness. Aggregate interlock arising from the interaction of the two rough joint surfaces is an important load transfer mechanism at contraction joints. Isolation joints are used at the intersection of pavements with structures, and in some cases, within pavements. Construction joints are required between paving lanes, and at the end of a pour. In contrast to contraction joints, construction joints have formed joint surfaces with load transfer taking place through keys and tie bars.

The statement made by Du Plessis and Freeme (1989) that mechanistic models capable of evaluating the behaviour of concrete pavements with respect to the separate and combined influences of dowels, drainage, subbase, shoulder configurations, etc. have yet to be developed, is still true. Analysis models of this type, emphasizing the need for effective load transfer mechanisms are required especially for pavements carrying low- to medium volume traffic, if these are to be considered competitive with flexible pavements.

1.2 OBJECTIVE OF THE STUDY

The primary objectives of this research were:

a) To take into account existing methods for modelling aggregate interlock shear transfer to develop a model applicable to South African conditions that reflects variations in joint load transfer with joint opening, load magnitude, subbase support, aggregate size and concrete properties. This was in order to provide an improved aggregate interlock load transfer equation for the new South African mechanistic concrete pavement design method and application software, cncRisk.

b) To evaluate jointed concrete pavement response in terms of deflections, to static and moving impulse or dynamic loads (equivalent to traffic loads).

In the context of this thesis, modelling can be defined as the execution of pre-planned tests in a laboratory under controlled conditions using materials commonly used in the construction of concrete pavements in South Africa in order to develop an equation simulating performance in the field.

The secondary objectives were:

a) To obtain field measurements of crack widths and load transfer efficiency of existing jointed concrete pavements to calibrate the laboratory results.

b) To investigate existing methods for modelling steel dowel/concrete interaction at joints in jointed concrete pavements to determine a universal design model.

1.3 SCOPE OF THE STUDY

The scope of this study mainly involved the following:

a) Defining the rigid pavement system.

b) A detailed literature review of the main jointed concrete pavement load transfer mechanisms, namely, aggregate interlock and steel dowels.

c) Theoretical three-dimensional finite element (3D FE) modelling using the computer software programme EverFE (Davids et al, 1998) to determine ranges for input variables that could be expected during studies on part-slab sections in the laboratory. Both aggregate interlock and steel dowel load transfer mechanisms were modelled theoretically, as well as the combined effect of aggregate interlock and steel dowel load transfer mechanisms

d) Determining aggregate interlock load transfer efficiency through laboratory studies on part-slab sections.

e) Comparison of theoretical and laboratory modelling results with crack width and load transfer efficiency results obtained from testing actual in-service jointed concrete pavements in the field.

The scope of this study did not include laboratory modelling of steel dowel load transfer devices. This was only done theoretically. Voids beneath the concrete due to erosion of the subbase were also not investigated.

1.4 METHODOLOGY

In order to obtain a sound foundation for modelling load transfer at a joint in a concrete pavement a review of historical developments of rigid pavement design procedures had to be performed, together with a literature review of available rigid pavement response models, including two- and three-dimensional finite element techniques.

Theoretical analyses of full-scale concrete pavement models were first analysed using the 3D FE computer software programme EverFE (Davids et al, 1998). This was in order to determine the ranges for the different input variables that could be expected during experimental studies in the laboratory. Both aggregate interlock and dowel/concrete interaction was evaluated using EverFE.

In the laboratory, however, the scope of the investigation had to be narrowed down to what could be achieved practically within the scope of the project. Instead of full-scale models, so-called part-slab studies were conducted, and only the aggregate interlock load transfer aspect was investigated in detail. The change in deflection, and shear stiffness with variations in aggregate size, and joint opening were monitored. Instrumentation included thermocouples to collect slow responses due to environmental temperature influences. Linear variable displacement transducers (LVDT's) and strain displacement transducers collected fast responses induced by dynamic and static loads. The testing also included determining the relevant engineering properties for South African concrete aggregates.

The concrete pavement part-slab sections were constructed on rubber mats to simulate a liquid (Winkler) foundation. Constructing the slabs on rubber mats, made it possible to repeat experiments with the same founding conditions, which reduced the number of variables that had to be taken into consideration during calculations.

The success of the studies has laid the foundation for future testing involving dowel bars, as well as different subbase types to study the effect of erosion.

The software package, EverFE, which permits 3D FE models to be run on desktop computers, was recently developed in the USA. This package still needed 'field data" to validate the theoretically

calculated stresses and strains at the joint in the concrete pavement using South African materials and under our local environmental conditions.

As it was identified that the current relationship used in the South African concrete pavement design manual (Manual M10, 1995) modelling the mechanism of concrete joints in shear (aggregate interlock) was not accurate, especially for the smaller sized coarse aggregates used in the construction of concrete, the focus of this study was therefore to develop a more accurate formula through laboratory testing.

1.5 ORGANISATION OF THE THESIS

This thesis is organised as follows:

a) Chapter 1 serves as introduction to the thesis.

b) Chapter 2 contains the literature review. The literature review includes a definition of the rigid pavement system and a survey of the historical developments of rigid pavement design procedures, including two- and three-dimensional finite element techniques. It explains the mechanics of aggregate interlock and provides an overview of past attempts to model this phenomenon. It also covers the modelling of dowels and dowel-slab interaction as presented in the literature. The main aim of the literature review was to obtain guidance for laboratory modelling.

c) Chapter 3 presents a summary of the results obtained during laboratory modelling and also summarizes results obtained from field investigations on in-service concrete pavements in South Africa.

d) Chapter 4 describes how the laboratory and field data was analysed in the development of an improved modelling equation.

e) Chapter 5 describes the application of the model developed in this study.

f) Chapter 6 presents conclusions and recommendations for future research.

CHAPTER 2: LITERATURE REVIEW AND GUIDANCE FOR MODELLING

TABLE OF CONTENTS

		Page
2	**LITERATURE REVIEW AND GUIDANCE FOR MODELLING**	**2-1**
2.1	**INTRODUCTION**	**2-1**
2.2	**RIGID PAVEMENT SYSTEM**	**2-1**
2.2.1	Introduction	2-1
2.2.2	Pavement system	2-1
2.2.3	Load transfer definitions	2-3
2.2.4	Load transfer mechanisms	2-5
2.2.5	Rigid pavement foundations	2-8
2.2.6	Summary of rigid pavement system	2-8
2.3	**OVERVIEW OF HISTORICAL DEVELOPMENTS**	**2-9**
2.3.1	Introduction	2-9
2.3.2	Westergaard theory	2-9
2.3.3	Elastic layer theory	2-13
2.3.4	Finite element model development	2-15
2.3.5	Rigid pavement joints	2-17
2.3.6	The effects of moment and inertia	2-19
2.3.7	A mechanistically and risk based design method for concrete pavements in southern Africa (Strauss et al., 2001)	2-21
2.3.8	Summary of historical developments	2-36
2.4	**AGGREGATE INTERLOCK**	**2-36**
2.4.1	Introduction	2-36
2.4.2	Theoretical aggregate interlock modelling	2-38
2.4.3	Laboratory studies	2-47
2.4.4	Joint deterioration mechanisms	2-52
2.4.5	Summary of aggregate interlock modelling	2-56
2.5	**DOWEL MODELLING**	**2-57**
2.5.1	Introduction	2-57
2.5.2	Analytical dowel modelling	2-58
2.5.3	Finite element dowel modelling	2-66
2.5.4	Combined aggregate interlock and dowel modelling	2-67
2.5.5	Summary of dowel modelling	2-72
2.6	**GUIDANCE FOR LABORATORY MODELLING**	**2-73**

LIST OF TABLES

Table 2.1: Overview of 2D FE models for rigid pavements (Hammons and Ioannides, 1996, with modifications by author) 2-15
Table 2.2: Summary of features of 3D FE studies 2-16
Table 2.3: Summary of laboratory studies by various researchers 2-48

LIST OF FIGURES

Figure 2.1: Typical rigid pavement system (Hammons and Ioannides, 1996) 2-2
Figure 2.2: Concept of load transfer (Hammons and Ioannides, 1996) 2-2
Figure 2.3: Illustration of 0% and 100% load transfer efficiency 2-4
Figure 2.4: Effect of aggregate interlock at joints or cracks (Manual M10, 1995) 2-5
Figure 2.5: Effect of load transfer devices (Manual M10, 1995) 2-7
Figure 2.6: Schematic layout of plate loading test (Huang, 1993) 2-10
Figure 2.7: Foundation displacement under a loaded plate for Winkler and elastic solid foundations (Hammons and Ioannides, 1996) 2-14
Figure 2.8: Dowel installations at Lockbourne and Sharonville Test Tracks (Sale and Hutchinson, 1959) 2-19
Figure 2.9: Measured surface deflection versus speed 2-27
Figure 2.10: Performance curves used by various designers. 2-29
Figure 2.11: Triangular distribution of input variables. 2-31
Figure 2.12: Simplified simulation flowchart. 2-32
Figure 2.13: Example of the Main control panel. 2-33
Figure 2.14: Example of the Advanced input panel. 2-34
Figure 2.15: Example of the Statistics panel 2-35
Figure 2.16: Crack plane and distribution of aggregate particles (Davids et al., 1998a) 2-39
Figure 2.17: Deformed cracked plane (Davids et al., 1998a) 2-40
Figure 2.18: Subdividing aggregate particles and cement paste into discrete particles (Davids et al., 1998a) 2-42
Figure 2.19: LTE_{Δ} as a function of dimensionless joint stiffness (AGG/kl) (Ioannides and Korovesis, 1990) 2-45
Figure 2.20: Endurance of joints (Colley and Humphrey, 1967) 2-51
Figure 2.21: Effect of repetitive loading on the development of dowel looseness (Teller and Cashell, 1958) 2-60
Figure 2.22: Winkler foundation between dowel and slab (Friberg, 1940) 2-60
Figure 2.23: Analysis of dowel bar support (Friberg, 1940) 2-61
Figure 2.24: Sliding shear behaviour at a constant crack width of 0,5 mm (Soroushian et al., 1988) 2-68
Figure 2.25: Deflection LTE in the wheel path – aggregate interlock versus combined effect of aggregate interlock and dowel action (no gap around dowel) 2-68

Figure 2.26: Maximum shear stress at joint in wheel path – aggregate interlock versus combined effect of aggregate interlock and dowel action (no gap around dowel) 2-69
Figure 2.27: Total shear force transferred across joint – aggregate interlock versus combined effect ofaggregate interlock and dowel action (no gap around dowel) 2-70
Figure 2.28: Deflection LTE in the wheel path – 9 mm maximum sized aggregate – combined affect of aggregate interlock and dowels (gap around dowel) 2-70
Figure 2.29: Deflection LTE in the wheel path – 63 mm maximum sized aggregate – combined affect of aggregate interlock and dowels (gap around dowel) 2-71

LIST OF SYMBOLS

a	Radius of applied load
agg	Nominal size of 20% biggest particles in concrete mix
AGG	Aggregate interlock joint shear stiffness per unit length of crack/joint
A_d	Cross-sectional area of dowel
A_z	Cross-sectional area of dowel effective in shear
AIF	Aggregate interlock factor
β	Relative stiffness of dowel/concrete system
C	Load transfer coefficient
c	Dowel bar radius
$[C]$	Damping matrix
D	Slab stiffness
Δ_L	Maximum edge deflection of the loaded slab
Δ_s	Aggregate interlock wear out
Δ_U	Maximum edge deflection of the adjacent unloaded slab
Δ_f	Maximum edge deflection with no joint
Δ_{di}	Deflection of any given dowel relative to the concrete
Δ_0	Deflection of the dowel relative to the concrete at the face of the joint
dia	Diameter of steel bar (dowel)
Δ	Deflection of the plate / shear displacement
EI	Endurance index
E_c	Modulus of elasticity of concrete
E_d	Modulus of elasticity of dowel
E_e	Equivalent subgrade support stiffness
E_s	Modulus of elasticity of soil
e	Effective length
$\{F\}$	Vector of nodal point forces
FE	Finite element

FWD	Falling Weight Deflectometer
F_x	Total force in X-plane
F_y	Total force in Y-plane
f_{cu}	Concrete cube crushing strength
Gd	Shear modulus of dowel bar
h	Concrete slab thickness
I_d	Moment of inertia of the dowel
J	Total stiffness ratio
J_{AI}	Dimensionless aggregate interlock stiffness ratio
J_D	Dimensionless dowel stiffness ratio
h_e	Effective concrete slab thickness
J	Corner stress coefficient (load transfer coefficient) Joint stiffness computed on transverse crack
JE	Joint effectiveness
K	Slab support modulus / dowel support modulus
$[K]$	Stiffness matrix
k	Modulus of subgrade reaction
L	Length of the slab
l	Radius of relative stiffness
LTE	Load transfer efficiency
LTE_Δ	Deflection load transfer efficiency
LTE_σ	Stress load transfer efficiency
$[M]$	Mass matrix
μ	Poisson's ratio for concrete / coefficient of friction between paste and aggregate
μ_d	Poisson's ratio of dowel
μ_s	Poisson's ratio for steel / soil
n	Number of load applications
n_{ij}	Number of axle load applications for current sub increment i and load group j
p	Pressure on plate loading test plate
P	Load, representing wheel load
P_d	Load on a dowel
P_i	Shear force acting on any particular dowel, transferred across the joint
P_L	Portion of load supported by loaded slab
P_T	Total load transferred across entire length of joint
P_U	Portion of load supported by unloaded slab
ΣA_x	X-projection of the sum of the most probable contact areas
ΣA_y	Y-projection of the sum of the most probable contact areas
σ	Maximum tensile stress
σ_b	Bearing stress of concrete
σ_E	Edge stress
σ_L	Maximum bending stress in the loaded slab

σ_U	Maximum bending stress in the adjacent unloaded slab
σ_f	Maximum bending stress for the free edge loading condition
σ_{pu}	Stress normal to the contact area
S	Dowel spacing
τ	Shear stress
τ_{pu},	Stress tangential to the contact area
τ_{stress}	Shear stress on the transverse crack
τ_{ref}	Reference shear stress derived from Portland Cement Association test results
TLE	Total load efficiency
$\{u\}$	Vector of nodal point displacements
$\{\dot{u}\}$	Vector of nodal point velocities
$\{\ddot{u}\}$	Vector of nodal point accelerations
v	Speed of heavy vehicles
$Void$	Length of void below slab
w	Joint/crack opening
w_i	Crack width in sub-increment i
W	Width of the slab
x	Crack width
y	Relative vertical movement at joint

NOTE: Equations (2.29) and (2.32) contain constants a, b, c, d, e, f, and g which are defined together with the equations on p4-18 and p4-19.

2 LITERATURE REVIEW AND GUIDANCE FOR MODELLING

2.1 INTRODUCTION

An in depth literature review has been conducted to lend guidance to the laboratory modelling envisaged for this thesis. This chapter deals with the definition of the rigid pavement system, historical developments in the field of concrete pavement modelling, aggregate interlock and dowel modelling.

Each paragraph has a short introduction, as well as a summary at the end.

2.2 RIGID PAVEMENT SYSTEM

2.2.1 Introduction

In the following paragraphs the rigid pavement system is defined, definitions are presented for deflection load transfer and stress load transfer developed in practice. An explanation is given of the different load transfer mechanisms encountered, and rigid pavement foundations are also described.

2.2.2 Pavement system

A rigid pavement system may be defined as a pavement structure in which the primary load-supporting element comprises a rigid layer/slab constructed from relatively thin Portland cement concrete (Manual M10, 1995). Concrete slabs are finite in length and width and are constructed over one or more foundation layers (Hammons and Ioannides, 1996). Figure 2.1 shows a representation of a typical rigid pavement system subjected to static loading. When a slab-on-grade is subjected to a wheel load, it develops bending stresses and distributes the load over the foundation. However, the response of these finite slabs is controlled by joint or edge discontinuities. Edge loading can increase the stress in the slab by up to 50% and stress in the slab support by up to 150% compared to internal loading (Manual M10, 1995). By their nature, joints are structurally weakening components of the system. Almost any type of crack in a slab (or unsealed joint) eventually allows water to enter the sublayers. This may facilitate erosion of the subbase with a subsequent loss of slab support. This increases slab deflection and shear stress on the jointing system. Material is displaced by erosion, or the subgrade subsides and a void develops under the slab leading to a further increase in stress until the stress is high enough to cause additional cracking in the slab. Thus, the response and effectiveness of joints are primary concerns in rigid pavement analysis and design.

A conceptual view of the mechanism of load transfer is presented in Figure 2.2. The concept of load transfer is fairly simple: stresses and deflections in a loaded slab are reduced if a portion of the load is transferred across the joint. Load transfer is important and fundamental to rigid pavement design procedures. Load transfer can vary with concrete pavement temperature (see paragraph 2.4), age,

moisture content, construction quality, magnitude and repetition of load and type of joint (Hammons and Ioannides, 1996).

When a joint is capable of transferring load, statics dictate that the total load (P) must be equal to the sum of that portion of the load supported by the loaded slab (P_L) and the portion of the load supported by the unloaded slab (P_U), i.e.:

$$P_L + P_U = P \tag{2.1}$$

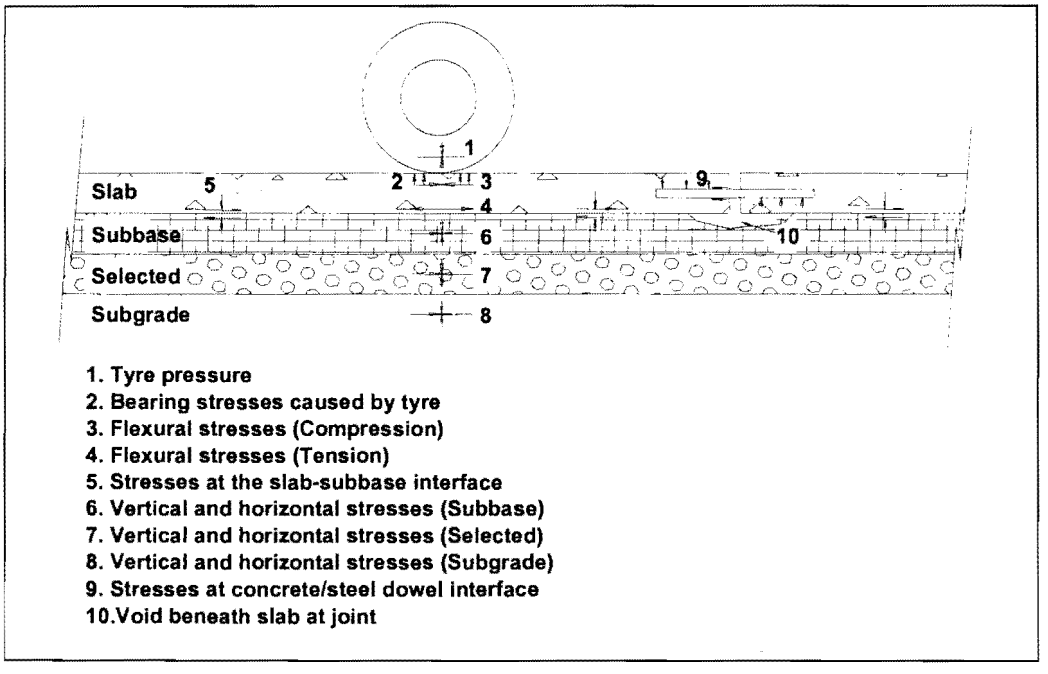

Figure 2.1: Typical rigid pavement system (Hammons and Ioannides, 1996)

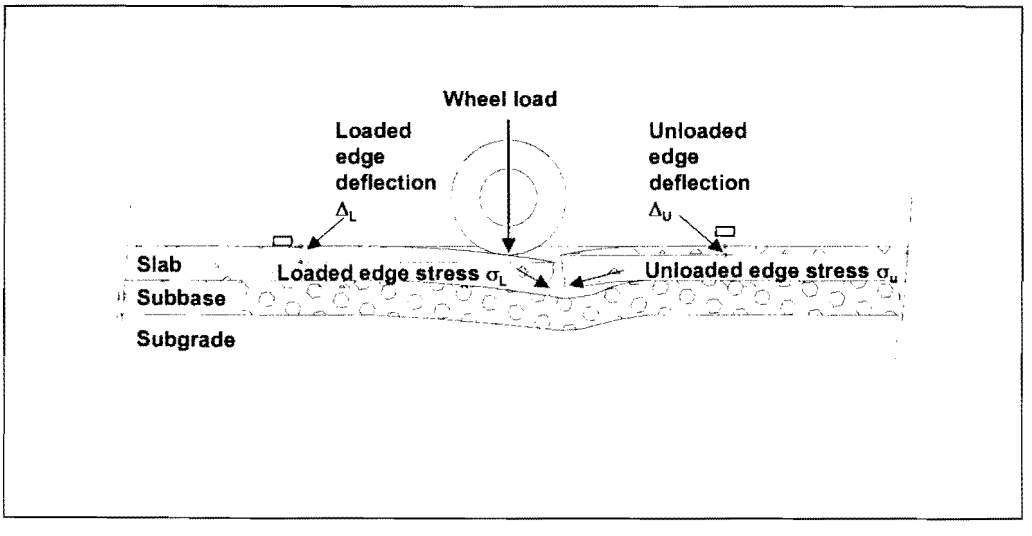

Figure 2.2: Concept of load transfer (Hammons and Ioannides, 1996)

Load may be transferred across a joint by shear or bending moments. However, it has been commonly argued that load transfer is primarily caused by vertical shear. In either case, the following relationship applies:

$$\sigma_L + \sigma_U = \sigma_f \tag{2.2}$$

Where:

σ_L = Maximum bending stress in the loaded slab;

σ_U = Maximum bending stress in the adjacent unloaded slab; and

σ_f = Maximum bending stress for the free edge loading condition.

Because maximum slab deflections are also directly proportional to applied load under the stated conditions, it follows from Equation (2.1) that

$$\Delta_L + \Delta_U = \Delta_f \tag{2.3}$$

Where:

Δ_L = Maximum edge deflection of the loaded slab;

Δ_U = Maximum edge deflection of the adjacent unloaded slab; and

Δ_f = Maximum edge deflection with no joint.

2.2.3 Load transfer definitions

Deflection load transfer efficiency (LTE_Δ) is defined as the ratio of the deflection of the unloaded slab (Δ_U) to the deflection of the loaded slab (Δ_L) as follows:

$$LTE_\Delta = \Delta_U/\Delta_L \; x \; 100 \; percent \tag{2.4}$$

The main load transfer mechanism in both doweled and un-doweled joints is shear (through dowel action and aggregate interlock), provided that the deflection load transfer efficiency (LTE_Δ), is in excess of about 80% (Ioannides, 1991).

Figure 2.3 illustrates load transfer efficiency in terms of deflection.

Stress load transfer efficiency (LTE_σ) is defined as the ratio of the edge stress in the unloaded slab to edge stress in the loaded slab as follows:

$$LTE_\sigma = \sigma_U / \sigma_L \; x \; 100 \; percent \tag{2.5}$$

Load transfer (LT) in the FAA rigid pavement design procedure is defined as that portion of the edge stress (σ_E) that is carried by the adjacent unloaded slab, as follows:

$$LT = \left[\frac{\sigma_U}{\sigma_f}\right] = \left[\frac{\sigma_E - \sigma_L}{\sigma_f}\right] = \left[1 - \frac{\sigma_L}{\sigma_f}\right] \tag{2.6}$$

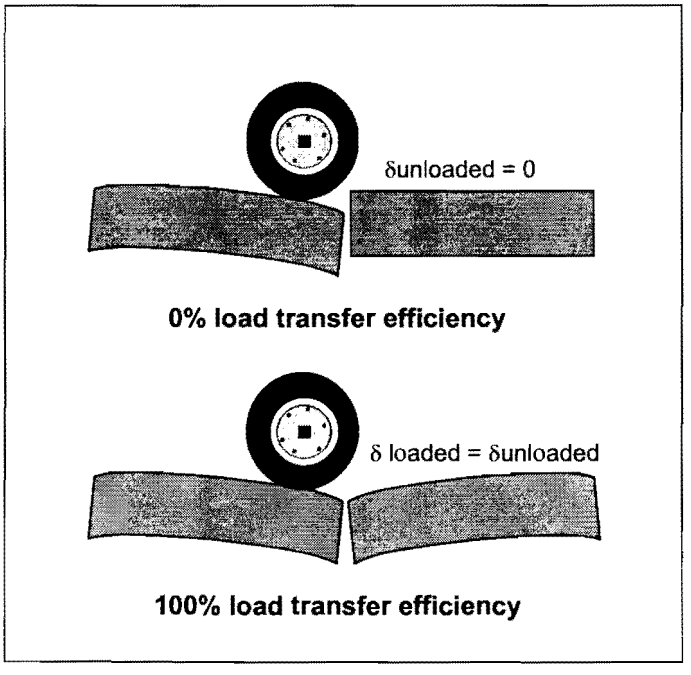

Figure 2.3: Illustration of 0% and 100% load transfer efficiency

The range of LTE_Δ and LTE_σ is from zero to one, while the range of LT is from zero to 0,5. Equation (2.6) can be related to Equation (2.5) as follows:

$$LT = \frac{LTE_\sigma}{1 + LTE_\sigma} \tag{2.7}$$

The US Army Corps of Engineers' design criteria prescribe LT = 0,25, effectively reducing the design stress and allowing a reduced slab thickness. This accepted value is primarily based upon test sections trafficked from the mid-1940's to the mid-1950's (Hammons and Ioannides, 1996). If the load transfer assumption is violated through a degradation of the joint system, the pavement life can be significantly reduced.

2.2.4 Load transfer mechanisms

Load transfer at joints is accomplished by two primary load transfer mechanisms:

a) Dowel bars.
b) Aggregate interlock.

Dowel bars are often placed across a joint to provide load transfer through dowel action and to maintain slab alignment. Dowels are smooth, round bars with bond intentionally broken on one half to allow longitudinal movement of the slabs (see Figure 2.1).

Aggregate interlock is a load transfer mechanism that relies on shear forces developed at the rough vertical interface of a concrete pavement joint. These shear forces are caused by mechanical interlock between the rough vertical surfaces of the joint and by sliding friction (see Figure 2.4).

Deformed steel bars, often called *tie bars*, can be placed across the joint (normal to the plane of the joint) to hold slab faces in intimate contact. Bond between the concrete and bar develops in both slabs; thus movement normal to the joint is restrained. Diameter, length and spacing of tie bars are fixed by design criteria. However, load transfer due to dowel action of tie bars, is small in comparison to that provided by dowel bars.

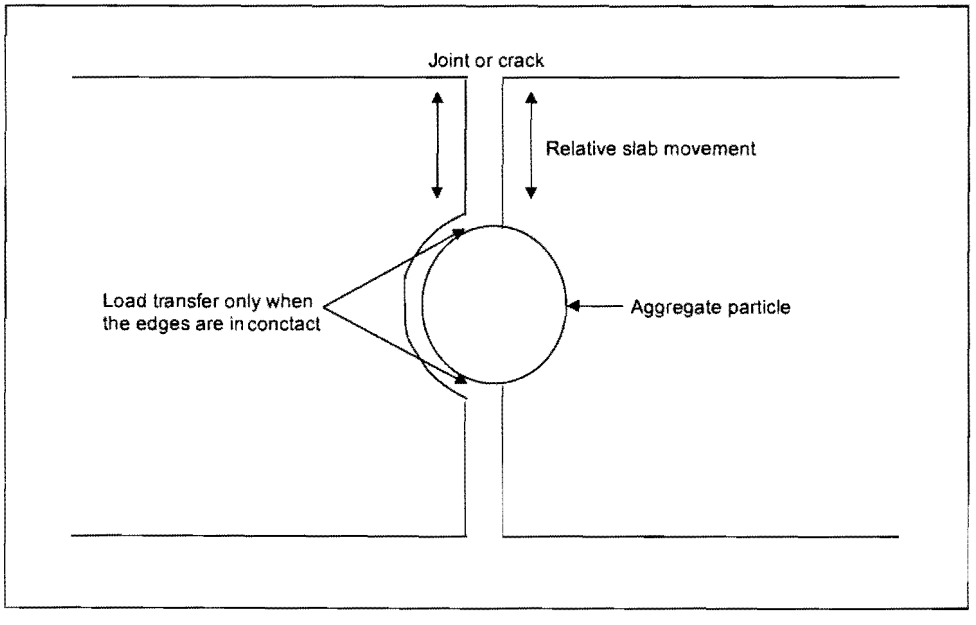

Figure 2.4: Effect of aggregate interlock at joints or cracks (Manual M10, 1995)

Figure 2.5 indicates the effect of different load transfer devices on relative movement, as determined for Manual M10: Concrete Pavement Design and Construction (1995). The top part of the figure shows the relative effect of dowel bars and the bottom part the relative effect of aggregate interlock.

The three major types of joints are:

a) Contraction joints.
b) Construction joints.
c) Isolation joints.

Contraction joints, used to control cracking in the concrete and to limit curling and warping stresses in the slab, are formed by introducing a weakened plane into the concrete and allowing a crack to form at the weakened plane. Typically, sawing a groove in the concrete while it is curing creates the weakened plane. Contraction joints may be plain (often called dummy joints), doweled, or tied (often called hinged joints).

Construction joints are required between lanes of paving and where it is necessary to stop construction within a paving lane. The two most common types of load transfer devices in construction joints are dowels and keyways.

Isolation joints are used at the intersections of pavements with structures, and in some cases, within pavements. Their primary purpose is to relieve compressive stresses induced by expansion of the concrete caused by temperature and moisture changes against relatively immovable objects such as foundations, drainage structures, and etcetera. Isolation joints may contain dowels or have thickened edges. To obtain load transfer at an isolation joint, a load transfer device is required (usually a dowel bar).

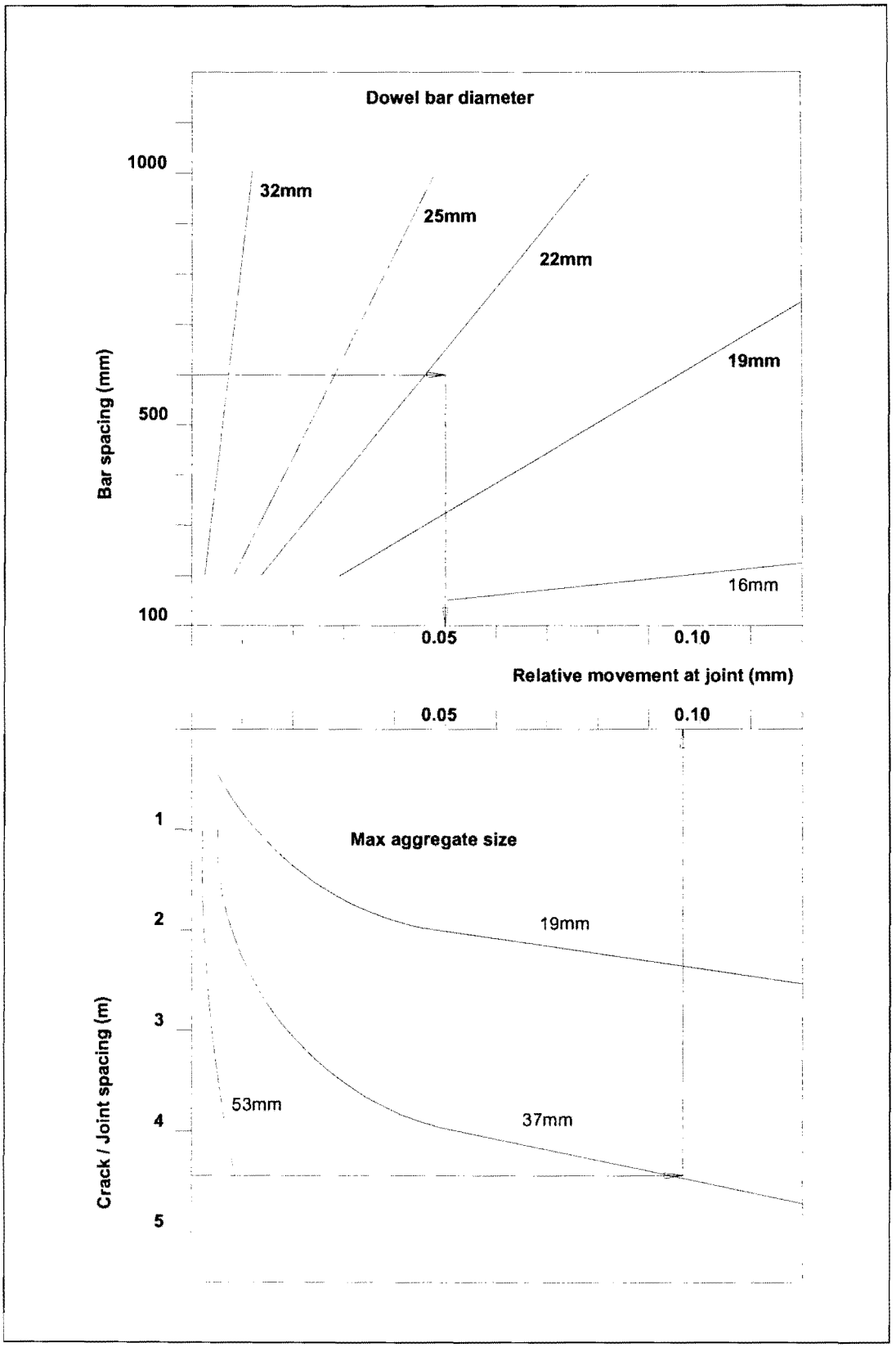

Figure 2.5: Effect of load transfer devices (Manual M10, 1995)

2.2.5 Rigid pavement foundations

The slab may be placed directly on the subgrade; however, most current practice has slabs placed on an unbound or bound subbase. Such subbase layers may be constructed to:

a) Provide uniform bearing support for the pavement slab.
b) Provide a construction platform.
c) Protect the subgrade from frost effects (not normally applicable to South African conditions).
d) Produce a suitable surface for operating construction equipment.
e) Improve foundation strength.
f) Prevent subgrade pumping.
g) Provide drainage of water from under the pavement.

An unbound subbase may be a densely graded granular material or an open-graded or free-draining granular material. The subbase may be bound with Portland cement, a lime-fly ash blend, bitumen, or other agent.

One or more subbases may be present in the pavement system. These subbases may be a lesser quality material and may be chemically stabilised. The subbase provides additional strength to the pavement system, provides more uniform support over variable soil conditions, and may provide protection against frost damage and swelling. Stabilised subbases need to be structurally considered as part of the concrete slab, rather than as part of the subgrade.

The subgrade is naturally occurring soil, compacted naturally occurring soil, or compacted fill. It may be subject to pumping, collapsing sands, frost damage, swelling (expansive soils/clays), or unstable (earth fills). Subgrade soils will have different values of strength depending on its soil classification, moisture conditions, and compaction.

2.2.6 Summary of rigid pavement system

In summary, the rigid pavement system has been defined as a pavement structure in which the primary load-supporting element comprises a rigid layer/slab constructed from relatively thin Portland cement concrete (Manual M10, 1995). Concrete slabs are finite in length and width and are constructed over one or more foundation layers (Hammons and Ioannides, 1996). Dowels bars or aggregate interlock at contraction, construction, or isolation joints accomplishes load transfer. The foundation layers or subbase primarily have to provide uniform bearing support for the pavement slab and as such need to be of high quality material.

2.3 OVERVIEW OF HISTORICAL DEVELOPMENTS

2.3.1 Introduction

A survey of past developments of rigid pavement design theory is presented, with specific reference to the work done by Westergaard, and the limitations of his theory, together with a literature review of available rigid pavement response models, including two- and three-dimensional finite element techniques. This provides insight into the current state-of–the-art of rigid pavement analysis tools.

This paragraph also presents a short overview of the development of the South African concrete pavement design manual (Manual M10), as well as the main reason for the motivation of the research presented in this thesis.

2.3.2 Westergaard theory

The design of rigid pavements and the name Westergaard have been synonymous for the past 80 years.

Professor Harald Malcolm Westergaard published a series of papers containing relationships for calculating stresses in rigid pavements based upon elastic theory. His pioneering work was first published in Danish in 1923 (Westergaard, 1926). However, this work was not widely read, and in 1926, he published a method in English for calculating stresses in rigid pavements (Westergaard 1926). He developed relationships for stresses *by assuming the slab to act as a homogeneous, isotropic, elastic solid in equilibrium, and by assuming that the reactions of the subgrade to be vertical only and to be proportional to the deflections of the slab* (Westergaard, 1926; Hammons and Ioannides, 1996).

Westergaard characterized the subgrade by the *modulus of subgrade reaction (k)*, which is a measure of the stiffness of the subgrade, and is defined as the reactive force (pressure) generated by unit displacement (deflection) of the subgrade surface. Subgrade reaction (k) is normally determined from a loading test on a circular plate, 762 mm (30 inch) in diameter (ASTM D1196-93, 1997). To minimize bending, a series of stacked plates should be used. The load is applied to the plates by a hydraulic jack. A steel beam tied to heavy mobile equipment can be used as the reaction for the load. Three dial gauges located at the outside edge, 120 degrees apart, measure deflections of the plate. The support for the deflection dials must be located as far from the loaded area as possible, usually not less than 4,5 m (15 feet). Figure 2.6 is a schematic layout of the plate-loading test. The load is applied at a predetermined rate until a pressure of 70 kPa (10 psi) is reached. The pressure is held constant until the deflection increases not more than 0,025 mm (0,001 inch) per minute for three consecutive minutes.

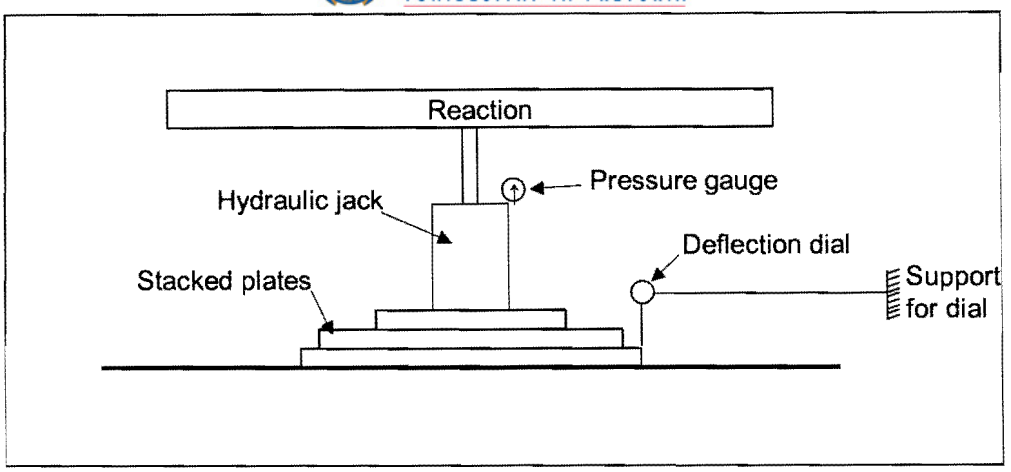

Figure 2.6: Schematic layout of plate loading test (Huang, 1993)

The average of the three dial readings is used to determine the deflection. The modulus of subgrade reaction is then given by:

$$k = \frac{p}{\Delta} \tag{2.8}$$

Where:

p = Pressure on the plate (kPa or psi); and

Δ = Deflection of the plate (mm or inch)

The principles of dimensional analysis were used in the interpretation of data pertaining to the response of rigid pavement systems, derived from either field measurements or from analytical studies (Ioannides, 1990). The governing principle was stated as follows: "The fundamental relationships in the physical world are essentially non-dimensional, existing between non-dimensional independent variables and non-dimensional dependent variables. This is self evident, since order in nature pre-existed the conventional definitions of units of measurement."

On the basis of this hypothesis Ioannides (1990) showed that the fundamental independent variable determining the response of a slab relative to the subgrade (analysed using plate theory), is the dimensionless load size ratio (a/l), where a is the radius of the loaded area and l is the radius of relative stiffness of the slab-subgrade system. This term in the Westergaard theory that quantifies stiffness of the slab relative to that of the subgrade, is expressed by the following relationship:

$$l = \sqrt[4]{\frac{E_c h^3}{12(1-\mu^2)k}} \tag{2.9}$$

Where:

E_c = Modulus of elasticity of concrete (MPa);

h = Concrete slab thickness (mm); and

μ = Poisson's ratio of concrete.

In Equation (2.9) it is assumed that the response of a slab can be compared to that of a plate on a bed of springs, the so-called Winkler foundation. Westergaard (1926) solved for the ratio $\sigma h^2/P$ as a function of ratio a/l where σ is the maximum stress, P is the magnitude of the applied load, and a is the radius of the circular area upon which the applied load acts for the following three cases:

a) Wheel load close to the corner of a semi-infinite slab (critical stress at the top of the slab, causing corner breaks).
b) Wheel load at the interior of an infinite slab (critical tension occurs at the bottom of the slab under the centre of the load circle).
c) Wheel load at the edge of a semi-infinite slab (critical stress is a tension at the bottom of the slab under the centre of the load circle).

Westergaard considered two cases for the edge load case:

a) The load distributed over the area of a full circle, or
b) The entire load distributed over the area of a semi-circle (the more severe case if the tyre was operating on the very edge of the pavement with no support under half of the tyre, as occurs on a severely faulted pavement).

During 1933 Westergaard modified his 1926 formulae to reflect the conditions of the Road Tests conducted at Arlington, VA, in 1932. Westergaard extended his procedures to airfield pavements in 1938, again revising his formulae to account for the larger contact area of aircraft tyres (Westergaard 1941).

Although Westergaard considered the interior, corner, and edge loading cases in his early works, he concentrated on interior loadings. Ioannides, Thompson and Barenberg (1985) found that several of the equations ascribed to Westergaard in the literature are incorrect due to typographical errors or misapplication. They also reported that the 1926 equation for edge loading was incorrect.

It was not until 1947 that Westergaard (1947) published relationships that were valid for computation of stresses caused by edge loading of large wheel loads on large contact areas. His revised formulas allowed the load to be characterised as an ellipse rather than being limited to a circular tyre print. Ioannides, Thompson and Barenberg (1985) recommended the use of these equations as being more accurate than the 1926 equations.

Still, several investigators noted repeatedly that although the Westergaard solutions agreed fairly well with their observations for the interior loading condition, it failed to give even a close estimate of the response of the edge and corner loading. Ioannides, Thompson and Barenberg (1985) felt that the time-honoured Westergaard solutions deserved a thorough re-examination, using the tool of finite element analysis (ILLI-SLAB). They developed improved expressions for maximum corner loading responses, as summarised in Appendix A.

During 1951 Pickett and Ray (Hammons and Ioannides, 1996) developed graphical solutions for the Westergaard theory in the form of response charts. These charts / nomograms were presented for four different load cases: interior loading assuming a dense liquid subgrade, interior loading assuming an elastic solid subgrade, edge loading assuming a dense liquid subgrade, and load placed at *l*/2 from an edge assuming a liquid subgrade.

2.3.2.1 Westergaard theory limitations

There are several limitations to the Westergaard theory, namely (Hammons and Ioannides, 1996):

a) All pavement layers below the slab must be represented by a single parameter, the modulus of subgrade reaction. In practice, however, a pavement normally has several layers of materials, including bound or unbound subbases and selected layers with each layer having an increase in quality and stiffness. This leads to a decrease in exactness of the analysis.

b) The foundation layer is assumed to respond linear-elastically. Most subgrade materials are non-linear, stress-dependant and change with time and environment.

c) It was assumed that the slab is in full contact with the subgrade at all points. It does not therefore take into account voids developed due to pumping, or slab/subgrade separation due to warping and curling.

d) Westergaard assumed the slabs were infinite (for the interior load case) or semi-infinite (for the edge and corner load cases); the slabs extend far enough from the loaded area that boundaries (discontinuities such as joints or cracks) have no effect on the solution. In practice this is not the case, because rigid pavement slabs tend to be relatively narrow and have many cracks and joints.

e) Load transfer cannot be directly modelled. Load transfer is assumed to be a constant 25 percent for airport pavement design. A more rational method of analysing load transfer is required for mechanistic evaluation of rigid pavements.

f) The thickness of the slab must be uniform, which makes it impossible to analyse thickened edge slabs or slabs of non-uniform thickness.

In a recent study conducted by Ioannides et al. (1999), they reconsidered the Westergaard solution to curling due to temperature differentials, and noted the following further limitations to the Westergaard theory:

a) The slab was assumed to have continuous contact with the subgrade (infinite slab self-weight).

b) It was assumed that the principle of superposition with regard to the summation of load-induced and thermal stresses could be applied.

c) Assuming a linear temperature variation through the slab thickness was considered adequate.

d) The slab response under night time conditions was assumed to be a mirror image of the corresponding behaviour under daytime conditions.

2.3.3 Elastic layer theory

The elastic layer theory was first formulated for a point load and one layer by Boussinesq and later generalised for a uniformly distributed load acting over a circular area and two or more layers, by others. Where manual solutions of one- or two-layer elastic systems to one circular load were cumbersome, computerised solutions have made it possible to analyse a system of many layers subjected to multiple loads. Among these programmes are BISAR, CHEVRON, ELSYM5, and JULEA.

The basic assumptions of the elastic layer theory are:

a) All materials in the system are assumed to be homogeneous, isotropic, and linear elastic; thus each pavement layer can be represented by three parameters: thickness, modulus of elasticity, and Poisson's ratio. Each layer may have different elastic properties.

b) Each layer is infinite in horizontal extent, and the bottom layer extends vertically to infinity.

c) The load is static and is uniformly distributed over one or more circular areas. Most programmes assume the load to be entirely vertical, although some can accommodate horizontal components.

d) The layers are continuously in contact. Also, the degree of restraint between adjacent layers must be assumed. Common assumptions are that the adjacent layers are fully bonded or that they are frictionless. Some programmes can allow any degree of restraint between these two extremes.

Because of the assumptions of the elastic layer models, it holds certain limitations for the analysis of rigid pavements:

a) Joint and cracks in rigid pavements are ignored, as the model assumes each layer to be infinite in horizontal extent. Cracks in stabilised layers are also ignored.

b) Each material is assumed to be linear elastic, leading to inconsistencies in stress calculations in the foundation layers.

For the case with an elastic solid foundation the radius of relative stiffness (l) is expressed as follows:

$$l = \sqrt[3]{\frac{E_c h^3 (1-\mu_s^2)}{6(1-\mu^2)E_s}} \tag{2.10}$$

Where:

E_s = Modulus of elasticity of the soil (MPa); and

μ_s = Poisson's ratio of the soil.

The difference between a spring-supported Winkler foundation and an elastic solid foundation is illustrated in Figure 2.7. Although the elastic solid foundation is often considered as a more realistic soil representation, it has not been used extensively in concrete pavement analysis and design. This is probably because elastic solid is a continuum model, and sometimes fails to simulate the behaviour of real soils, which are particulate media, especially under conditions of edge and corner loading (Khazanovich and Ioannides, 1993).

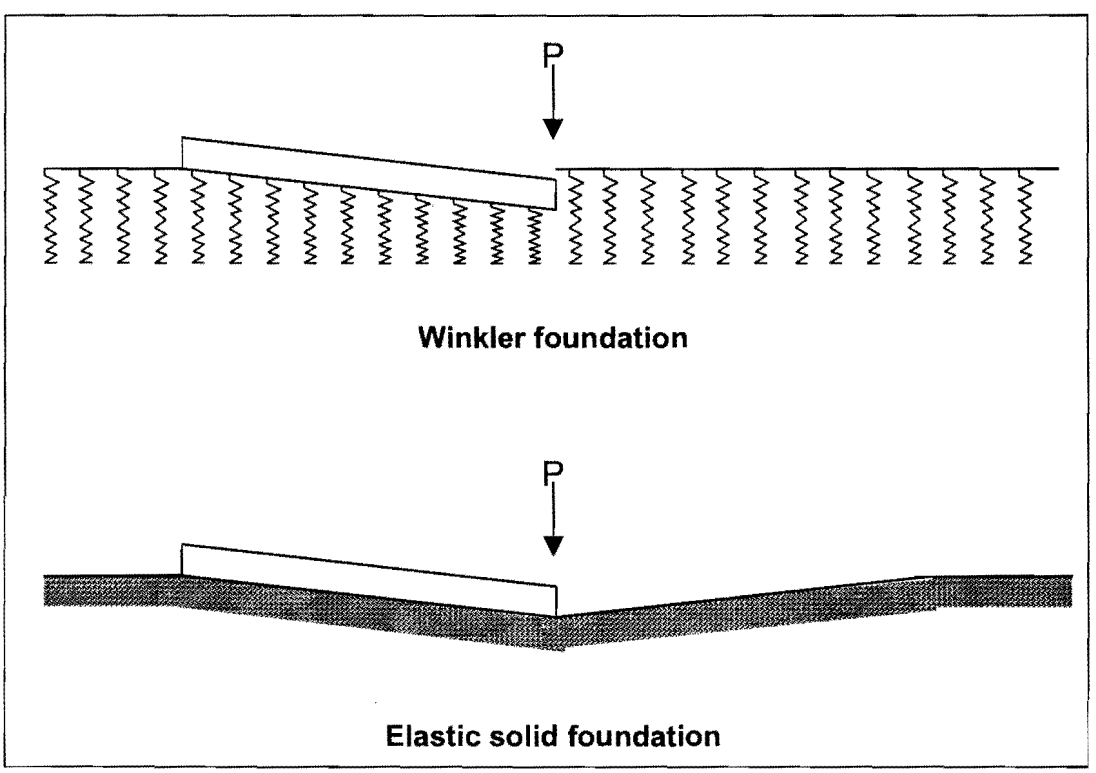

Figure 2.7: Foundation displacement under a loaded plate for Winkler and elastic solid foundations (Hammons and Ioannides, 1996)

2.3.4 Finite element model development

The finite element (FE) method is a powerful numerical analysis technique that has been successfully used to solve a broad class of boundary value problems in engineering. The FE method to model joint and edge discontinuities has led to its emergence as the analysis method of choice for rigid pavement research (Hammons and Ioannides, 1996). In line with this statement, it is remarkable to note that up to approximately 1994, most of the FE research studies conducted were two-dimensional (2D), whereas there are a relatively large number of three-dimensional (3D) studies that were published during the period 1994 to 1999.

Certain key attributes of the more common FE programmes as reported in the literature are summarised in Tables 2.1 (2D studies) and 2.2 (3D studies).

Table 2.1: Overview of 2D FE models for rigid pavements (Hammons and Ioannides, 1996, with modifications by author)

Programme name	Slab model	Load transfer	Foundation model(s)
ILLI-SLAB (Tabatabaie and Barenberg, 1980)	2D medium thick plate	Linear spring, beam element on spring foundation	Winkler, Boussinesq, non-linear, two- and three-parameter models
ILLI-SLAB (Ioannides et al. 1985b)	2D medium thick plate	Linear spring, beam element on spring foundation	Winkler, Boussinesq, two-parameter models
ILLI-SLAB (Ioannides and Korovesis, 1990)	2D medium thick plate	Linear spring, beam element on spring foundation	Winkler
ILLI-SLAB (Khazanovich and Ioannides, 1993)	2D medium thick plate	-	Winkler, Boussinesq, non-linear, two- and three-parameter models
WESLIQID (Chou, 1981) and KENSLABS (Huang, 1993)	2D medium thick plate	Linear springs	Winkler
FEACONS III (Wu et al., 1993)	2D medium thick plate	Linear and torsional springs	Winkler
GEOSYS (Ioannides et al., 1985b)	3D brick element	None	3-D brick elements with stress-dependent subgrade model
ABAQUS (Kuo, 1994)	2D shell element 3D brick element	Linear and non-linear springs, interface elements, gap elements, multipoint constraints, explicit models	Winkler, 3-D brick element with linear and non-linear elastic, plastic, and visco-elastic constitutive models, user-defined models
DYNA-SLAB (Chatti et al, 1994)	2D plate element	Linear spring, beam element on spring foundation	Winkler and layered visco-elastic solid
ILLI-SLAB and JSLAB (Masad et al, 1997)	2D medium thick plate	Friction	Linear solid
ILLI-SLAB (and HVS) (Coetzee, 1989)	2D medium thick plate	Linear springs	Winkler

Table 2.2: Summary of features of 3D FE studies

Programme name	Loading	Slab(s)	Subbase layer(s)	Foundation	Dowels	Aggr. interl.
GEOSYS (Ioannides and Donnelly, 1988)	Static	Linear 8-noded brick elements		Non linear solid		
(Channakeshawa et al., 1993)	Static and temperature	Multiple and non linear		Winkler	Beams	
ABAQUS (Zaghloul et al., 1994)	Dynamic	Multiple and non linear	Non linear solid	Non linear solid	Bars	Friction
ABAQUS (Uddin et al., 1996)	Dynamic (FWD)	Multiple and linear	Linear solid	Linear solid	Beams	Friction
ABAQUS (Kuo et al., 1996)	Static and temperature	Multiple and linear	Linear solid	Winkler	Beams	Springs
ABAQUS (Hammons, 1998)	Dynamic (FWD)	2D shell 3D hexahedral	3D hexahedral	Winkler		Springs
Various programmes (Zaman and Alvappillai, 1995)	Static and dynamic	Linear		Winkler		
NIKE3D (Brill and Lee, 1999a, 1999b)	Static	Linear	Linear solid	Linear solid		
EverFE (Davids et al., 1998a, 1998b)	Static and temperature	Linear elastic	Linear elastic	Winkler	Beams	Shear

It is widely accepted that 3D FE models are necessary to adequately capture the structural response of rigid pavement systems (Lourens and Strauss, 1988; Davids et al., 1998a). However, there are still areas that must be addressed if realistic 3D finite element models are to be routinely used for the evaluation, retrofit, and design of rigid pavements:

a) Beyond permitting dowel slip, dowel-slab interaction has not been considered, except by Channakeshawa et al. (1993), and more recently by Davids et al. (1998a). EverFE models the portion of the dowels within the slab using an embedded quadratic beam element. This ensures no loss in solution accuracy over a conventional formulation and permits the dowel to be de-bonded by releasing the dowel's axial degrees of freedom (Davids et al., 1998a). Paragraph 2.5 describes dowel modelling techniques in more detail.

b) Aggregate interlock has mostly been modelled using linear spring elements (Kuo et al., 1996), or assuming classical friction behaviour (Masad et al., 1997; Uddin et al., 1996; Zaghloul et al., 1994). In attempting to validate the use of ABAQUS for 3D FE modelling of joints in concrete airport pavements, Hammons (1998) also studied the aggregate interlock of joints in the *subbase* beneath the concrete slab. Both the joints in the concrete and in the subbase were modelled as springs across the crack. This approach did not capture the actual mechanism of aggregate interlock. In developing his aggregate interlock model for EverFE, Davids et al. (1998a) chose the two-phase constitutive model developed by Walraven (1981; 1994) to model aggregate interlock shear transfer (see paragraph 2.5). Laboratory studies are still required to determine optimal parameters for this model. *Load transfer across pavement joints due to aggregate interlock has to be determined under a variety of loadings, geometries, and joint openings for design purposes.*

c) Up till recently, the 3D FE models available could only be used in research applications due to computational requirements. During their research study, Lourens and Strauss (1988), made an attempt to develop nomograms for the mechanistic design of continuously reinforced concrete pavements, using finite element techniques. This was in an attempt to bridge the gap between sophisticated (first-world) design methods and the need for practical and directly applicable designs in remote (third-world) areas. This was also the method used to design the continuously reinforced concrete overlay during the rehabilitation of the N1 Ben Schoeman freeway between Buccleuch and Brakfontein Interchanges. Similarly, nomograms/response charts need to be developed (or existing response charts refined) for the mechanistic design of doweled jointed concrete pavements. Davids et al. (1998a), on the other hand, developed EverFE with the specific aim to make a 3D model available for implementation on desktop computers.

2.3.5 Rigid pavement joints

Early work by the US Corps of Engineers showed that design thickness of rigid pavement slabs was controlled relative to fatigue cracking, by the tensile stresses that occurred at the edges of the pavement slabs (Hammons and Ioannides, 1996). They conducted accelerated trafficking tests under controlled conditions during 1943. The tests were designed to permit a comprehensive evaluation of many of the factors influencing rigid pavement design. Each of the tests contained extensive strain and deflection measurements at slab interiors, edges and corners.

This work indicated that increasing the efficiency of joints through improved design methods reduced the edge stresses at both transverse and longitudinal joints. The transferral of loads across joints in a pavement is desirable to reduce the independent vertical movement of adjacent slabs and reduce the occurrence of distresses like spalling, faulting, and effects due to pumping (i.e. differential displacement).

The following ranking of joint types from the most to the least effective in terms of load transfer was made by Sale and Hutchinson (1959) based on the performance of test items in the Lockbourne No 2 Test Track:

a) Doweled contraction joint.
b) Doweled construction joint.
c) Keyed construction joint with tie bars.
d) Contraction joint.
e) Keyed construction joint.
f) Doweled expansion joint.
g) Free-edge expansion joint.

For doweled joints in thick concrete pavements, it was found that there was no apparent advantage in using structural shapes over conventional round bars (Hammons and Ioannides, 1996).

Observations at test tracks at Lockbourne and later at Sharonville, Ohio (Sale and Hutchinson, 1959), indicated that load transfer at doweled joints also varied with the methods of doweled joint construction. At both Lockbourne and Sharonville, the concrete slabs were cast against forms, and the dowels were locked into place in the forms. At Lockbourne, the dowels were installed by bonding one end in the concrete, pulling the forms off over the dowels, painting and greasing the exposed half of the dowel and then paving the adjacent lane. At Sharonville the dowels were installed by painting and greasing the end of the dowel in the first paving lane, turning and removing the dowel, removing the forms, reinserting the painted and greased end of the dowels into the same hole from which they were removed, and bonding the exposed end of the dowel into the adjacent lane. Strain gauges and deflection gauges were installed in the pavement on each side of the joints at both test tracks. A load cart with a twin tandem assembly was used to load the track in each case. The dowel installations at Lockbourne and Sharonville are shown graphically in Figure 2.8.

The most important result from these tests is that the construction method used at Lockbourne (in which the first end of the dowel was bonded) performed better (higher load transfer) than the construction method used at Sharonville. In both cases better load transfer was measured when the slab with the bonded end of the dowel was loaded, than when the slab with the un-bonded end of the dowel was loaded. Thus it was recommended that the dowels be installed with no manipulation of the dowel after concrete was placed to maximize the load transfer obtained by the doweled joint. Furthermore, load transfer across doweled joints resulted in an edge stress reduction of 25 percent. The load transfer computed from deflections was more than the load transfer computed from stresses. The load transfer across joints in multi-layer pavements is about the same as load transfer in single slab construction.

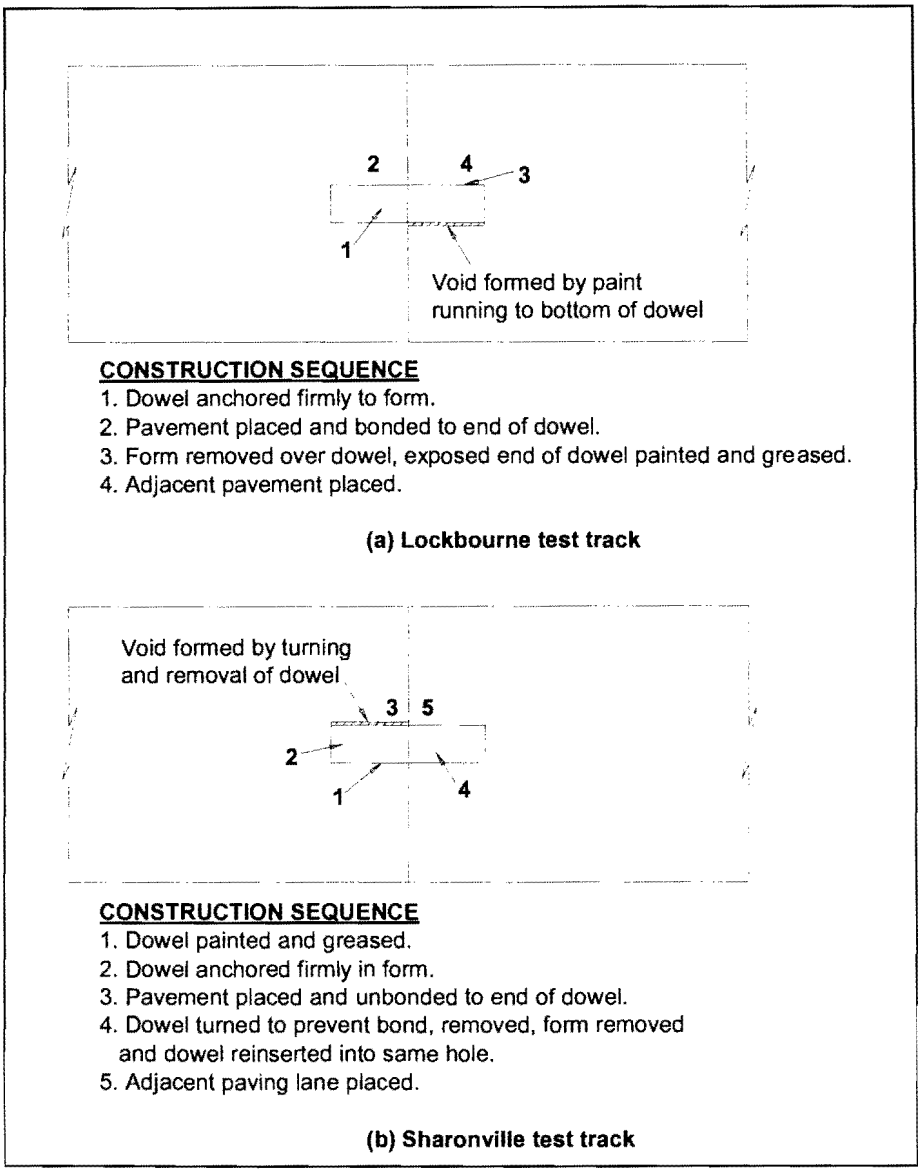

Figure 2.8: Dowel installations at Lockbourne and Sharonville Test Tracks (Sale and Hutchinson, 1959)

2.3.6 The effects of moment and inertia

The effects of moment and inertia were specifically investigated in order to gain an understanding of what the effect of a moving load could be on the load transferred across a crack/joint in a concrete pavement. One of the most common methods used in practice to determine deflection load transfer efficiency at a joint in a concrete pavement is by using a falling weight deflectometer (FWD). With the FWD, a static impulse load is applied by dropping a load onto the pavement on the one side of a crack/joint, and measuring the deflection at both sides. The deflection load transfer efficiency is then calculated using Equation (2.4). In practice, however, the loads applied to a pavement are not "one-

sided", but a dynamic load is transferred from one slab to the next. The response of the slabs therefore had to be captured under dynamic loading as well as under static loading to be able to capture real-life conditions and to compare the results.

The dynamic response of a pavement is fundamentally a function of the inertia and damping characteristics of the structure (Huang, 1993). These characteristics generally invalidate attempts to approach the problem with static or quasi-static analyses and experiments. In a study by Lourens (1991) the equation for motion was formulated as follows:

$$\{F\} = [K]\{u\} + [C]\{\dot{u}\} + [M]\{\ddot{u}\} \tag{2.11}$$

Where:

$\{F\}$ = Vector of nodal point forces;
$[K]$ = Stiffness matrix;
$\{u\}$ = Vector of nodal point displacements;
$[C]$ = Damping matrix;
$\{\dot{u}\}$ = Vector of nodal point velocities;
$[M]$ = Mass matrix; and
$\{\ddot{u}\}$ = Vector of nodal point accelerations.

The last two quantities in Equation (2.11) are exclusive to dynamic analyses and need some clarification. The term $[C]$ is necessary to dampen the induced movement, as an un-dampened system will oscillate up to infinity in time after acceleration. Damping therefore defines the loss of energy due to friction and other effects. The mass term $[M]$ and acceleration $\{\ddot{u}\}$ is Newton's Second Law of Motion, and can be viewed as the inertial effect or "resistance to movement" which is experienced when an attempt is made to accelerate an object.

Measurements on pavements and vehicles have shown that the frequency of dynamic loads at a discontinuity in a pavement stay more or less constant at about 3 Hz, and is apparently not affected by the speed of the vehicle (Papagiannakis et al., 1988; Sousa et al., 1988, Steyn and Visser, 2001). The forces developed by the vehicles vary according to a host of factors, the most important being the road roughness and suspension type, although contradicting results have been reported on this aspect. The dynamic forces reported were nearly always substantially higher than the static forces (Papagiannakis et al., 1988; Sousa et al., 1988), and measured forces of up to 150% of the static values have been reported (Bergan and Papagiannakis, 1984).

On the other hand, it was found that deflection and strain values generally decreased with increased speeds (Steyn and Visser, 2001). Stress values generally remained constant with increased speeds. Load magnitude showed good relationships with stresses in the upper part of the pavement structure, while load speed showed good relationships with the strains in the pavement structure. The expected

pavement lives calculated using the response parameters from a moving constant load analysis caused higher expected lives than when doing the calculation using static load data. The analysis of data from all the pavement response analysis methods used by Steyn and Visser (2001) at all load and speed conditions, indicated that the calculated stresses were not affected by load speed to the same magnitude as the calculated strains in flexible pavements.

Despite the fact that there is a difference between the response of the pavement under dynamic loading to the response under static loading, the static loading testing method, using the FWD still takes precedence. The main reason is that the equipment used for the FWD is less expensive than for, for example Weigh in Motion (WIM) or Stress in Motion (SIM) stations. On the other hand back-calculation from FWD data is a two-dimensional problem, and therefore simpler and more commonly used, whereas back-calculation from WIM/SIM data is a three-dimensional problem, requiring more sophisticated and time consuming methods.

2.3.7 A mechanistically and risk based design method for concrete pavements in southern Africa (Strauss et al., 2001)

A study was initiated in 1988 to investigate the performance of rigid pavements in South Africa and to develop design techniques based on South African experience (Strauss, 1992). The research study involved a field evaluation, laboratory study (Malan et al., 1988) and the development of a modelling technique based on finite element analysis.

During modelling of the pavements under investigation, significant differences in behaviour occurred for loading at the interior and loading at an edge or corner of a slab, emphasising the fact that edge load transfer has a marked influence on the performance of the pavement.

Evaluating the effectiveness of aggregate interlock for different types of mixes, an increase in relative movement was obtained with an increase in crack width. For the same crack width, concrete that cracked at 28 days allow ten times more relative vertical movement before aggregate interlock is enacted than concrete cracked at 3 days of concrete age. The same applied for concrete mixes with 25 mm aggregate, which showed 30 times more relative vertical movement than 50 mm aggregate concrete.

From this study, Strauss (1992) compiled an equation to predict the relative movement that takes place at an aggregate interlock joint in a concrete pavement, as follows:

$$y(x) = 114000 \frac{x^3}{agg^{4,5}} \qquad (2.12)$$

Where:

$y(x)$	=	Relative vertical movement (mm);
x	=	Crack width (mm); and
agg	=	Nominal size of 20% biggest particles in concrete mix / maximum aggregate size (mm) in concrete mix.

Equation (2.12) accepts that the age of cracking cannot be controlled, and assumes all cracks developed within 7 days. The research done by Strauss (1992) evolved into the production of Manual M10 (1995). Most of the design curves used in this manual were developed using linear elastic layered theory together with finite element analysis and were confirmed against presently used design procedures. The manual essentially followed a "recipe-type" approach to design and used a series of nomograms. The design process consisted of the following basic steps:

a) Estimating traffic loads and volumes.
b) Assessment of slab support conditions.
c) Joint design and load transfer mechanism identification.
d) Determining slab properties.
e) Calculation of concrete slab thickness.

The structural design of concrete overlays on flexible pavements was also included in Manual M10 (1995). The same theoretical base as for new pavements was used. Due to the fact that it is easy to determine the deflections of the surface to be overlaid, and that most settlement was assumed to have taken place, it was considered that the overlay design could be done with a higher degree of certainty than the design of new pavements.

Specifically for joint design, it was stated that load transfer efficiency could be improved by:

a) Large (greater than 26,5 mm) durable coarse aggregate.
b) Dowels.
c) Reduced joint opening.
d) Stiff subbases.

Specific guidelines for dowel design were also given in the manual, together with guidelines for the functional design parameters such as skid resistance, noise, glare and roughness. The manual also contained typical specifications for the construction of the underlying pavement layers, as well as for the concrete pavement itself.

Equation (2.12) was incorporated as the aggregate interlock model of Manual M10 (1995). However, this equation was only accurate for concrete constructed with a maximum aggregate size of around 26,5 mm; the aggregate used in the concrete constructed for the laboratory studies (Malan et al., 1988).

This will be demonstrated in more detail in the chapter dealing with the laboratory studies conducted for this thesis (Chapter 3).

The South African concrete pavement fraternity recognized the need to upgrade the South African Concrete Pavement Design and Construction Manual (Manual M10, 1995), to a manual based on mechanistic design principles with the aim of increasing the market share for concrete roads. It became apparent from overseas research, performance of local pavements and some instrumented sections of a concrete inlay on the National Route 3, that current concrete design methods were inherently conservative and consequently resulted in expensive pavements.

A number of strategy sessions identified the need for a departure from existing practice. A new design method was needed that utilised a mechanistic approach and would result in more cost-effective pavements (for equivalent performance to asphalt pavements). This approach is fuelled by the fact that concrete pavements are increasingly utilised as overlays on old flexible pavements where characteristics are determined through linear elastic theory and software packages. An integration of flexible and rigid mechanistic design approaches is therefore becoming more and more important. The new method was, however, to be pragmatic and aimed at ordinary pavement design practitioners rather than researchers and academics.

Simultaneously it was also decided to develop a simple, user-friendly software programme as part of the manual. Among the critical input parameters that were identified at the outset of this whole process, was an aggregate interlock load transfer constant, Ca. The fact that the format of the aggregate interlock equation itself was still uncertain was emphasized and it was recognised that further research was required to ascertain a more accurate, mechanistic formula.

A survey of the South African road network indicated that the great majority of structural failures of road pavements could be attributed to construction and materials problems. Structural failures were thus caused by deficiencies built into the pavement, which were aggravated by traffic and environmental factors. It was also established that the traditional approach, using single values for input parameters, was not ideal as uncertainty in the input was not translated into uncertainty in the output and therefore in the inherent risk of the design.

The design package had therefore to incorporate variability of the different parameters. Its structure should also enable it to be used to assess the relative effects of poor construction, higher than planned for variation in properties and to develop a bonus/penalty scheme for contractual purposes.

The basic principles incorporated in the new manual and the software programme, as well as a description of input data and interpretation of the output is given below. The specific area where the research conducted for this thesis had to make a contribution to the design modelling is also pointed out in the following paragraph.

2.3.7.1 Modelling of performance

Based on the requirement that the design procedure should be user friendly and that the software needed to run on relatively inexpensive and readily available hardware, the use of sophisticated methods in calculating pavement response was precluded. However it was recognised that, in order to develop suitable pavement response and performance models, the latest technological tools had to be employed. The decision was therefore made to develop a database using finite element techniques, multi-layer analysis software packages, instrumented pavement sections measuring dynamic effects and the actual performance of the concrete road network to develop performance equations.

Maximum tensile stress in a concrete slab that is placed on an elastic support can be calculated using several methods (Hogg, 1938; Skarlatos and Ioannides, 1998), the most familiar being Westergaard (1926). The following relationship indicates the basic format of these theories:

$$\sigma = f\left(C, \frac{P}{h_1^{\,2}}, \sqrt[4]{\frac{D}{K}}\right) \qquad (2.13)$$

Where:

σ	=	Maximum tensile stress close to a joint or crack in the pavement (MPa);
C	=	A coefficient that primarily depends on load/slab configuration and load transfer at a crack or joint (mm);
D	=	Slab stiffness (MPa);
K	=	Slab support modulus (MPa);
P	=	Load (kN); and
h	=	Slab thickness (mm).

Tensile stress close to the joint or crack is calculated since structural failure affecting performance can usually be associated with it.

Coefficient C, the load transfer coefficient, depends on the extent of load transfer at a joint or crack through aggregate interlock or dowels (longitudinal reinforcement for continuously reinforced pavements).

The magnitude of slab loading, P, for a given load application can be defined in terms of wheel loading with due consideration for the effect of dynamic loading and speed of loading.

Slab stiffness, D, is a function of slab thickness and concrete stiffness.

Slab support modulus, K, is not only dependent on the stiffnesses and thicknesses of the supporting layers, but also on the uniformity of the support. Relative settlement of sub-layers and/or erosion under traffic loading and the presence of water creating voids will have an influence on slab support.

The ratio of slab tensile stress/slab tensile strength has always been used in calculating the number of load applications N of magnitude P to failure:

$$N = a\left(\frac{tensile\ stress}{tensile\ strength}\right)^{b} \tag{2.14}$$

Where:

N	=	Number of load applications to failure;
a	=	Damage constant; and
b	=	Damage factor.

Based on the discussion above the modelling can be subdivided into:

a) A load transfer component.
b) Slab loading through moving traffic.
c) Slab support including voids under the slab.
d) Slab characteristics and stress calculations.
e) Structural performance as a function of the stress/strength ratio.

2.3.7.1.1 Load Transfer at the Joint/Crack

Load transfer can be achieved in two ways namely aggregate interlock and dowel action of longitudinal steel bars. In order to isolate the effect of load transfer at a joint/crack on slab stress from the influence of slab support as far as possible, the relative vertical movement at the joint/crack due to a load moving across the joint/crack is taken as indicative of joint/crack shear stiffness.

Based on work by Walraven (1981) as well as a laboratory study of some typical South African concrete mixes using hard, crushed, granitic material (Strauss, 1992), the following was found for aggregate interlock:

$$y(x) = f\left(\sqrt{n}, \frac{1}{E_c}, \frac{x^{1,5}}{agg}\right) \tag{2.15}$$

Where:

$y(x)$, x, agg		As defined for Equation (2.12)
E_c	=	Modulus of elasticity of the concrete (MPa); and
n	=	Number of load applications.

By this stage the format of the relative movement equation already changed from the version published earlier by Strauss (1992). Note that the *agg* parameter has no exponent anymore, and that the *x* of the latter version is raised to the power 1,5, instead of 3, as previously. As mentioned in Chapter 1, the research conducted for this thesis was therefore primarily aimed at developing a new aggregate interlock load transfer equation, covering the normal range of maximum sized crushed aggregates (19,0 mm to 37,5 mm) used in the construction of concrete pavements in South Africa.

Applying the fundamental theory of dowel design (Yoder and Witczak, 1975) relative vertical movement at a joint/crack with steel bars through it can be written as a function:

$$y(x) = f\left(P_d, \left(\frac{1}{E_c}\right)^{0,75}, \left(\frac{1}{dia}\right)^{1,75}, \sqrt[4]{\frac{1}{E_d}}, \sqrt[4]{n}\right) \tag{2.16}$$

Where:

P_d = Load on a dowel (kN);

E_c = Modulus of elasticity of the concrete (MPa);

dia = Diameter of steel bar (dowel) (mm);

E_d = Modulus of elasticity of dowel / steel bar (MPa); and

n = Number of load applications.

In order to translate relative vertical movement at the joint/crack into a C value as depicted in Equation (2.13) above, the following relationship is used:

$$C = f\left(\sqrt{y(x)}\right) \tag{2.17}$$

Where C, the load transfer coefficient, is in the order of 0,16 for interior loading and 0,55 for free edge loading of a slab (no load transfer to the next slab). These values of C were determined for typical South African roads with slab thickness ranging from 150 to 250 mm, concrete cube strengths of about 40 MPa after 28 days and fairly stiff subgrade support.

2.3.7.1.2 Loading of the Pavement

External loading of the pavement is primarily through moving truck traffic. In order to determine amongst other factors, the influence of speed on stress in the slab, trial pavement sections were instrumented and tested under different speeds of a standard loaded dual-wheel single-back-axle truck. A typical plot of speed versus surface deflection for three different types of pavements is shown in Figure 2.9 for illustrative purposes (Lourens and Strauss, 2000). It is clear from the data that the un-dowelled jointed pavement is much more affected by speed (109% increase in deflection from static

loading) if compared with dowelled jointed (62%) and continuously reinforced concrete (31%). The simplified equation to depict this in terms of horizontal tensile stress in the concrete is:

$$\text{Stress} = f\left(\frac{P}{v^{0.2C}}\right) \tag{2.18}$$

Where:

v = Speed of loading (km/h); and

C = Load transfer coefficient.

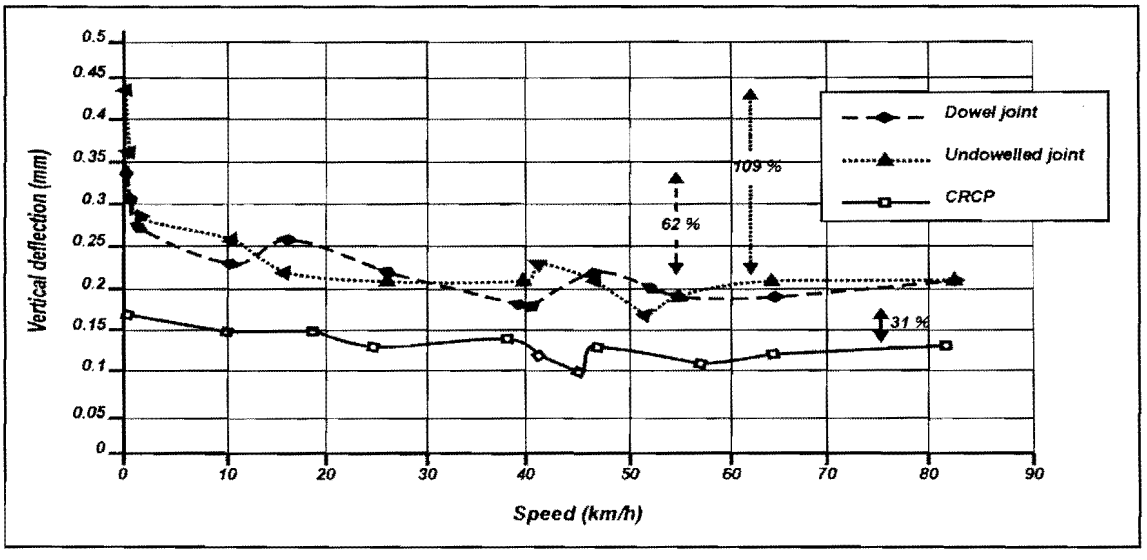

Figure 2.9: Measured surface deflection versus speed

2.3.7.1.3 Slab Support

Slab support is provided through several layers of natural materials, some of which are modified or stabilised and the top layer, the subbase, consisting of asphaltic, cemented or high quality granular material. Since concrete overlays on flexible pavements are also becoming more popular, the use of multi-layer linear elastic software programs to calculate not only residual life of the old pavement, but also its stiffness as an input into the design of overlays, is essential.

Although it is recognised that a stabilised subbase could structurally be considered as part of the concrete, during the development of cncRisk, slab support was simplified into a two-layer system, namely the subbase and an equivalent stiffness representing the contribution of lower layers. Using a multi-layer linear elastic program the equivalent stiffness of the layers below the subbase, which render the same tensile stress in the slab, could therefore be calculated

Voids below the slab, as a result of erosion or pumping of the subbase, or settlement in the lower layers, can increase tensile stress within the slab by up to 40% if compared to uniform slab support conditions (Dominichini and La Torre, 1998; Strauss and Lourens, 1998).

2.3.7.1.4 Slab Geometry and the Calculation of Stress

Recognising the need for simple equations, an attempt was made to utilise finite-element modelling together with actual measurement of strain on concrete roads under dynamic loading to develop models through regression techniques. A database was developed using a three-dimensional non-linear dynamic finite-element programme (STATAN), a three- dimensional linear elastic multi-layer programme (ELSYM5) and field measurements on pavements under traffic (Lourens and Strauss, 2000). Eight variables were introduced to develop the basic equation: load transfer constant C, void length, concrete stiffness E_c, slab thickness h_1, subbase stiffness E_2, subbase thickness h_2, subgrade stiffness E_e and speed of loading. Submodels for load transfer through aggregate interlock and dowel action of steel bars, the effect of different loads and surface pressures and the combination of sublayers to form an equivalent subgrade stiffness E_e were developed separately using different databases.

The equation for maximum tensile stress at a joint/crack under dynamic truck loading finally arrived through regression analyses is:

$$Stress = constant\left[\frac{(Void+1)^{0,80(C-0,1)}C^{0,45}\ E_c^{\ 0,60}}{h_1^{\ a}(h_2E_2)^{0,08}\left(3\sqrt{v+1}\right)^{0,40C}\ E_e^{\ 0,27}}\right] \quad (2.19)$$

Where:

$Void$	=	Length of void below slab (m);
C	=	Load transfer constant derived from Equations (2.15), (2.16) and (2.17);
$E_c h_1$	=	Slab stiffness and thickness (MPa, mm);
$E_2 h_2$	=	Subbase stiffness and thickness (MPa, mm);
E_e	=	Equivalent subgrade support stiffness (MPa);
v	=	Speed of heavy vehicles (km/h);
a	=	$1,95/(h_2 E_2)^{0,05}$; and
$constant$	=	Depends on wheel load and surface pressure.

The data on which the above equation is based was generated for 4,5 m joint spacing, a concrete shoulder 2,5 m wide, two travelling lanes each 3,7 m wide and the loading is by an 80 kN single axle with double wheels.

As mentioned, the load transfer constant, C in Equation (2.19) depends on the extent of load transferred through either aggregate interlock or dowels. The smaller of the values calculated with Equations

(2.15) and (2.16) is used. Furthermore, in Equation (2.19) C has a coefficient of 0,45. In the event of an interior loading condition where C is in the order of 0,16, the numerical value becomes 0,44 once the coefficient has been applied, which is nearly three times higher than the original value. Similarly for a free edge where C is in the order of 0,55, the calculated value becomes 0,76, which is less than twice the original value. Equation (2.19) therefore becomes less sensitive to a change in the load transfer constant, the larger the movement and the smaller the load transfer efficiency of the joint.

2.3.7.1.5 Structural Performance

Many different performance curves or transfer functions are being used by designers to convert stress to expected number of load applications to failure. Figure 2.10 shows some typical data obtained from the literature. Both the RISC (Majidzadeh and Ilves, 1983) and ARE (Treybig et al., 1977) curves are based on AASHTO data, the first assuming a terminal serviceability index of 2,0 and the second (ARE) a terminal serviceability of 2,5. Both these curves are based on the format of Equation (2.14) and thus the value of b for RISC is 4,29 and that of ARE 3,21. Darter (1977) used laboratory beam fatigue tests to produce the curve in Figure 2.10, which is similar to the findings of other laboratory studies (Hilsdorf and Kesler, 1966). The performance curve used by PCA (1984) is also illustrated in this figure and is used, in similar format, for design procedures in Australia and Canada.

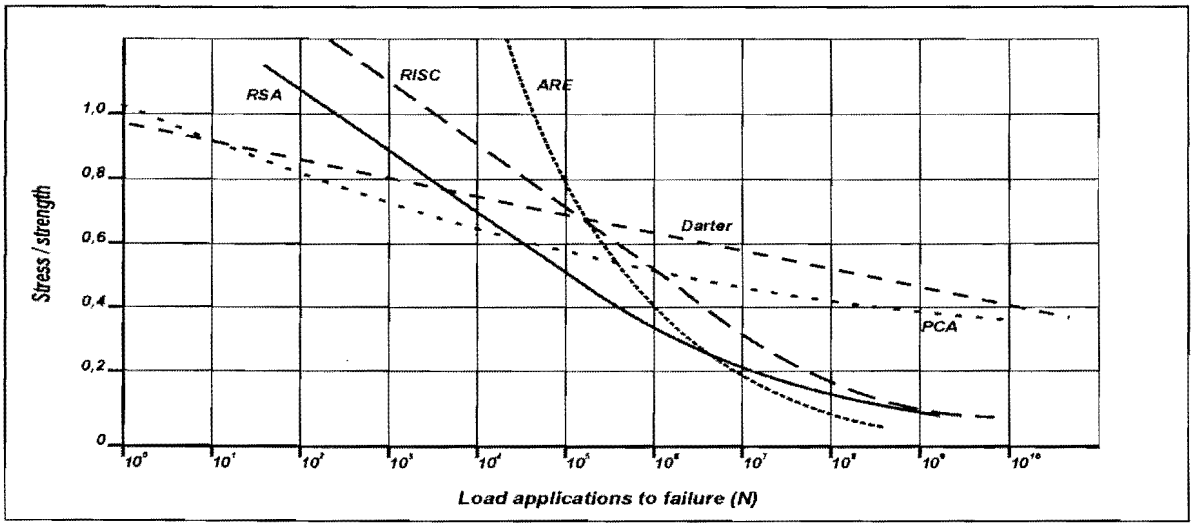

Figure 2.10: Performance curves used by various designers.

Using Equation (2.14) as a basis for the performance curve, as was done by Majidzadeh and Ilves (1983) and Treybig et al. (1977), the constant a leads to the situation that at high stress ratio e.g. 1,0, the number of load applications to failure is between 2 300 and 230 000. To overcome this problem, a can be defined as a function of the category of road in terms of the number of vehicles for which the pavement is designed. The curve depicted as *RSA* in Figure 2.10 is being used in the model until such

time that present research suggests an improvement. The value of b for this curve in Equation (2.14) is 4,2.

2.3.7.1.6 Deflection at a Joint

Using the same database that was developed for generating the equation for stress and supplementing with calculated field-measured information, the relationship for maximum deflection at a joint is:

$$Deflection = constant \left(\frac{C^{0,4} \left(void + 1\right)^{0,2}}{h_1 E_c^{0,25} \left(h_2 E_2\right)^{0,1} E_e^{0,4} \left(v + 1\right)^{0,02/C}} \right) \tag{2.20}$$

Where the constant depends on surface loading determined through. vehicle traffic or by falling weight deflectometer.

2.3.7.2 Design evaluation based on the view of consequences

2.3.7.2.1 Background

An effective but simple approach was adopted to evaluate the quality of design and thus facilitate competent decision-making. The approach is based on the evaluation of consequences. The consequences of a certain pavement design are expressed in terms of three output variables, namely risk of premature pavement failure, excessive deflection, and – in case of continuously reinforced concrete – excessive crack spacing.

Conceptually, pavement failure occurs when demand exceeds supply. In practice this happens when the number of load applications n a pavement is supposed to carry over the design period exceeds the number of load application N the pavement can carry at an acceptable level of structural and/or functional integrity. The ratio n / N is called cumulative damage CD. By definition $CD = n / N$. The risk R of premature pavement failure is defined as the probability of n being greater than N. In other words, R is the probability (P) of cumulative damage CD being greater than unity:

$$R = P\{CD > 1\} \tag{2.21}$$

One should mention that the complement of risk, i.e. $1 - R$, is called *reliability*.

2.3.7.2.2 Input

The proposed design method, cncRisk, requires five input constants, namely the Damage factor b, Damage constant a (as in Equation (2.14)), Ratio $k1 = E_c f$, Ratio $k2 = ITS / f$ (where f is the flexural

strength of the concrete and *ITS* the Indirect Tensile Strength), and Steel diameter *dia*. Apart from these, the method relies on nineteen input variables, such as aggregate size, crack width, slab thickness and others. For a concrete pavement with a concrete shoulder, traffic loading is considered as interior loading, whereas for a concrete pavement with no shoulder, traffic loading is considered as edge loading.

Due to uncertainty, the designer may find it difficult to determine appropriate values for these variables. Many designers realise the uncertainty about correct input and, consequently, try to avoid the use of single point-estimates. Instead, they prefer indicating a range of reasonable practical values. Triangular probability distribution was used to express the stochastic nature of input variables. A triangular distribution is defined by three parameters, namely a minimum practical value, the best estimate, and a maximum practical value (see Figure 2.11). The triangular distribution has been chosen in preference to the Normal, Lognormal, Gumbel or Weibull types of probability distribution, because the determination of its parameters appeals to intuition, and is conducive to a direct application of the designer's experience.

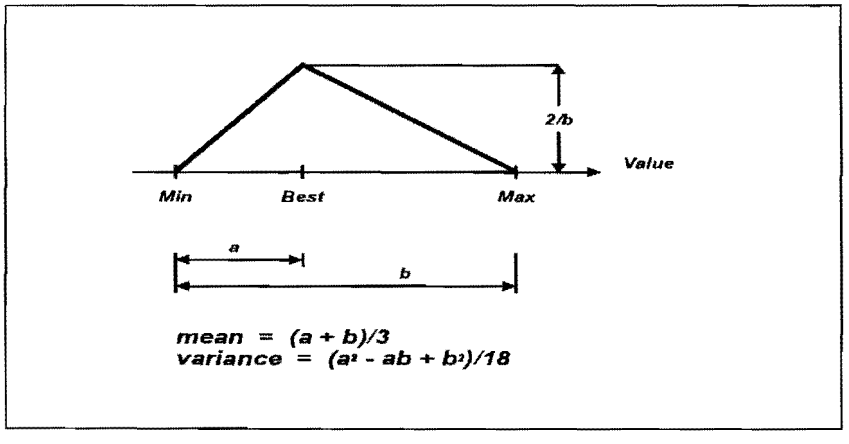

Figure 2.11: Triangular distribution of input variables.

Of the nineteen input variables eighteen have triangular distributions, whereas one – the dynamic axle load – follows an empirical distribution. A practical example of such an empirical distribution of axle loads, which was obtained from weigh-in-motion measurements, is shown in Figure 2.14.

2.3.7.2.3 Output

Because of the complexity of calculations, a Monte Carlo simulation technique was used to translate the uncertainty about the input into the uncertainty about the output. The magnitude of this uncertainty was established in terms of the probability distributions of the output variables, namely the cumulative

damage *CD*, pavement deflection *y*, and crack spacing *x*. The risk of premature failure *R* is then represented by the area of the *CD* distribution that lies right of the line for *CD* = *1*, outside the graph (see Figure 2.15).

The simplified flowchart on which the Monte Carlo simulation was based is shown in Figure 2.12.

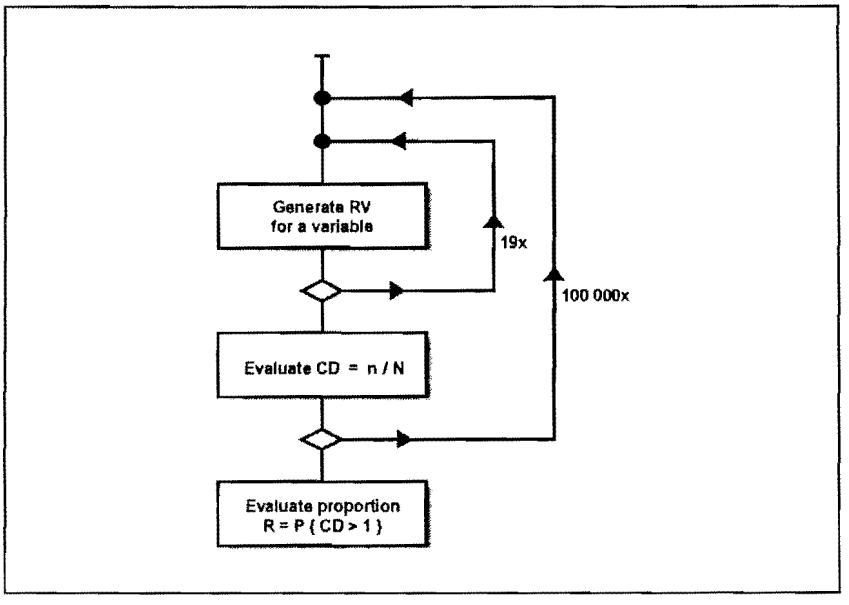

Figure 2.12: Simplified simulation flowchart.

2.3.7.2.4 Computer Simulation Program

A computer program was developed to perform the above simulation. The program is called CncRisk and runs on a PC under the Windows operating system. The user interface is divided into five panels, namely Main control, Statistics, Advanced input, Operating instructions and Manual highlights. A panel can be selected by clicking its tab.

Main control panel

Figure 2.13 shows the Main control panel of the program, together with default values of the input variables and constants. The values of main output variables – risk, deflection and crack spacing – are also shown on this panel. In addition, three dials are displayed. During a simulation run, the needles indicate the current level of cumulative damage, deflection and crack spacing, respectively, to continuously inform the user.

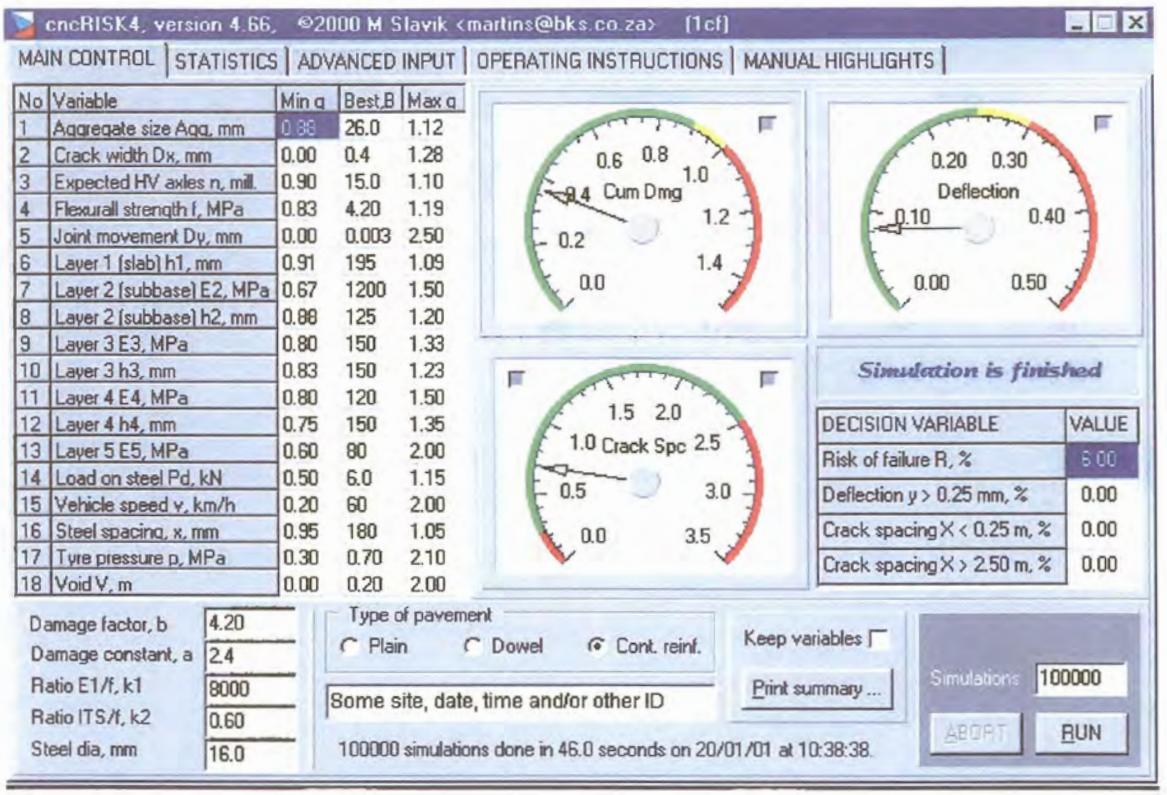

Figure 2.13: Example of the Main control panel.

The minimum and maximum practical values of the input variables are entered as factors q, by which the best value is multiplied to obtain the respective extreme. Three main types of concrete pavement – plain, dowelled and continuously reinforced – are selectable by means of 'radio' buttons. The number of simulations can be selected from 1 000 to 10 000 000.

Although a small number of simulations will be done very quickly, it may produce jagged output distribution curves and give dissimilar output figures for repeated simulation runs. In contrast to the above, a large number of simulations (say, over 100 000) will take more time to complete, but will yield relatively smooth probability distribution curves, and ensure good repeatability of output results.

Advanced input panel

The panel called Advanced input, which is shown in Figure 2.14, gives the user an opportunity to enter the distribution of dynamic axle loads that are applicable in his or her case. A typical distribution can be selected from a provided list. Alternatively, entering frequencies can create an individual distribution. In any case, a frequency plot is shown in a graph to guide the user. Also, the presence of a shoulder is selectable on this panel.

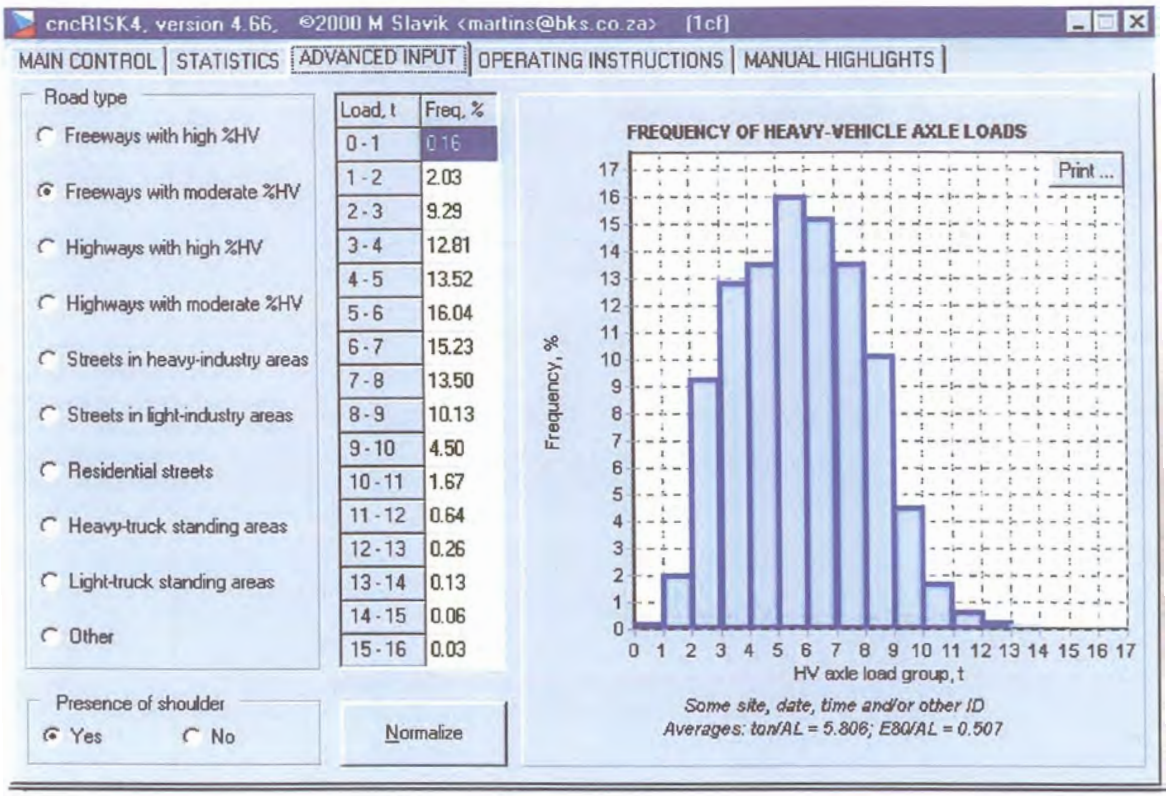

Figure 2.14: Example of the Advanced input panel.

Statistics panel

The probability distributions of the output variables, together with other figures of interest, are shown on the panel called Statistics – see an example in Figure 2.15. As mentioned earlier, the quality of design is reflected by the three main output variables, namely cumulative damage, deflection, and crack spacing in case of continuously reinforced concrete. To facilitate evaluation and competent decision-making, certain standards were laid down to guide the designer. As a rule of thumb, the risk R should not exceed 5% in case of national and strategic roads, 7% in case of provincial and less important roads, and 10% in case of low-standard roads. Similarly, the probability of deflection at a joint or crack exceeding 0,25 mm should also comply with the above standards. These percentages can also be applied to the probability of excessive crack spacing, which should never be less than 0,25 m and never more than 2,50 m. This deflection of 0,25 mm is associated with an 80 kN load on a single axle with double wheels; 40 kN on each side of the axle.

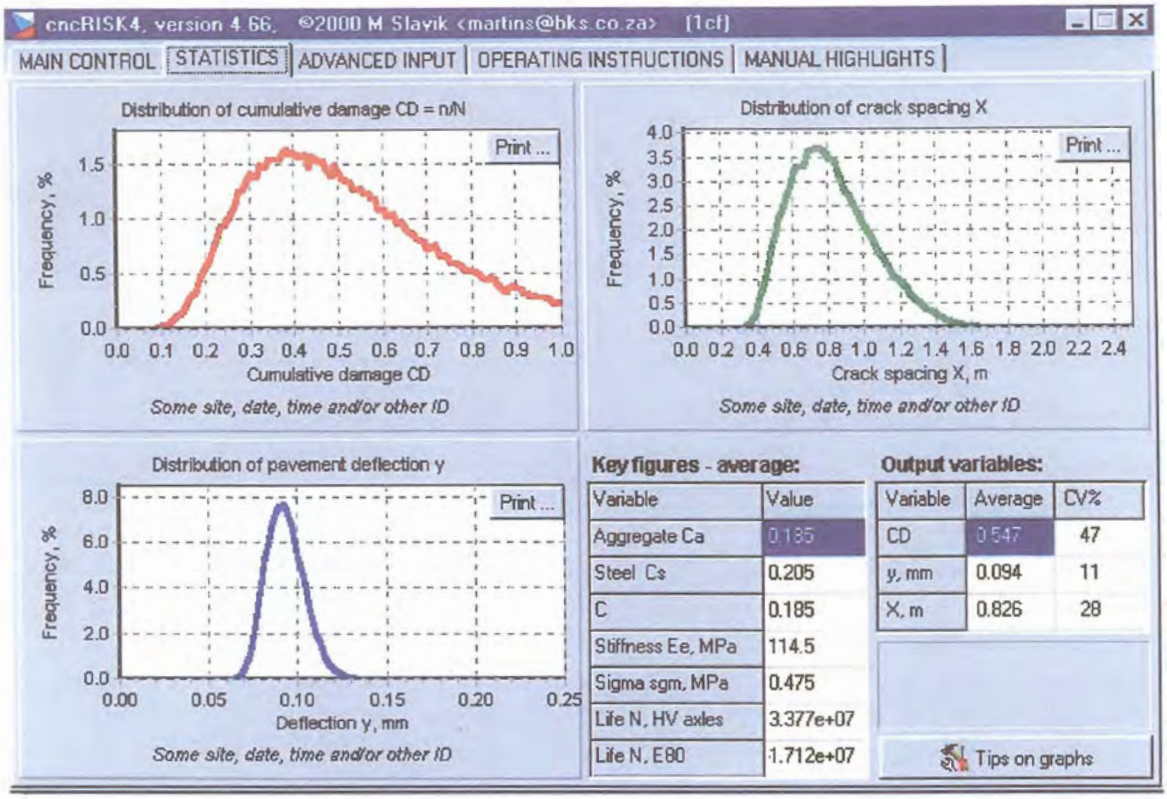

Figure 2.15: Example of the Statistics panel

One should consider the relation between the above figures and the uncertainty about the input. A conservative uninformed, or unsure designer would specify the respective triangular distributions with low minimum, and high maximum, practical values. This will result in "fat" distributions of the output variables, with probabilities exceeding the recommended figures. To bring the figures down to the standard, a stronger – and more expensive – design will have to be employed. The extra cost of such a design can then be viewed as a cost of imperfect knowledge of the input.

2.3.7.2.5 General

Apart from the research conducted for this thesis to develop the aggregate interlock load transfer function; research is also under way to further develop the load transfer function for dowels. This will increase the accuracy of the stress equation. However, the refinement of the performance curve is of the greatest importance and, in order to increase confidence in the prediction of performance, the program has been released for use by a selected group of practitioners. Feedback from them on the performance of pavement structures together with further research using the Heavy Vehicle Simulator (HVS) will be implemented during further development of the software.

2.3.8 Summary of historical developments

All design methods universally recognise the need to consider the subgrade, material characteristics, environmental effects, and the traffic anticipated in the design period. The concept of serviceability-performance, and a quantitative definition of "failure" are necessary. Stability or "balance" should be maintained throughout the various phases within the design period for repetitive permanent deformation, as well as repetitive fatigue of cemented layers. The pavement tends to reach a state of equilibrium during each of these phases within which a temporary imbalance may exist due to material changes (with time, water ingress, and changes in support).

Up till recently, the 3D FE models available could only be used in research applications due to computational requirements. Most researchers therefore tended to focus on developing empirical methods. These methods, however, were complicated as illustrated by the formulas and derivatives shown in Appendices A and B. Davids et al. (1998a), on the other hand, developed EverFE with the specific aim to make a 3D model available for implementation on desktop computers.

The "recipe-type" approach previously followed in Manual M10 (1995) for the design of concrete pavements in South Africa was conservative and resulted in expensive pavements. A new design method was needed that utilised a mechanistic approach and would result in more cost-effective pavements (for equivalent performance to asphalt pavements). An integration of flexible and rigid mechanistic design approaches was therefore becoming more and more important. The new method was, however, to be pragmatic and aimed at ordinary pavement design practitioners rather than researchers and academics (Strauss et al., 2001).

2.4 AGGREGATE INTERLOCK

2.4.1 Introduction

Aggregate interlock was first recognised as a beneficial load transfer mechanism in the early 1900s, when the popularity of Portland cement concrete as a paving material was beginning to increase. Aggregate interlock is a natural mechanism effective in transferring loads across discontinuities, such as joints and cracks in plain or reinforced concrete pavement systems. Only a shear action is operative in this mechanism. In contrast, load transfer devices such as dowel bars also involve bending, thus creating an interest to investigate load transfer by aggregate interlock (Ioannides and Korovesis, 1990).

Because of its questionable long-term endurance record in the United States of America (USA), aggregate interlock is not relied on as a primary load transfer mechanism in jointed concrete pavements, except perhaps in low volume roads. Abrasion and attrition of the aggregates coupled with temperature variations causing a fluctuation in the size of the opening at the discontinuity can result in

a significant decrease in the effectiveness of this mechanism over time (Ioannides and Korovesis, 1990).

The poor performance of joints/cracks relying on aggregate interlock only, and conclusions from the Bates Road Test, conducted near Bates in Illinois (Older, 1924), led to the conclusion that once cracks had formed in plain concrete, they tended to propagate rapidly and deteriorate badly under a small number of load repetitions. In contrast cracks developing in reinforced concrete pavement sections remained tight, deteriorated slowly, and exhibited overall much better behaviour. Therefore it was concluded that "when roughened edges of two slabs are held firmly together the aggregate interlock may be expected to function perfectly and permanently as a load-transfer medium" (Benkelman, 1933).

Various experimental studies on aggregate interlock shear transfer in concrete pavements demonstrated that joint shear transfer effectiveness and endurance depend on many factors including joint width, slab thickness, load magnitude, foundation type, subgrade modulus, and aggregate shape (Colley and Humphrey, 1967).

Research by Walraven (1981) into shear transfer across discrete cracks in concrete has shown the mechanics of aggregate interlock shear transfer to be highly complex. In addition to contact between sharp edges of aggregates on joint surfaces, there may be localised crushing of the cement paste and the aggregate, as well as entry of loose materials. The amount of crushing and the bearing area of the surfaces depends on the joint opening, normal restraint of the joint, the strength of the concrete (both the paste and the aggregate), and the size and distribution of the aggregate particles. Walraven (1981) stated that the modelling of aggregate interlock shear transfer in rigid pavements should take all these factors into account.

During finite element (FE) modelling of aggregate interlock shear transfer in rigid pavement systems, most researchers tend to use discrete linear spring elements (see paragraph 2.3). While this may be considered reasonable for an examination of the effect of aggregate interlock shear transfer effectiveness on the global slab response, it does not permit modelling of local response at the joint. Even when the use of linear springs is appropriate, the rational choice of a spring stiffness may be difficult, if not impossible, and the appropriate spring value is valid only for one model geometry, set of material properties, and loading. The need for the more realistic FE modelling of aggregate interlock shear transfer was recognised by Davids et el. (1998a). They chose the two-phase model developed by Walraven (1981) to model aggregate interlock shear transfer in the FE software EverFE.

A literature review, distinguishing between theoretical modelling, laboratory studies, and field investigations has been conducted to provide an overview of past attempts to model this phenomenon and to explain the mechanics of aggregate interlock. The focus of the literature review was to investigate methods used during previous studies, to assist in the design of the experiments, and the compilation of the test programme for the current study.

2.4.2 Theoretical aggregate interlock modelling

2.4.2.1 Micro-mechanics-based model

Probably the most important development in the theoretical modelling of aggregate interlock in concrete was the development of the two-phase model by Walraven (1981). This model is based on a statistical analysis of the crack structure and the associated contact areas between the crack faces as a function of the displacements, w (crack width), and Δ (shear displacement), and the composition of the concrete mix.

The fundamentals on which the study was based are that concrete can be represented as constituted by two distinct materials, the hardened cement paste, and a collection of embedded aggregate particles. Generally the strength and stiffness of the aggregate particles are greater than those of the matrix, however, the contact area between both materials, the bond zone, was assumed to be the weakest link of the system.

The micro-roughness of the crack, caused by the aggregate particles projecting from the crack plane, was assumed to dominate the macro-roughness, due to overall undulations of the crack faces. Because of the large plastic deformations of the cement paste due to pore-volume reduction, the cement paste was idealised as obeying a rigid-plastic stress-strain law. The aggregate was idealised as incompressible.

The aggregate particles were modelled as spheres of varying size, distributed according to a Fuller curve. The aggregate particles intersect the crack plane at various depths, depending on their statistical distribution within the concrete matrix as shown in Figure 2.16.

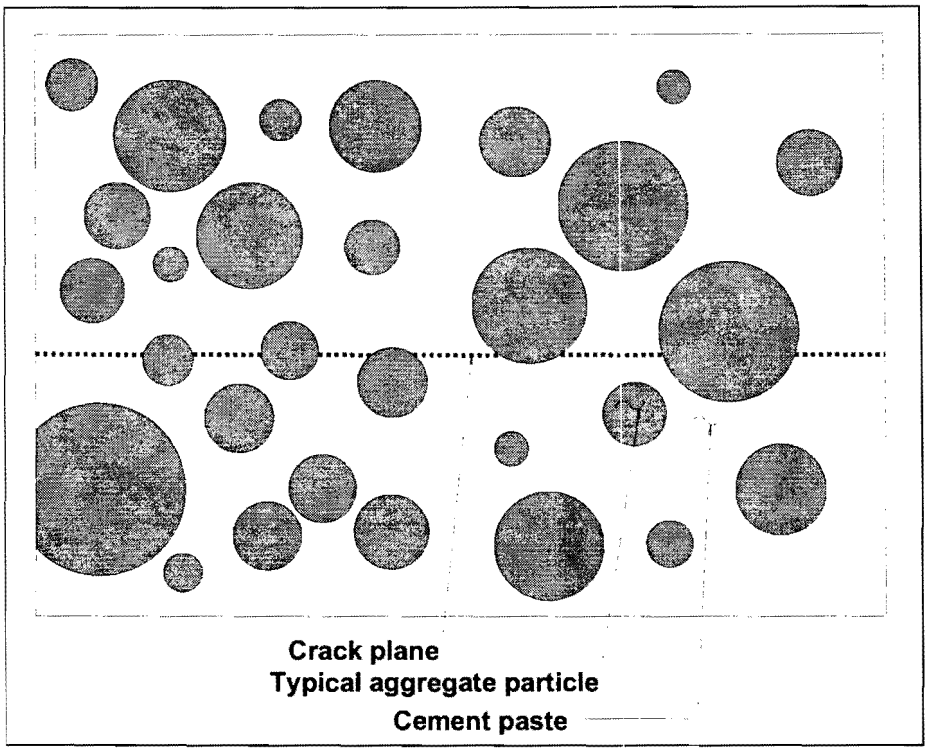

Figure 2.16: Crack plane and distribution of aggregate particles (Davids et al., 1998a)

As a result of these assumptions, it is possible to consider a cracked concrete body as an assemblage of a large number of slices each of finite width, thus reducing the crack to a two-dimensional problem of finite width. The stresses at the contact area are resolved into a stress, σ_{pu}, normal to the contact area and a stress, τ_{pu}, tangential to this area (see Figure 2.17). These stresses are interrelated by the condition that the contact areas are about to slide and therefore:

$$\tau_{pu} = \mu.\sigma_{pu} \tag{2.22}$$

Where μ is the coefficient of friction between the paste and the aggregate, and σ_{pu} is the ultimate strength of the paste, which can be calculated as follows:

$$\sigma_{pu} = 6{,}39 f_{cu}^{\,0{,}56} \tag{2.23}$$

Where:

f_{cu} = Concrete cube crushing strength (MPa)

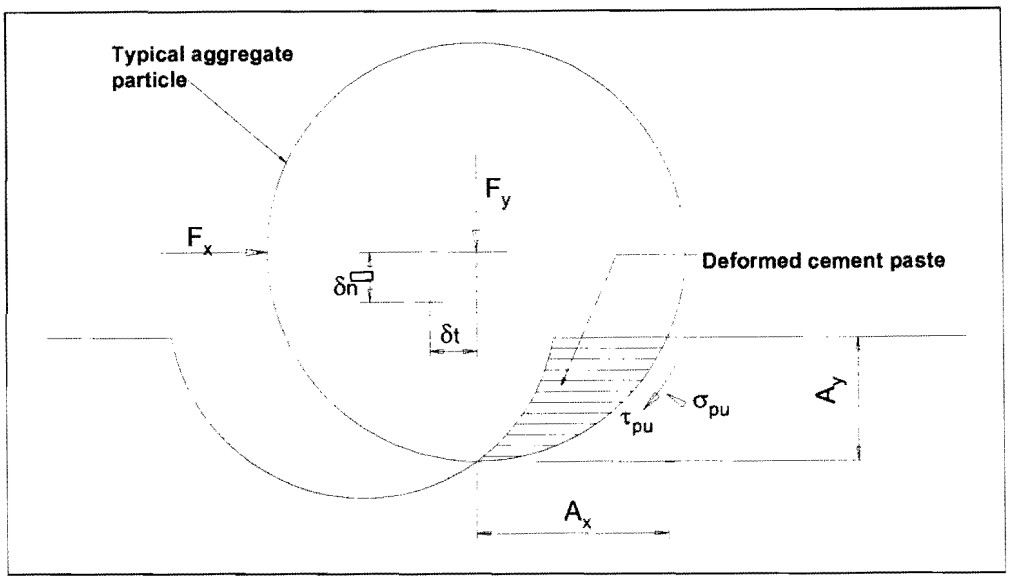

Figure 2.17: Deformed cracked plane (Davids et al., 1998a)

The equilibrium of the crack plane requires that the net forces be balanced as follows:

$$F_x = \sigma_{pu}\left(\Sigma A_y + \mu \Sigma A_x\right) \tag{2.24}$$

$$F_y = \sigma_{pu}\left(\Sigma A_x - \mu \Sigma A_y\right) \tag{2.25}$$

Where:

ΣA_x = X-projection of the sum of the most probable contact areas; and

ΣA_y = Y-projection of the sum of the most probable contact areas.

The determination of the x- and y-projections is based on the statistical distribution of the aggregate in the concrete matrix, and the geometry of the spherical aggregate particles intersecting the crack plane at a given tangential and normal displacement.

In an attempt to verify the theory, a series of tests were run in which the crack width was maintained at a constant value, and the shear stress, normal stress, and shear displacement were measured. The values of σ_{pu}, and μ were determined to provide the best fit to the experimental data for a crack opening of 1,0 mm. These values were then used to calculate the stress-displacement curves for other crack opening values. The theory was generally in good agreement with the experimental data for all values of crack openings. In addition, parametric studies were conducted which allowed the role of friction between aggregate and matrix, the contribution of various aggregate fractions to transmissions of stresses in the crack, the influence of aggregate size, and of the grading curve to be studied.

Building forth on the same physical and mechanical concepts developed in his initial study (Walraven, 1981), Walraven (1994) presented a model that makes it possible to explain and predict the behaviour of cracks under cyclic loading.

Walraven (1994) recognised the fact that the behaviour of cracks under cyclic shear loading is characterised by a considerable irreversible damage of the crack faces. The response of cracks to reversed and alternate actions can only be well described if load-history effects are taken into account. The load-history of rough cracks subjected to earthquake loading, can be determined from the severity of the earthquake, which in turn can be related to the cyclic loading of traffic across a joint in a concrete pavement, relying on aggregate interlock load transfer.

Tests on cracks subjected to earthquake loading showed that there is a considerable difference between the first and the subsequent loading cycles. Irreversible damage to the cement matrix takes place when the hard aggregate particles are pushed into this softer cement matrix. Any new cycle of loading leads to further damage of the crack faces, resulting into steadily increasing values of the shear displacement and the crack width at peak loading.

The statistical basis for the aggregate particle distribution is identical to that developed for the previous study by Walraven (1981). To simplify calculations, both the distribution of particle diameters and all possible embedment depths were added one by one into a finite number, with the embedment depth assumed to be uniformly distributed between a minimum of zero and the maximum of the radius of a given particle. This allows the representation of an aggregate particle D_{ij} with diameter $D_i = (0,1i - 0,05)D_{max}$ and embedment depth $d_j = 0,1j[(1/2)D_i]$ as shown in Figure 2.18. For each embedment/diameter combination, D_{ij}, the cement paste is subdivided into a finite number of layers, allowing computation of the projected contact area by summing the contact areas of the individual paste layers. Figure 2.18 gives a graphical representation of this discretisation.

For a given normal and tangential displacement of the crack plane, the likely contact area for any particle diameter is determined by summing the contact areas for all embedments and multiplying by n_i, the likely number of occurrences of D_i. The total contact area is then determined by summing over all particle diameters, and the shear and normal stresses may be computed by using Equations (2.24) and (2.25).

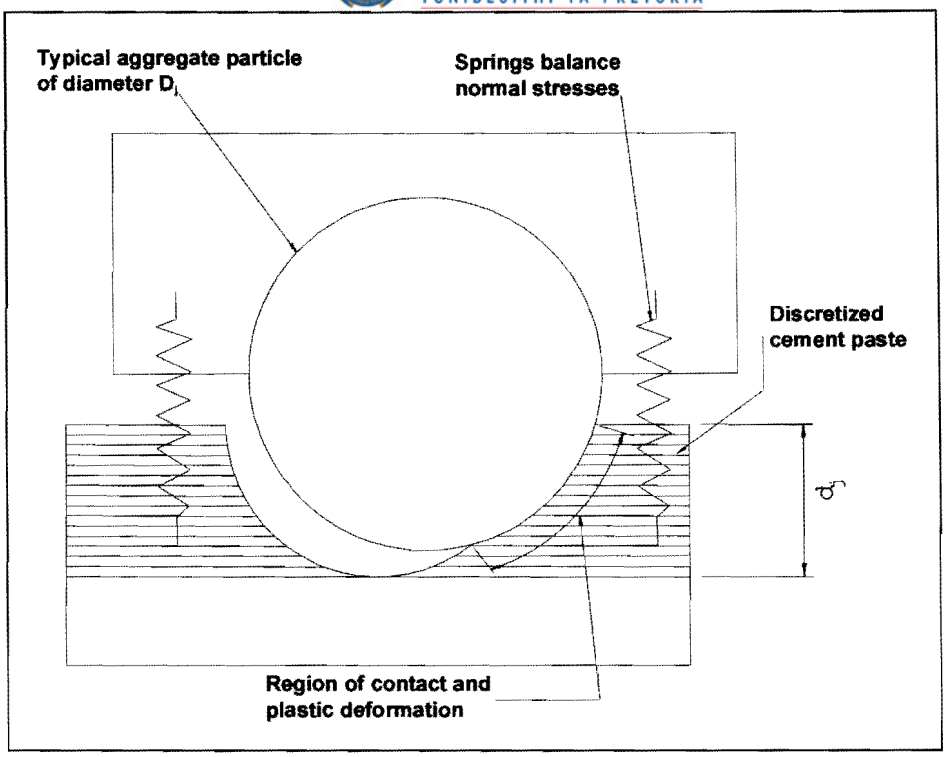

Figure 2.18: Subdividing aggregate particles and cement paste into discrete particles (Davids et al., 1998a)

The normal stresses generated across the crack are balanced by the springs assumed to cross the crack plane as shown in Figure 2.18. These springs may represent some external restraint mechanism, or reinforcing bars intersecting the crack plane. The discretisation of the cement paste also allows the damage to the cement paste to be updated throughout the loading history by tracking the geometry of the paste layers for each particle diameter/embedment depth combination. A simple programme may be written to perform simulations of both static and cyclic loading for different parameters such as initial crack opening, restraining spring stiffness, etc.

Up to now, it has been assumed that the aggregate is so strong, that no aggregate particle will fracture during cracking of the concrete, so that all the particles in the crack contribute to the aggregate interlock mechanism. To take this effect into account the fracture index, C_f was introduced. This is used to proportionally reduce both the shear and normal stress transferred across the crack, and account for the fracturing of the aggregate particles. The value of C_f is characteristic of the specific concrete mixture, and must be determined from static load testing of a specimen and curve-fitting the resulting data.

Some of the relevant conclusions to these studies were:

a) The experimental results were adequately described by the adopted physical model.

b) The mechanism of aggregate interlock can only be adequately described if normal stress, shear stress, crack width, and shear displacement are all involved.

c) All particle fractions contribute qualitatively in the same way to the transfer of stresses across the crack; only fractions containing particles with a diameter smaller than two times the crack width may be considered to be inactive.

d) A friction coefficient of, $\mu = 0{,}4$, between the aggregate particles and the matrix, independent of the concrete quality and the level of the stresses, results in the best fit between experimental data and the model. The yielding strength of the cement paste, which has to be used to obtain the best results, is a function of the concrete strength. Both parameters are in good agreement with experimental data described in the literature.

e) The resistance to shear deformations is governed by the concrete strength, with the diameter of the aggregate playing a secondary role.

f) The grading curve of the aggregate has some influence on the shear stiffness at larger crack widths. The development of the normal stresses is hardly influenced.

g) The behaviour of cracks, subjected to cyclic loading can be well explained and described by the theoretical model.

h) The load-history effect is caused by crushing of the matrix, irreversibly damaging the matrix during load cycles, which in turn influences the behaviour during the next cycles of loading.

i) The influence of the damage on the geometrical shape of the crack faces can be followed cycle by cycle.

2.4.2.2 Empirical and semi-empirical models

Reinhardt and Walraven (1982)

Following on the development of the micro-mechanics-based theoretical model and to increase the database on aggregate interlock, Reinhardt and Walraven (1982) conducted a series of experimental investigations. Push-off type tests were conducted on specimens with embedded bars (reinforcing bars intersecting the crack plane), as well as on specimens with external restraint bars. The advantage of these tests was that the normal stresses acting on the crack plane could be measured directly on the restraint bars. Typical measurements in these tests were the shear stress, the normal stress, the crack opening, and the shear displacement.

Millard and Johnson (1984)

In an attempt to study the internal mechanisms of shear transfer and dowel action across a single crack to enable more accurate modelling of shear stiffness, Millard and Johnson (1984) *devised tests of a new type* to examine independently the aggregate interlock and dowel action (see paragraph 2.5) effects in reinforced concrete. The primary goal of the aggregate interlock tests was comparison with previously developed theoretical models, including that developed by Walraven (1981).

The aggregate interlock test results showed that the two-phase model by Walraven (1981), involving a combination of crushing and sliding of the crack faces, is the most realistic one. In this model, shear

forces were resisted by a combination of crushing and sliding of the rigid spheres into and over the softer cement matrix: contact and interaction between spheres projecting from opposite crack faces was not considered. Closely similar results were obtained from nominally identical specimens. It was deduced from this repeatability that the aggregate interlock mechanism is not dependent upon the random path of propagation of a tensile crack. There was crack widening associated with shear slip, regardless of the size of the initial crack width. Increasing axial stiffness increased the shear stiffness and ultimate shear stress. For tests where the crack width was allowed to increase under increasing shear stress, the concrete strength had only a small effect on the ultimate shear stress. The test with a constant crack opening exhibited significantly higher ultimate shear stress and stiffness than similar tests, which permitted progressive crack opening. The conclusion that bearing/crushing predominates for small crack widths (≤ 0,25 mm) and sliding predominates for larger crack widths was not supported by these test results.

Soroushian, Obaseki and Choi (1988)

Soroushian et al. (1988) investigated the combined effect of aggregate interlock and dowel action in reinforced concrete against sliding shear at a crack.

Algorithms were developed for predicting the aggregate interlock constitutive behaviour using some empirical formulations. The analytical results obtained from these algorithms compared well with tests performed with either constant or variable crack widths. A numerical study with the developed algorithms indicated that sliding shear stiffness and strength provided by aggregate interlock increased significantly with decreasing crack width, and increasing concrete compressive strength, and also increased to some extent with increasing maximum aggregate size and restraining stiffness.

At typical crack widths (of the order of 0,5 mm), as the sliding shear deformations increased, the aggregate interlock tended to become more dominant over dowel bars in contributing to the sliding-shear resistance of cracks in typical reinforced concrete beams. The dominance of aggregate interlock was expected to diminish at very large crack widths or when cyclic loadings reduced the roughness of the crack faces.

Ioannides and Korovesis (1990)

During a mechanistic analysis of aggregate interlock load transfer mechanisms Ioannides and Korovesis (1990) developed the dimensionless joint stiffness parameter, *AGG/kl*. Aggregate interlock (or any pure-shear device, in general) was modelled in ILLI-SLAB as a set of linear springs, acting at each node along the discontinuity.

Seasonal variations in the efficiency of load transfer at the cracks were also noted. These were the result of expansion of the slabs in the summer, and their corresponding contraction in the winter. Joint opening was clearly established as a major determinant of aggregate interlock and efficiency of load transfer. Results of non-destructive testing (NDT) using the Falling Weight Deflectometer (FWD)

suggested that an increase in ambient temperature improve the efficiency of joints/cracks that are free to open or close.

At the commencement of the FE investigation the problem was described as fairly complex, even after the simplifying assumptions of linear elasticity, plate theory, and dense liquid (Winkler) foundation have been adopted. The purpose of the assumptions was to reduce the number of variables involved and thus improve the engineer's ability to understand, if not solve, the problem. The effect of the size of the loaded area was analysed, as well as the effect of slab length and width. The results of previous studies were also re-interpreted.

The major relationship established in this study is depicted in the form of an S-shaped curve, which is a non-dimensional plot of LTE_{Δ} versus AGG/kl (see Figure 2.19). This S-curve (Equation (B.44), Appendix B) offers the designer the possibility of investigating the factors influencing the spring constant AGG, which characterises the aggregate interlock shear stiffness per unit length of crack (AGG is also commonly referred to as the aggregate interlock factor (AIF)). This parameter expresses the relative stiffness of the joint itself to the stiffness of the pavement system in which it is installed. A large AGG for a crack indicates that the crack is relatively stiff, and has a good potential for aggregate interlock load transfer. Computation of this parameter involves determining LTE_{Δ}, obtaining k and l, and then using the graphical relation between LTE_{Δ} and AGG/kl, developed through a theoretically based (mechanistic) design approach to determine AGG.

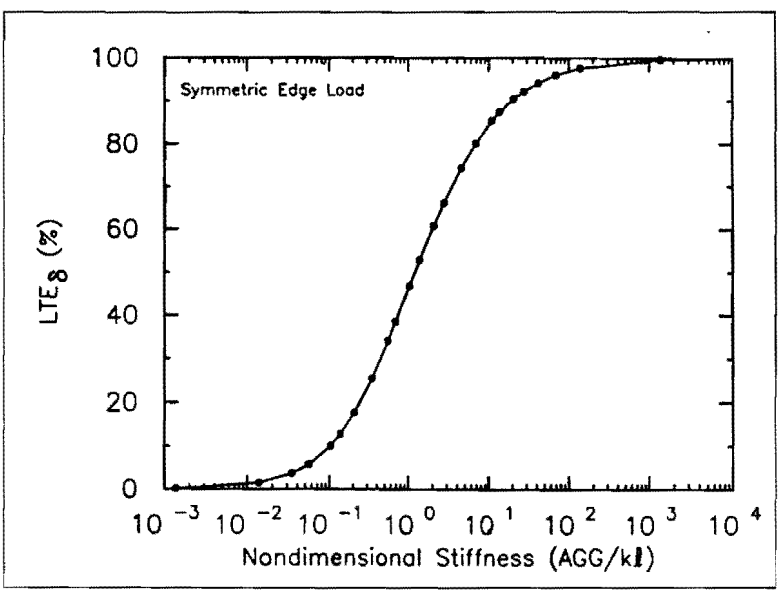

Figure 2.19: LTE_{Δ} as a function of dimensionless joint stiffness (AGG/kl) (Ioannides and Korovesis, 1990)

When determining the effect of the size of the loaded area, it was found that the load size ratio (a/l) (where a is the radius of the applied load) influences LTE_σ significantly. At any value of LTE_Δ, much higher LTE_σ values are obtained as a/l increases, i.e. as the load becomes less concentrated. The effect of slab length and slab width was also specifically investigated by determining the effect of the slab size ratios (L/l and W/l), (where L and W are the length and width of the slab, respectively) on LTE_Δ and LTE_σ. Both the slab length and slab width investigations suggested that slab size effects on TLE, LTE_Δ, and LTE_σ are not significant.

One of the primary concerns in designing load transfer mechanisms for a pavement system is the possibility of a detrimental effect when external loads and a temperature differential are considered simultaneously. Daytime conditions are often considered to be critical when combined with an externally applied load. Three loading conditions were analysed: external load only, curling only, and curling and external loading combined. Under curling-only conditions, joint stiffness caused by a pure-shear mechanism does not affect the response of either a short or a long slab. In contrast, a mechanism that involves bending as well may be expected to increase the curling-only stresses, particularly in shorter slabs. Thus, a pure-shear load transfer system would reduce edge stresses caused by the load, without increasing the curling-only stresses. This response would be especially desirable during the early life of the pavement system when the slab strength has not yet developed fully.

The methodology described in this mechanistic design approach by Ioannides and Korovesis (1990) offer the possibility to back calculate in situ joint stiffness using NDT data and to re-interpret available laboratory and field test results. They also concluded that the long-held false perception pertaining to the uniqueness of the relationship between deflection load transfer efficiency and stress load transfer efficiency should be abandoned.

Ioannides, Alexander, Hammons and Davis (1996)

Ioannides et al. (1996) applied the principles of dimensional analysis and Artificial Neural Network Training (ANN) to concrete pavement joint evaluation. Using these principles they developed a method for assessing the deflection and stress load transfer efficiencies of concrete pavement joints and for back-calculating joint parameters.

The computer programme BACKPROP 3.0 was used to train the algorithm using data developed by numerical integration of Westergaard-type integrals. The predictions of the programme were verified by comparisons with closed-form and finite element solutions pertaining to data collected at three major civilian airports in the United States. They further demonstrated that significant savings could be achieved through reduction of the dimensionality of the problem, which could be reinvested by broadening the range of the applicability of the neural network.

Dong and Guo (1999)

The Runway Instrumentation Project at Denver International Airport, as a part of the Federal Aviation Administration (FAA) airport pavement research program, started in 1992. Dong and Guo (1999) used a Heavy Falling Weight Deflectometer (HFWD) in conjunction with deflectometers and strain gauges installed in the pavement to collect data to investigate the behaviour of the joints and interfaces in the pavement.

Load transfer efficiency at the joints was measured in terms of deflection transfer efficiency (DTE) and stress transfer efficiency (STE). All transverse joints were un-doweled, relying on aggregate interlock load transfer, and all longitudinal joints were either hinged or doweled. The hinged joints experienced the highest DTE, followed by the doweled joints, with the transverse joints the lowest. The FAA design specification assumes STEs of 25%. For hinged joints the STE was higher than 25% and for the doweled joints slightly less than 25%. For the transverse joints the STE was almost totally lost after only three years.

During this study, it appeared as if environmental effects played a more important role than the traffic load on the reduction of load transfer capability of the transverse joints. Although no serious structural distresses were observed during the investigation, it was verified that cold weather might significantly reduce the load and deflection transfer capability of transverse joints.

Wattar, Hawkins and Barenberg (1999)

Wattar et al. (1999) confirmed through laboratory studies that the two-phase model, initially developed for a crack width of 1 mm could adequately describe the static loading behaviour of aggregate interlock joints with large crack widths. In this instance a crack width of 2 mm was used. The authors further stated that additional experimental testing was needed to finalise an analytical model for joint shear behaviour, and suggested that the primary tests should involve subjecting the specimens to cyclic loading at constant amplitude stresses until failure occurs.

2.4.3 Laboratory studies

Various researchers have attempted to measure load transfer at joints in concrete pavements through laboratory studies. These models varied from full-depth pavement structures constructed in a test box (Colley and Humphrey, 1967; Jensen, 2001), to part-slab test specimens on a simulated subgrade (Buch, 1998; Wattar et al., 1999; Vandenbossche, 1999).

Table 2.3 presents a summary of some of the laboratory studies conducted by various researchers. The variables considered significant to the performance of aggregate interlock joints are singled out.

Table 2.3: Summary of laboratory studies by various researchers

Reference	Concrete strength and model size	Aggregate size and type	Crack width	Load	Foundation support	Crack inducer
Colley and Humphrey, 1967	38,5 MPa. 1168,4 mm wide, 5,5 m long, and 177,8 mm / 228,6 mm thick	38 mm – natural siliceous gravel and dolomitic crushed stone.	0,1 mm to 2,54 mm.	40 kN load applied to both sides of crack with two actuators at a simulated speed of 48,3 km/h on circular loading plates.	Silty clay soil subgrade, with two types of subbase – sand-gravel and cement-treated material	Removable metal strip + groove in top of concrete directly above metal strip.
Millard and Johnson, 1984	29 – 52 MPa. 300 mm high x 125 mm wide x 100 mm thick - short test specimen 2/300 mm high x 225 mm wide x 100 mm thick for long test specimen	10 mm rounded gravel.	0,063 mm to 0,75 mm.	Shear loading through direct forces acting through knife-edge bearing adjacent to crack up to 4 MPa.	-	Applying a direct tensile force to the end plates.
Buch, 1998	38 MPa. 254 mm thick x 915 mm long x 1220 mm wide.	19,0 mm and 25 mm -crushed limestone and river gravel.	0 mm to 1,4 mm.	40 kN load applied to both sides of crack with two actuators at a simulated speed of 48,3 km/h on circular loading plates.	FABCEL-25 neoprene pads with a k-value of 27 MPa/m.	Metal strip inserted in fresh concrete.
Wattar et al., 1999	39 MPa. 305 x 305x 610 mm.	25 mm – river gravel	2 mm.	Horizontal shear force applied statically, and at constant amplitude.	-	Tensile force a few hours after casting
Jensen, 2001	30,6 – 34,8 MPa 250 mm thick, 3 m long, 1,8 m wide	25 mm limestone and 25 mm and 50 mm glacial gravel	0,1 mm to 2,5 mm.	Cyclic wheel load of 40 kN at one side of crack at 3 Hz.	Michigan Highway foundation: 102 mm open-graded drainage course on a 400 mm thick subbase.	Slab subjected to horizontal displacement at surface slot, 7 to 10 days after casting

There was no correlation between the sizes of the models used, nor the concrete strengths achieved, although the average was approximately 37 MPa. The maximum aggregate sizes used, varied from 10 mm to 50 mm. The researchers basically used the types of aggregate available in their immediate vicinity, and therefore there was also no real relationship as far as aggregate type is concerned. Consensus was however reached that the more angular the aggregate, the greater the load transfer potential.

Both Colley and Humphrey (1967) and Jensen (2001) tested up to a maximum crack width of 2,5 mm. Repetitive testing showed that the deflections tended to reach an upper asymptote from a crack width of 2,5 mm and larger. This region was therefore considered to represent the contribution from the elastic deformation of the foundation, where aggregate interlock did not play the primary role in the results obtained anymore.

The maximum load applied to large-scale models (Colley and Humphrey, 1967; Buch, 1998; Jensen, 2001) were 40 kN. This represented the load on one side of a standard 80 kN single axle heavy vehicle with two wheels on each side of the axle.

Foundation support models also differed greatly, varying from neoprene pads with an equivalent k-value of 27 MPa/m (Buch, 1998) to a typical Michigan Highway foundation (Jensen, 2001). To further contribute to dissimilarities in the laboratory studies, the methods used to induce a crack/joint in the test specimens, also differed. Two of the studies induced cracks by inserting metal joint formers in the fresh concrete (Colley and Humphrey, 1967; Buch, 1998), two studies used direct tensile forces (Millard and Johnson, 1984; Wattar et al., 1999), and a third method used was the application of a horizontal displacement with the aid of a surface slot by Jensen (2001).

Invariably, laboratory studies went hand-in-hand with either finite element analyses or theoretical modelling. Test results were mostly calibrated with field investigations. Colley and Humphrey (1967) collected data from in service pavement joints instrumented in a manner similar to the laboratory slabs. Millard and Johnson (1984) used Walraven's model to calibrate the aggregate interlock test results. Buch (1998) used the finite element programme ILLI-SLAB to conduct theoretical modelling, as well as dimensional analysis procedures to develop a non-linear regression equation to predict load transfer efficiency. Wattar et al. (1999) also used Walraven's two-phase model for theoretical analysis, as well as the test data obtained by Colley and Humphrey (1967). Jensen (2001) focussed mainly on the data obtained from the laboratory study, but also made use of Colley and Humphrey's (1967) data.

Apart from the definition of deflection load transfer efficiency already given in paragraph 2.2 (equation (2.4)), load transfer/joint effectiveness was also rated by the following equation (Colley and Humphrey, 1967; Ioannides and Korovesis, 1990):

$$JE(\%) = \frac{2\Delta_U}{\Delta_L + \Delta_U}(100) \tag{2.26}$$

Where:

JE = Joint effectiveness;

Δ_L = Deflection of loaded slab; and

Δ_U = Deflection of unloaded slab.

As illustrated in Figure 2.3, if load transfer at a joint was perfect, the deflections of the loaded and unloaded slabs would be equal, and the effectiveness would be 100%. Depending on the specific data set, this latter equation (2.26) tends to give values 1% to 2% higher than the former (2.4).

Further to determining the load transfer efficiency at joints, researchers also attempted to develop methods to determine equivalence of performance, for example:

Colley and Humphrey (1967) developed a summary statistic of joint performance, called the endurance index (EI), through regression analysis. This index is expressed in percent and is obtained by dividing the area under the curve of effectiveness versus cycles by the area that would be developed if the joint retained an effectiveness of 100 percent throughout one million load applications. This equation included only data obtained from the rounded natural gravel. The equation is as follows:

$$EI = 230\frac{h_e}{Pw}\sqrt{k} \tag{2.27}$$

Where:

h_e = Effective thickness (inch);

k = Modulus of subgrade reaction (pci);

P = Wheel load (lb); and

w = Joint opening (inch)

The nomograph developed from Equation (2.27) is presented in Figure 2.20.

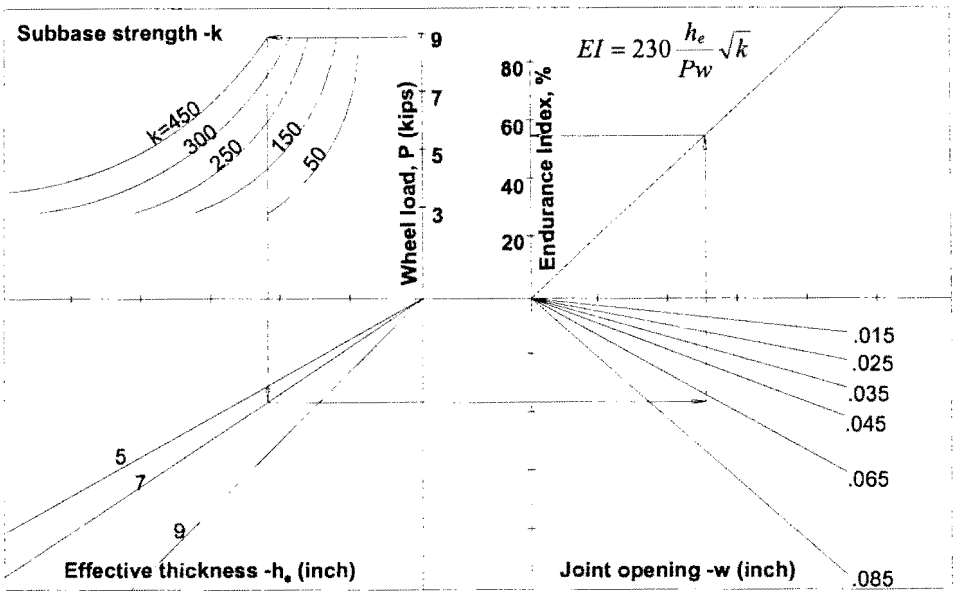

Figure 2.20: Endurance of joints (Colley and Humphrey, 1967)

Frabizzio and Buch (1999) found that fatigue cracking, caused by repeated cycles of temperature curling and moisture warping, combined with repeated loading applications of traffic load at mid-slab location, is a major source of transverse cracking in jointed concrete pavements (JCP's). Data obtained from forty-nine test sites, comprising of in-service JCP's throughout southern Michigan was used in the field investigation. Sites were chosen to represent each of four concrete coarse aggregate types: carbonate, natural gravel, recycled concrete, and slag. Each site was 25 to 65 m long and consisted of two to eight slabs. Jointed plain and jointed reinforced concrete pavements were not distinguished from one another, as it has often been found in practice that the reinforcing steel has fallen to the bottom of the slab or has been sheared off during crack formation. The effect of temperature reinforcement was therefore not considered.

The primary objective was to use field data to identify significant design parameters that affect the occurrence and performance of these transverse cracks. Another objective was to demonstrate how crack performance could be characterised using performance parameters. A void analysis procedure was also performed to characterise void potential near selected cracks and joints.

Of the parameters used to characterise crack performance were:

a) Transferred load efficiency (*TLE*), a derived parameter, which quantifies load transfer efficiency in terms of load itself (rather than deflection); the ratio of the amount of load transferred across a crack to the total applied load. The ideal condition is where the load is equally shared between both sides of a crack, in other words where *TLE* = 50%.

b) P_T; the total shear load transferred from the loaded to the unloaded side of a crack along its length, is directly derived form *TLE* using (Ioannides and Korovesis, 1990):

$$P_T = \frac{TLE}{100\%} \times P \tag{2.28}$$

Where:

P_T = Total shear load transferred (kN);
TLE = Total load efficiency (%); and
P = Total load (kN).

P_T and *TLE* provide the same information regarding characterisation of crack performance, but in different forms. It was suggested that P_T be used rather than *TLE*, as it has a more physical meaning than its counterpart (Ioannides and Korovesis, 1990).

c) The aggregate interlock shear stiffness per unit length of crack, *AGG*, parameter was computed by determining LTE_Δ, obtaining k and l, and then using the graphical relation between LTE_Δ and AGG/kl, developed through a theoretically based (mechanistic) design approach by Ioannides and Korovesis (1990) (see Figure 2.19).

Performance parameter thresholds were developed for LTE_Δ, P_T and *TLE* with limits that allow for evaluation of cracks in a pavement network. Ideally, rehabilitation activities would be performed before the parametric values reach threshold limits, allowing the integrity of cracked JCPs to be restored, prior to the development of crack-related distresses. A threshold value of 70% for LTE_Δ is commonly accepted. Similar values were not established for P_T and *TLE* prior to this study. In developing these thresholds, it was necessary to establish an indicator of the ability of the transverse crack to transfer load, other than the crack performance parameters. Faulting was selected as this indicator, as inadequate load transfer is a mechanism for faulting. The appropriate threshold value for P_T was determined as 16,5 kN, and for *AGG* as 200 MPa.

2.4.4 Joint deterioration mechanisms

As important as it is to define the load transfer mechanisms, it is equally important to define the joint deterioration mechanisms. The main mechanisms that cause joint deterioration are: aggregate wear out, loss of dowel support, and development of erosion as it pertains to faulting in jointed concrete pavements or punch-out development in continuously reinforced concrete pavements (Jeong and Zollinger, 2001). Of these three mechanisms, aggregate wear out will be discussed here, whereas dowel looseness is described in the following paragraph. As it has been envisaged to construct the experimental slabs on a rubber foundation, the mechanism of subbase erosion is cancelled out of the present study, although it is still considered for follow-up studies.

Two studies were singled out to describe the results of research work that has already been conducted on the subject of aggregate wear out or abrasion within the crack face, namely: the development of the volumetric surface texture (VST) test by Vandenbossche (1999), and the function developed by Jeong and Zollinger (2001).

Vandenbossche (1999) was part of the team at the University of Minnesota that developed the VST test. Although this test was developed to provide an estimate of the load transfer potential available through aggregate interlock across a concrete fracture plane, it was also stated that the test could provide an estimate of the abrasion that has taken place since fracture.

The test apparatus consisted of a spring-loaded probe with a digital readout, mounted on a frame over a computer-controlled microscope of the type typically used to obtain linear traverse and other measurements of concrete air void systems. The distance from an arbitrarily established datum to the fractured surface at any chosen point was measured in a predetermined grid pattern to map the three-dimensional fractured surface. A 3,2 mm grid was established by determining how far apart readings could be measured while still maintaining a precision of $\pm$ 0,0001 cm^3/cm^2 over a specified area, regardless of the positioning of the grid. The average area measured was about 161 cm^2 per specimen. After completion of this testing the surface texture was quantified in terms of a VST ratio (VSTR), defined as the ratio of the volume of texture per unit surface area (in cm^3/cm^2). A high VSTR indicated a rough surface texture, while a low value indicated a smooth texture.

To validate the VST test, tests were performed on both laboratory and field specimens. The laboratory study included tests performed on flexural beam specimens broken after 18 h, 7 days, and 28 days of curing. The beams were companion specimens cast in conjunction with full-scale concrete pavement test slabs, which were cracked 18 h after casting and were then subjected to simulated vehicle loads after 28 days of curing. Deflection, load and crack width data were collected for each slab. VST testing was also performed on cores retrieved from cracks and un-doweled joints of several concrete pavements across the USA. Joint and crack load transfer measurements were obtained for each pavement section by using a falling weight deflectometer at the time that the cores were retrieved.

Both the laboratory and the field data indicated a significant increase in VSTR with an increase in maximum aggregate size (an increase in maximum aggregate size from 38 to 63 mm, increased the VSTR by 66%), especially for angular aggregates. Durable (limestone) aggregates also had higher VSTRs than weaker aggregates (slag). The same applied to concrete prepared with virgin aggregates compared to recycled rounded aggregate concrete. A further observation was that cracks tended to propagate through weaker aggregates and around stronger aggregate particles, and that weaker aggregates tended to abrade more easily under repeated joint and crack movements.

Vandenbossche (1999) stated that this study had demonstrated that the VST test provides a means of accurately measuring surface texture so that the selection of concrete aggregates can be performed with

consideration of potential aggregate interlock at cracks and un-doweled joints. It also provides the engineer with an early indication of the extent of aggregate wear out that could be expected from a particular aggregate size, type, gradation, or blend.

Jeong and Zollinger (2001) investigated all three joint deterioration mechanisms as part of the prediction of faulting or punch-out distress at a joint or crack (The combined effect of aggregate interlock and dowel modelling is discussed in paragraph 2.5.4). They built forth on the work conducted by Ioannides and Korovesis during 1990 and 1992 (Ioannides and Korovesis, 1990; Ioannides and Korovesis, 1992) as the basis for this prediction.

It is generally accepted that joint or crack opening affects the degree of load transfer as far as it is sustained through aggregate interlock. Based on research the following relation has been established (Jeong and Zollinger, 2001):

$$\log(J_{cki}) = a.\exp\left[-\exp\left(-\frac{J_s-b}{c}\right)\right] + d.\exp\left[-\exp\left(-\frac{s_0-e}{f}\right)\right] + g.\exp\left[-\exp\left(-\frac{J_s-b}{c}\right)\right] x \exp\left[-\exp\left(-\frac{s_0-e}{f}\right)\right] \quad (2.29)$$

Where:

a	=	-4,00;
b	=	-11,26;
c	=	7,56;
d	=	-28.85;
e	=	0,35;
f	=	0,38;
g	=	56,25;
J_s	=	Load transfer on the shoulder of longitudinal joint;
s_0	=	Shear capacity $ae^{-0.039\omega}$, with a = 0,55 to 1,3 as a function of slab thickness = $0,0312h^{1,4578}$;
τ	=	Shear stress on the crack face = s_0P/h^2;
P	=	Wheel load; and
h	=	Slab thickness.

The shear capacity term (s_0) in Equation (2.29) is a significant parameter in the transfer of load relative to the aggregate interlock mechanism that can be used to represent the deterioration or wear out of aggregate interlock due to load repetition. The function for aggregate interlock wear out is important to account for the development of punch-out or faulting distress (Jeong and Zollinger, 2001):

$$\Delta s_{ij} = \sum_i \sum_j (0{,}069 - 1{,}5317 e^{-w_i/h}) \left(\frac{n_{ij}}{10^6}\right) \left(\frac{\tau_{stress}}{\tau_{ref}}\right) \quad (2.30)$$

Where:

n_{ij} = Number of axle load applications for current sub increment i and load group j;

τ_{stress} = Shear stress on the transverse crack;

τ_{ref} = Reference shear stress derived from Portland Cement Association test results; and

w_i = Crack width in sub-increment i.

Shear stresses (τ_{stress} and τ_{ref}) are computed as follows:

$$\tau_{stress} = sP_i / h^2 \quad (2.31)$$

$$\tau_{ref} = 111{,}1 . s_{pca} = 111{,}1 . [a + b \ln(J)^2 + c \ln(J) + de^{-1}] \quad (2.32)$$

Where:

s = Dimensionless shear;

J = Joint stiffness computed on the transverse crack;

a = 0,0848;

b = -0,000364;

c = 0,0188; and

d = -0,006357.

Equation (2.30) constitutes the wear-out function that allows for consideration of the deterioration of the aggregate interlock. Setting this equation to zero shear loss yields a threshold value of the dimensionless term ω/h = 3,1 below which no loss in shear capacity occurs. Examination of crack width data obtained from field measurements of continuously reinforced concrete pavements indicated that an LTE of about 91% is associated with a ω/h of 3,1. The data trends suggested that with an LTE above the 90 to 92% range, minimal loss of shear capacity is expected to occur. The crack widths were back calculated from Equations (B.44) (Equation (2.48)) and (2.29) for the given slab thickness and measured LTE. Equation (2.30) provides an estimate of the loss of shear capacity as a function of key slab characteristics and load repetition. The deteriorated level of shear capacity can be determined with the equation:

$$s_{new} = s_{old} - \Delta s \quad (2.33)$$

Where Δs is based on Equation (2.30) and s_{old} is the shear capacity before the loading increment and s_{new} is the resultant capacity due to the loading increment. The Δs may also be due to a change in the joint or crack opening. The new stiffness value can be determined with Equation (2.29) and s_{new}.

2.4.5 Summary of aggregate interlock modelling

This paragraph gives an overview of the studies conducted by various researchers on the subject of aggregate interlock shear load transfer at a joint in a concrete pavement. Although some of the studies used/tested the same micro-mechanics-based analysis model developed by Walraven, there were just as many different methods and models as research projects. Probably the only aspect these research projects really had in common was the fact that they all attempted to somehow understand the mechanics of aggregate interlock, and test/develop a method of quantifying it.

It has been agreed that the effectiveness of aggregate interlock load transfer at a joint in a concrete pavement depends on load magnitude, number of load repetitions, slab thickness, joint opening, subbase characteristics, subgrade bearing value, and aggregate angularity.

Aggregate interlock in cracks is not only a relation between shear stresses and shear displacements, but it is an interaction between normal and shear displacements on the one hand and normal and shear stresses on the other hand. The shear resistance depends on contributions from all particles with diameters larger than the crack width (Reinhardt and Walraven, 1982).

Studies conducted by Dong and Guo (1999), as well as by Vuong et al. (2001), indicated that environmental effects played a more important role than the traffic load on the reduction of load transfer capability of transverse joints relying on aggregate interlock load transfer. Although no serious structural distresses were observed during these investigations, it was verified that cold weather might significantly reduce the load and deflection load transfer efficiency of transverse joints. Hot weather on the other hand can cause such high compressive stresses in the pavement that blow-ups can occur.

The width of the joint/crack opening controlled the performance of the joint (Jensen, 2001). Opening the joint by 0,8 mm resulted in a loss of load transfer of 50% (Buch, 1998). In other words, aggregate interlock was considered effective in stress control when the joints were closed or under compression, but that it was not dependable when the joints opened 0,9 mm or more, irrespective of the maximum size of the aggregate in the concrete.

The surface texture of the crack directly influences the aggregate interlock and load transfer capacity of the joint. The texture of the crack face is a function of the coarse aggregate type, size, and gradation. It is also dependent on the maturity of the concrete. It is therefore logical that rough surfaced coarse aggregate will have better interlock characteristics than rounded smooth aggregate (Buch, 1998).

Davids et al. (1998) considered the micro-mechanics-based modelling technique of Walraven (1981) as the best choice for modelling aggregate interlock shear transfer. Davids et al. (1998) incorporated Walraven's model in the finite element models of the EverFE software programme. EverFE was

therefore considered the best tool available to conduct theoretical analyses, prior to laboratory studies, for the research project described in this thesis (see Appendix D).

In essence the VST (Vandenbossche, 1999) provides a practical tool for determining the aggregate interlock potential of a crack face, whereas the two-phase model by Walraven (1981) provides the theoretical tool, and the S-curve developed by Ioannides and Korovesis (1990) a mechanistic method.

The VST can also be used to provide an estimate of the abrasion or aggregate wear out that has taken place since fracture (Vandenbossche, 1999), together with the aggregate interlock wear-out function developed by Jeong and Zollinger (2001).

2.5 DOWEL MODELLING

2.5.1 Introduction

As was stated in paragraph 2.4, load transfer at joints is accomplished by two primary load transfer mechanisms, namely aggregate interlock and dowel bars. Aggregate interlock load transfer has been dealt with in detail in the previous paragraph and although the main objective was to investigate aggregate interlock load transfer through laboratory modelling, dowel modelling is just as important and warranted an in depth discussion.

Dowel bars have been used as load transfer devices in jointed concrete pavements at least since 1917 (Teller and Cashell, 1958). The use of dowel bars was justified by the fact that it prevents faulting, reduce pumping, and reduce corner breaks. The design of dowel bar diameter, length, and spacing, is based mostly on experience. For normal concrete pavements in South Africa the slab length, aggregate size, dowel diameter and spacing, are usually specified as 4,5 m, 37,5 mm maximum, 22 mm bars spaced at 600 mm, respectively (Manual M10, 1995).

Across the 50 states of America, however, disparities existed among the practices adopted by agencies, as well as among those reported from other countries (Ioannides et al., 1990). The main reasons were:

a) The theoretical treatment of the pertinent problems was still fairly elementary and strictly applicable to only highly idealised conditions.
b) Climatic and geotechnical conditions varied widely from state to state and from country to country.
c) The number, frequency, magnitude and geometry of traffic loadings were considerably different in each locality, and the concepts used to reduce mixed traffic to a design traffic number were sometimes flawed.

d) A large degree of empiricism derived from local experience entered the design and construction approaches of each agency.

This paragraph presents an overview of previous investigations by which various researchers attempted to develop fundamental design theory based on mechanistic design principles for the modelling of doweled slab-on-grade pavement systems. The logic behind the development of the dowel bar model used in the three-dimensional finite element (3DFE) computer programme, EverFE (Davids et al., 1998a; 1998b), is also summarised. Further literature reviews on the subject of modelling of dowel-shear load transfer across cracks in concrete pavements that have merit are summarised in Appendix C.

2.5.2 Analytical dowel modelling

The first procedure for the design of doweled joints in concrete pavements was presented by Westergaard (1926). However, the main theoretical definition of dowel behaviour to date has been presented by Friberg (1940). Experimental evidence presented by Teller and Cashell (1958) that suggested a direct exponential relation between dowel diameter and efficiency of load transfer lent credibility to the Friberg methodology. Furthermore, Teller and Cashell (1958) provided data suggesting that an increase in the modulus of subgrade reaction, k will cause a decrease in the amount of load transferred. This indicated that a dowel would show its highest effectiveness on a flexible subgrade where it is needed, and its lowest effectiveness on a stiff subgrade where it is not needed.

The length of dowel embedment necessary to develop maximum load transfer is not a constant function of dowel diameter as has sometimes been assumed. With a 19,0 mm (¾ inch) dowel diameter, maximum load transfer requires an embedded length of about eight dowel diameters. With larger dowels, such as the 25,4 mm (1 inch) and 31,8 mm ($1^1/_4$ inch) diameters, full load transfer is obtained with a length of embedment of about six diameters, both initially and after hundreds of thousands of repetitive loading (Teller and Cashell, 1958).

An experimental study by Snyder (1989) verified that a larger diameter dowel would ensure smaller dowel deflections, leading to reduced concrete bearing stresses and simultaneous decreased dowel looseness. The condition of dowel looseness has an important effect on the structural performance of the dowel; since it can function at full efficiency only after this looseness is taken up by load deflection. This is true for both initial looseness and that which develops during repetitive loading. *Tests that do not include repetitive loading and complete stress reversal provide no information on this important condition and no measure of its effects* (Teller and Cashell, 1958).

During the laboratory study conducted by Teller and Cashell (1958) the increase in looseness around the dowel, developed during the first 40 000 load application cycles, equalled that developed by the subsequent 1,96 million (up to 2 million) cycles (see Figure 2.21).

Another subject of debate was the number of dowels effective in distributing the load. Based upon Westergaard's theory, Friberg (1940) noted that for loadings a considerable distance from the edge, the maximum positive moment occurs beneath the load, and the maximum negative moment occurs a distance 1,8*l* from the point of loading. Beyond 1,8*l*, sometimes referred as the effective length (*e*), the moment changes very little. Finite element (FE) studies led to the conclusion that the assumption by Friberg was appropriate but that the effective length was 1,0*l*. These conclusions are appropriate for a single wheel loading only; multiple gear configurations will lead to different values of the effective length. Two important conclusions that have been a prominent point of debate in the decades that followed, even to the present day, are (Ioannides et al., 1990):

a) Only the two, or at most four, dowels nearest to the load need to be considered as active, since the contribution of more remote bars is negligible.
b) Dowels are affective in reducing bending stress developed in the loaded slab only if they are spaced closely enough (at less than 600 mm (2 ft) apart).

It is thought that bearing stresses under the dowel are responsible for spalling and looseness of the dowels. Analytical methods for quantifying the bearing stresses in dowel bars have been in existence since the late 1930's. Several investigators have presented formulae for calculating the concrete bearing stress. All of these formulations for bearing stress (σ_b) may be represented by the following relationship (Ioannides at el, 1990):

$$\sigma_b = A(structural) * B(load) \tag{2.34}$$

The first term *A*, is determined from the structural characteristics of the pavement system, while the second term, *B*, quantifies the transferred load.

Friberg (1940) based his analysis upon considering the dowel as a semi-infinite beam on a Winkler foundation (see Figure 2.22). His basic relationship for dowel stresses was:

$$\sigma_b = K\Delta_0 \tag{2.35}$$

Where:

K = Modulus of dowel support (FL^{-3}); and
Δ_0 = Deflection of the dowel with respect to the concrete at the face of the joint (L).

Friberg's (1940) analysis of dowel bar support is given in Figure 2.23, and his relationship for the maximum deformation of concrete under a dowel bar with a shear force P is given in Equation (2.36).

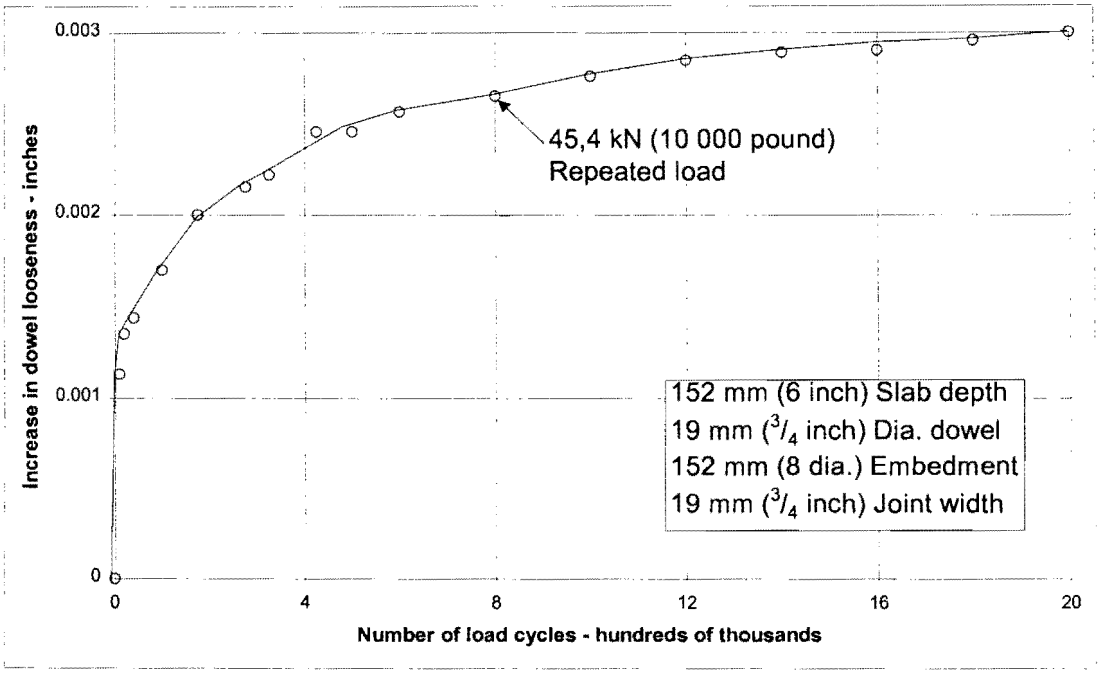

Figure 2.21: Effect of repetitive loading on the development of dowel looseness (Teller and Cashell, 1958)

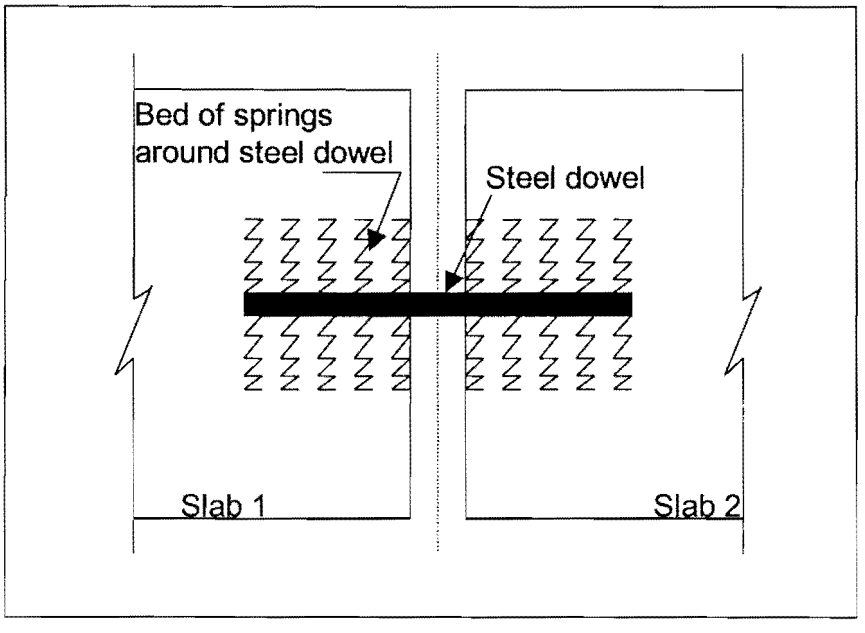

Figure 2.22: Winkler foundation between dowel and slab (Friberg, 1940)

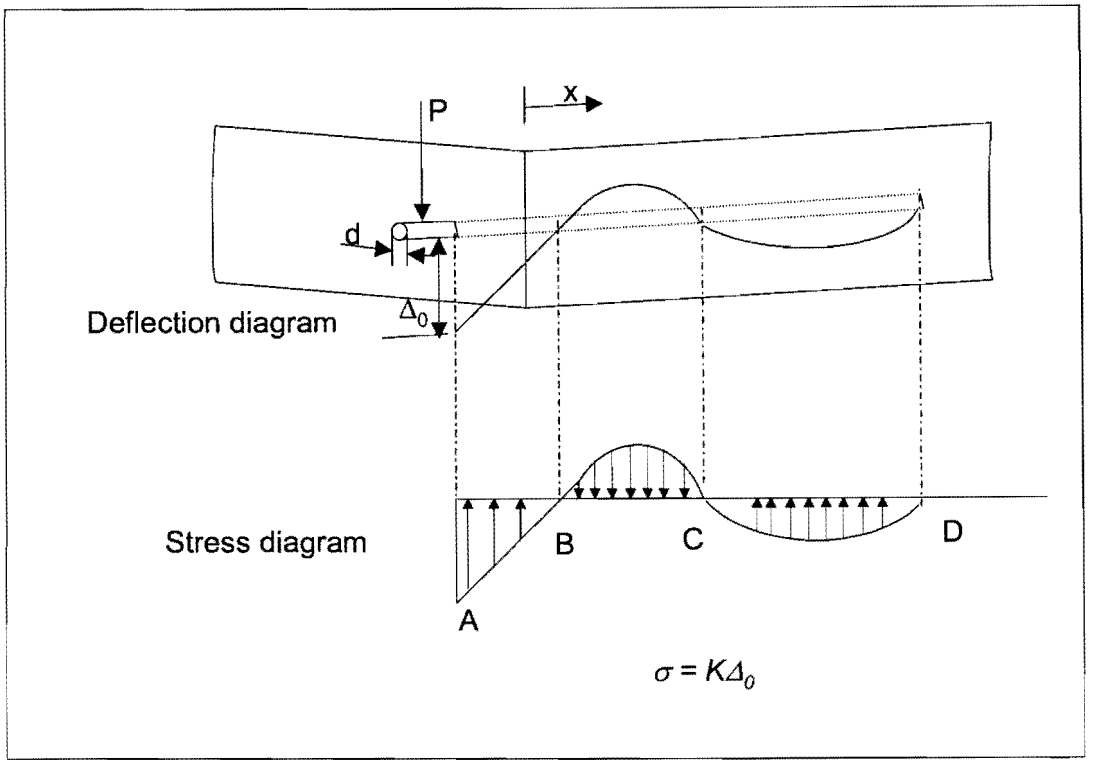

Figure 2.23: Analysis of dowel bar support (Friberg, 1940)

$$\Delta_0 = \frac{P_i}{4\beta^3 E_d I_d}(2 + \beta\omega) \tag{2.36}$$

Where:

Δ_0 = Deflection of the dowel relative to the concrete at the joint face (L);

P_i = Shear force acting on any particular dowel, transferred across the joint (F);

ω = Width of joint opening (L);

E_d = Modulus of elasticity of the dowel (FL^{-2}); and

I_d = Moment of inertia of the dowel (L^4).

Note that the primary dimensions are abbreviated as L for length and F for force.

For solid round bars,

$$I_d = \frac{\pi dia^4}{64} \tag{2.37}$$

Where *dia* is the dowel bar diameter (L) and β is the relative stiffness of the dowel/concrete system, as defined by Equation (2.38).

$$\beta = \sqrt[4]{\frac{Kdia}{4E_dI_d}} \tag{2.38}$$

The bearing stress on the concrete then becomes:

$$\sigma_b = \frac{KP}{4\beta^3 E_d I_d}(2 + \beta\omega) \tag{2.39}$$

Through dimensional analysis Ioannides et al., (1996) used the Friberg (1940) formula as basis and incorporated a dimensionless term quantifying the portion of the load carried by the critical dowel (f_{dc}), as shown in Equation (2.40):

$$\sigma_b = \frac{K(2 + \beta\omega)}{4\beta^3 E_d I_d} * P * TLE * f_{dc} \tag{2.40}$$

The critical dowel is the dowel carrying the largest shear force. Approximations for f_{dc} is given by S/e for edge load, and by $(2S/(e+S))$ for corner load, where:

e	=	Effective length;
S	=	Dowel spacing, and
TLE	=	$P_T/P * 100$, where:
P_T	=	Total load transferred across the entire length of joint.

In a study similar to the mechanistic analysis of aggregate interlock load transfer mechanisms (Ioannides and Korovesis, 1990) in which the dimensionless joint stiffness parameter AGG/kl, has been developed, Ioannides and Korovesis (1992) also developed the concept of a dimensionless joint stiffness for the doweled joint, D/skl. The major load transfer mechanism in doweled joints is also shear, since bending of the bar over the very small span afforded by the joint opening has a relatively minor effect.

Comparison of the stiffness matrices used to describe the aggregate interlock and doweled joint load transfer mechanisms in the ILLI-SLAB FE programme, suggested a correspondence between AGG and D/s where D is the composite shear stiffness of the supported dowel (FL^{-1}), and s is the dowel spacing (L). The dimensionless ratio D/skl is therefore the governing independent variable.

The ILLI-SLAB model considers the dowel bar as a thick beam element whose shear stiffness (i.e. resistance to deformation in the vertical direction) is $12C$ (FL^{-1}). This term expresses the shear force in the dowel per unit vertical deformation of the dowel. The support provided by the concrete matrix is modelled as a single spring that acts at the joint face and whose stiffness is dowel-concrete interaction

parameter (DCI) parameter (FL^{-1}). This is the shear force transferred by the dowel per unit deflection of the dowel with respect to the concrete matrix. For the supported dowel, therefore, the composite springs-in-series shear stiffness, D, is defined as (Ioannides and Korovesis, 1992):

$$D = \frac{1}{\frac{1}{DCI} + \frac{1}{12C}} \tag{2.41}$$

In which:

$$C = \frac{E_d I_d}{\omega^3(1+\phi)} \tag{2.42}$$

$$\phi = \frac{12E_d I_d}{G_d A_z \omega^2} \tag{2.43}$$

Where:

G_d = Shear modulus of dowel bar (FL^{-2}),

$$G_d = \frac{E_d}{2(1+\mu_d)} \tag{2.44}$$

Where:

E_d = Modulus of elasticity of dowel (FL^{-2}), as before;

μ_d = Poisson's ratio of dowel;

A_z = Cross-sectional area of dowel effective in shear (L^2);

$A_z = 0{,}9A_d$ for solid round bars, (2.45)

A_d = the cross-sectional area of the dowel (L^2), with

$$A_d = \frac{\pi dia^2}{4} \tag{2.46}$$

The DCI assuming the dowel to be a beam on a spring foundation (Friberg, 1940) is given by the following relationship:

$$DCI = \frac{P_i}{\Delta_{di}} = \frac{4\beta^3 E_d I_d}{(2+\beta\omega)} \tag{2.47}$$

Where:

Δ_{di} = Deflection of any given dowel relative to the concrete (L).

The proposed dimensionless independent variable (D/skl) lumps together all the necessary input parameters pertaining to the dowel bars (d, s, E_d, μ_d, K, ω), as well as those used in characterising the materials of a slab-on-grade pavement (k, E, H, μ). The only parameter missing is the embedment length, which, is not incorporated in the ILLI-SLAB model, either (Ioannides and Korovesis, 1992).

Guo, Sherwood and Snyder (1995) addressed this "missing" parameter by using ILLI-SLAB FE analyses in comparisons with experimental results to determine that the longer the dowel bar embedment length, the higher the load transfer capability of the dowel bar system. This led to an increase of maximum displacement and stress in the unloaded slab, a decrease of maximum displacement in the loaded slab, and more total shear force transmitted from the loaded to the unloaded slab. Also, when the half-embedded length is greater than five times the bar diameter, the difference of results between finitely and infinitely long dowel bar models can be neglected. Based on this, Guo et al. (1995) came to the conclusion that current dowel bars can be approximately modelled by assuming the embedded length to be infinitely long.

The dimensionless joint stiffness (*D/skl*) addressed earlier concerns that the behaviour of dowels is not merely a function of their own flexibility properties, but is influenced considerably by the stiffness characteristics (including slab thickness) of the entire pavement system in which they are incorporated.

Through a number of executions of the ILLI-SLAB FE code, the shear-only data plot exactly on the previously determined *AGG/kl* curve (See Figure 2.19). These results therefore confirmed the direct correspondence between *AGG/kl* and *D/skl*.

To complete the overview on analytical-empirical modelling by various researchers, the results of a few studies are presented below:

Buch and Zollinger (1996)

This paper presented the results of an in-depth study of factors that affect dowel looseness in jointed concrete pavements. The laboratory investigation revealed the influence of aggregate type (in relation to oxide content), aggregate texture and shape, bearing stress (dowel diameter and crack width), load magnitude, and number of load cycles on the magnitude of dowel looseness and the subsequent loss in load transfer efficiency (LTE) across saw-cut joints. They developed an empirical-mechanistic dowel looseness prediction model based on the experimental results.

The causes for initial dowel looseness were summarised as follows:

a) Coating applied to dowels to prevent bond or to protect the dowel bar against corrosion.
b) Water or air voids in the concrete around the dowels due to improper construction procedures.
c) Shrinkage of concrete during hardening.

A two-phase modelling approach was adopted: an experimental phase and an analytical phase. The variables considered for the model development were aggregate type and texture, dowel diameter, and magnitude of load. An experimental program was developed to study the effect of load cycles (N), and load (P) on the magnitude of dowel looseness.

Apart from conclusions that have already been drawn from the above-mentioned investigations, this specific study has shown the following:

a) The analysis of dowel looseness revealed that the magnitude of dowel looseness increased with increasing number of load cycles, and also that the magnitude of dowel looseness for a given load level was greater in specimens made with river gravel when compared with concrete samples made with limestone.
b) Further research must be conducted to develop a correlation between dowel looseness, aggregate angularity, and aggregate abrasive characteristics.
c) The prediction model (Friberg, 1940) can be further improved by investigating the influence of a non-dimensional parameter $\sigma_b h^2/P$ on dowel looseness. This will lead to the elimination of the variable P.

Hossain and Wojakowski (1996)

Hossain and Wojakowski (1996) reported the results of a survey, conducted over a period of 9 years, where six jointed reinforced concrete pavement (JRCP) and one jointed plain concrete (JPCP) pavement test sections were surveyed annually for faulting. The main focus of the investigation was to determine the effect of *concrete mix consolidation* with time on joint faulting and LTE.

Twenty-three test sections with lengths from 32 m to 1 584 m were constructed with various adjustments to vibrator settings (frequency and amplitude), concrete admixtures, and other special features of JRCP. Seven of these test sections were monitored for long-term performance for this joint faulting and LTE study.

Joint fault depth measurements were made with a fault meter built from the plans provided by the University of Illinois. Falling weight deflectometer (FWD) tests were done using a Dynatest-8000 FWD to assess the load transfer efficiencies of the joints.

The results of this study showed that:

a) As the original concrete density increased because of improved consolidation, the rate of increase of joint fault depth decreased at doweled joints.
b) The occurrence of joint faulting was much more severe when load transfer devices were not present.
c) Improved concrete mix consolidation appeared to improve load transfer, resulting in a lower rate of faulting.

2.5.3 Finite element dowel modelling

Certain key attributes of the more common FE programmes as reported in the literature have been summarised in Tables 2.1 (2D studies) and 2.2 (3D studies) of paragraph 2.3. During development of the 3DFE computer programme, EverFE, Davids et al. (1998a, 1998b) also conducted a review of current dowel modelling techniques. They confirmed that several different approaches have been used to model load transfer in jointed concrete pavements via dowel action, and that the interaction of the dowel and the slab is complex, but that it consists mainly of two portions, namely:

a) Looseness (gaps) between the dowel and the slab.
b) Compression of the slab around the dowel.

Several investigators had shown that dowel looseness has a significant effect on joint performance (Buch and Zollinger, 1996; Snyder, 1989). Zaman and Alvappillai (1995) did a two-dimensional (2D) FE study that explicitly considered dowel looseness. The study by Parsons, Eom, and Hjelmstad (1997) examined this problem with contact modelling using a 2D plane strain model.

Most attempts to model dowel-slab interaction approximately accounted for compression of the slab around the dowel by assuming a Winkler foundation between the dowel and the surrounding slab. This approach was even used before the development of the FE analysis. Investigators have typically modelled dowel bars with discrete beam elements between adjacent slabs having springs between the dowels and the slabs to account for the effect of dowel-slab interaction, as in ILLI-SLAB (Tabatabaie and Barenberg, 1980) and JSLAB. The spring stiffnesses were derived by considering the embedded portion of the dowel as an infinitely long beam on a Winkler foundation.

No 3DFE models have considered the effect of dowel looseness on joint performance. Davids et al. (1998a, 1998b) proposed and developed a new technique for modelling dowel load transfer, which relies on an embedded formulation of the dowel, and allows the explicit and rigorous consideration of gaps between the dowel and the slab through nodal contact modelling. The details for the necessary inclusion of a bond-slip law were also presented.

The dowel was modelled as an embedded quadratic beam element within a solid, quadratic, iso-parametric element. Three types of embedment were considered:

a) A bonded (axially constraining the dowel to the embedding element), constrained (constraint of transverse dowel displacements to the embedding element) embedded dowel.
b) A de-bonded, constrained dowel.
c) A de-bonded dowel with a gap.

Specific advantages of the embedding formulation are as follows:

a) Slab mesh divisions are not restricted to coincide with dowel lines.

b) The element may be de-bonded at selected nodes.

c) The non-linear effect of gaps between the dowel and surrounding slab concrete can be explicitly modelled.

d) The element stiffness is easily computed using a matrix transformation, and does not require special integration techniques. Both the effects of de-bonding and gaps are incorporated in this transformation.

e) The dowel element permits the incorporation of a general bond-slip law, making it appropriate for modelling reinforcement in conventional reinforced concrete structures.

2.5.4 Combined aggregate interlock and dowel modelling

Soroushian et al. (1988) investigated the combined effect of aggregate interlock and dowel action in reinforced concrete beam elements against sliding shear at a crack. Algorithms were developed for predicting the aggregate interlock constitutive behaviour using some empirical formulations. They concluded that at very small sliding-shear deformations (below 0,2 mm) the dowel action tended to dominate the shear resistance. At larger deformations, however, the aggregate interlock became more dominant. At sliding-shear deformations greater than 0,7 mm, about 65% of the total shear resistance in the case studied was provided by aggregate interlock. One of the results of their tests is given in Figure 2.24.

A theoretical analysis to determine the combined effect of aggregate interlock and dowel action was also conducted with EverFE (see Appendix D). The same model as the one used in aggregate interlock modelling with a cement stabilised subbase was used. To determine the effect of dowels in the model, 16 mm diameter dowels at 300 mm spacing were placed across the joint. During theoretical modelling the crack width was varied, while the gap around the dowel was initially kept constant.

The deflection LTE obtained for 9 mm and 63 mm aggregate sizes are presented in Figure 2.25. From this figure, it is obvious that the combined efficiency of aggregate interlock and dowels is far greater than for aggregate interlock only.

The maximum aggregate interlock shear stress measured in the wheel path was less for the combined aggregate interlock and dowel action models than for the models relying on aggregate interlock only (see Figure 2.26). This could be ascribed to the dowels relieving some of the stress in the aggregate.

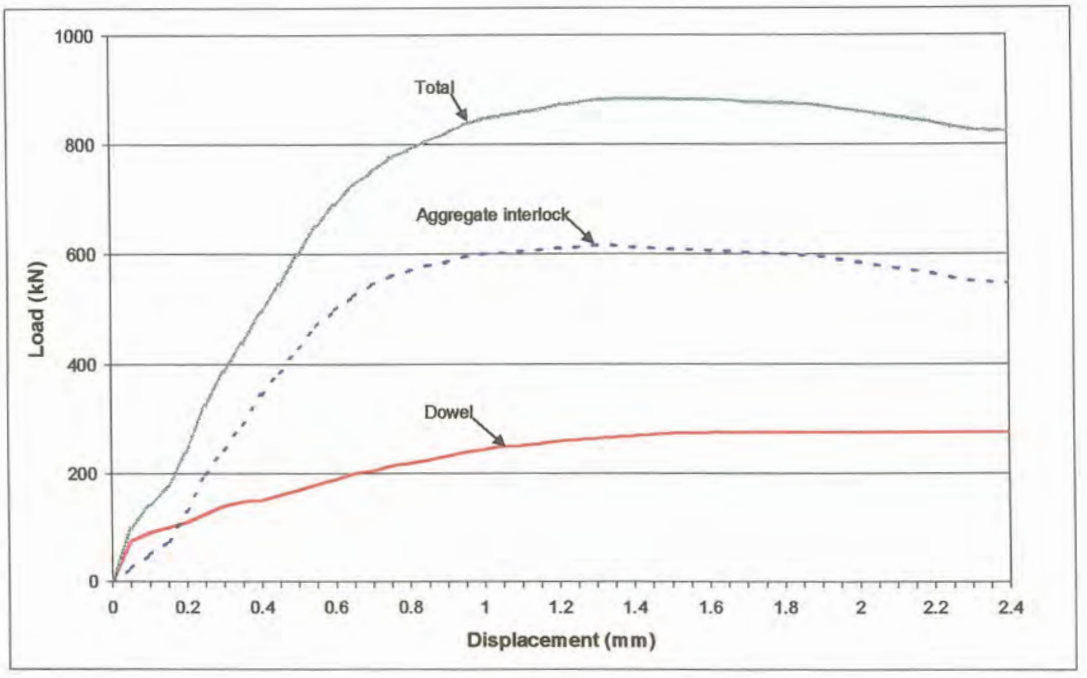

Figure 2.24: Sliding shear behaviour at a constant crack width of 0,5 mm (Soroushian et al., 1988)

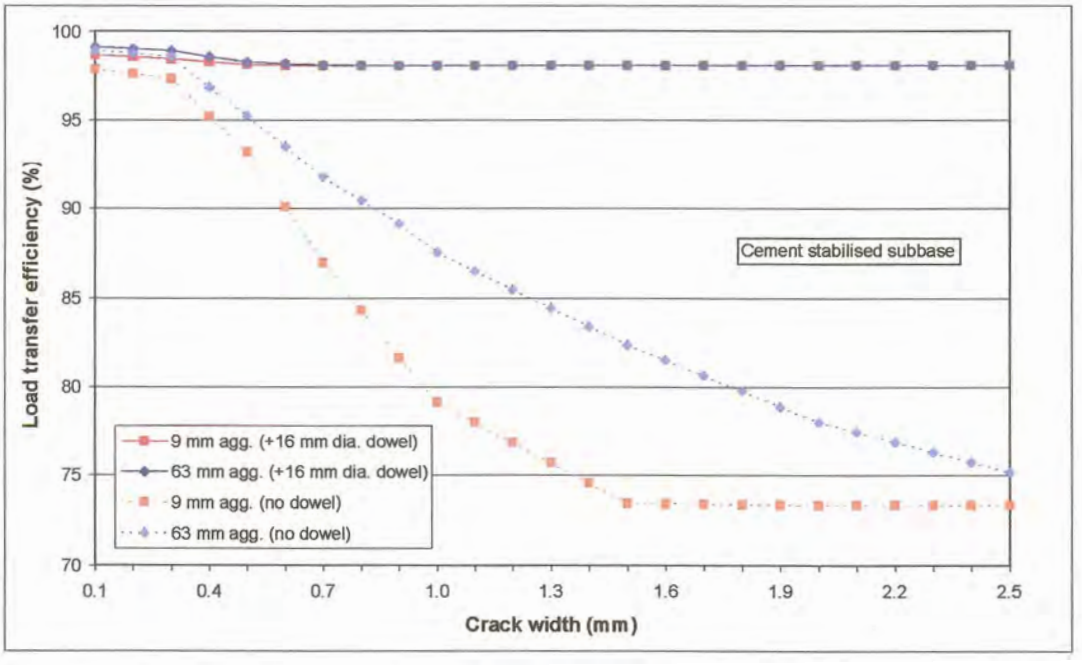

Figure 2.25: Deflection LTE in the wheel path – aggregate interlock versus combined effect of aggregate interlock and dowel action (no gap around dowel)

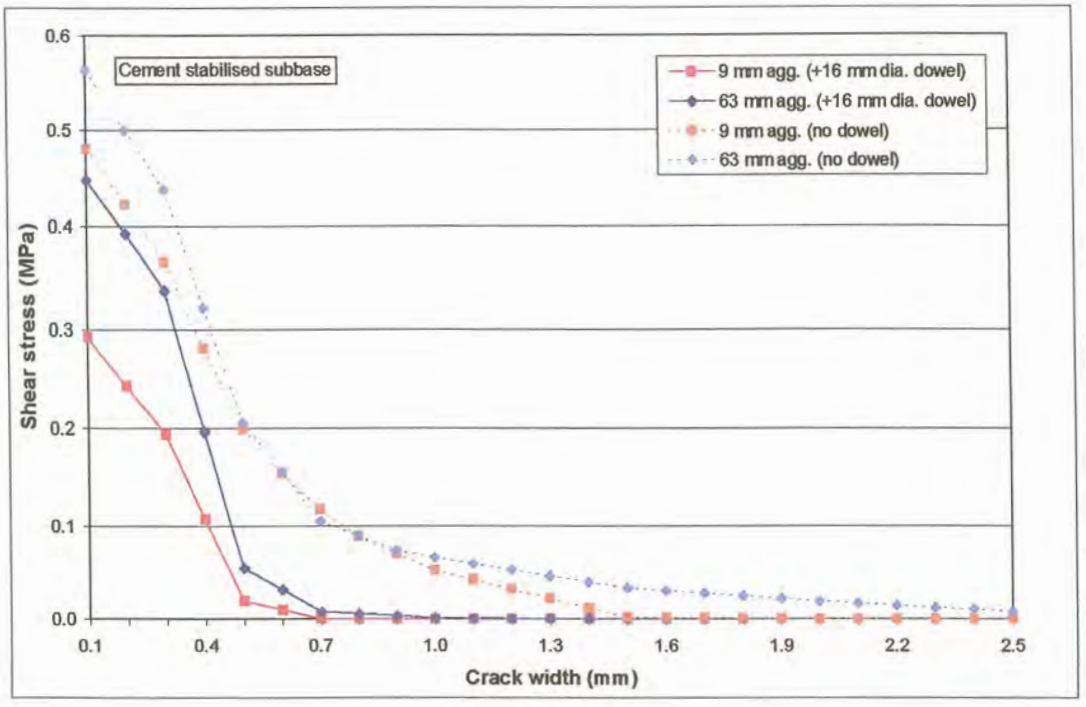

Figure 2.26: Maximum shear stress at joint in wheel path – aggregate interlock versus combined effect of aggregate interlock and dowel action (no gap around dowel)

Just as for the shear stress, the total aggregate interlock shear force transferred across the joint was also less for the combined model than for the aggregate interlock model, as can be seen from Figure 2.27.

The LTE of various dowel configurations was obtained during analyses with EverFE, for situations where the gap around the dowel was considered to be zero (see Appendix D). These analyses were repeated, but in the latter case the gap around the dowel was varied from 0,00 mm to 0,10 mm. The bigger the gap around the dowel, the lower the LTE. For comparison purposes, the values obtained for a joint relying on aggregate interlock only (no dowel), was also determined. At a gap of 0,10 mm the LTE approximated the "no dowel" case, which indicated that the dowel did not fulfil its purpose any more (see Figures 2.28 and 2.29). This emphasised the importance of considering a gap around the dowel as well, but also that high load transfer conditions are obtained through aggregate interlock (Jeong and Zollinger, 2001). The further analyses conducted with EverFE is described in detail in Appendix D.

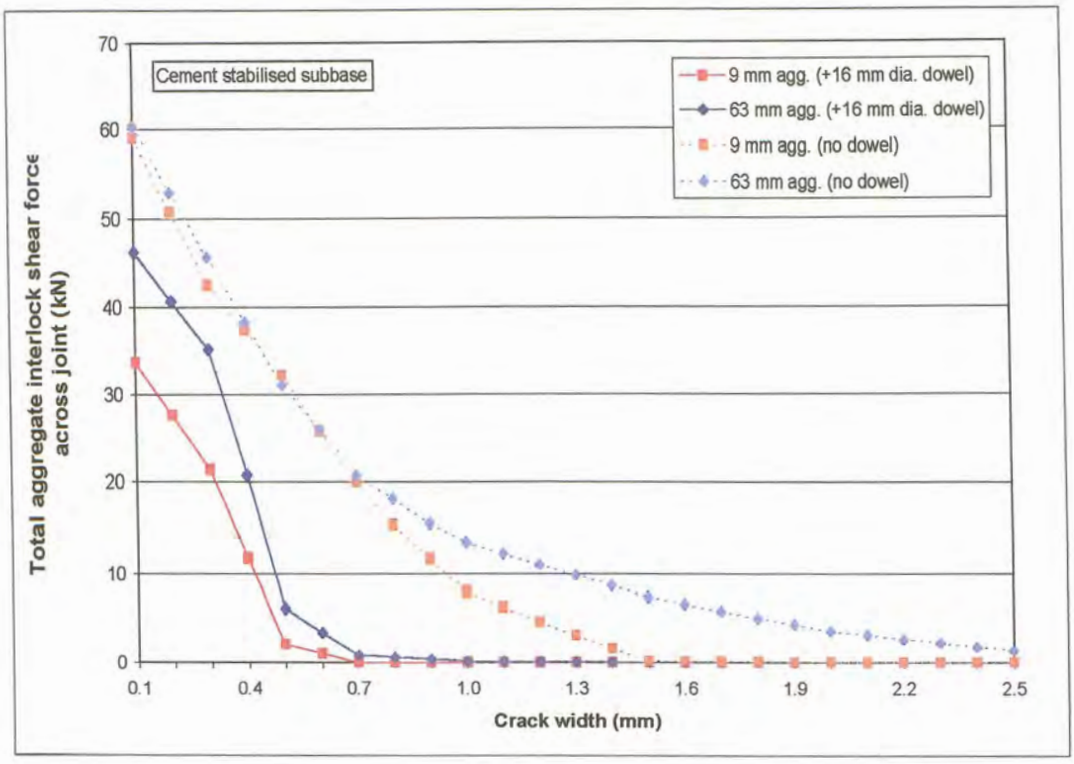

Figure 2.27: Total shear force transferred across joint – aggregate interlock versus combined effect of aggregate interlock and dowel action (no gap around dowel)

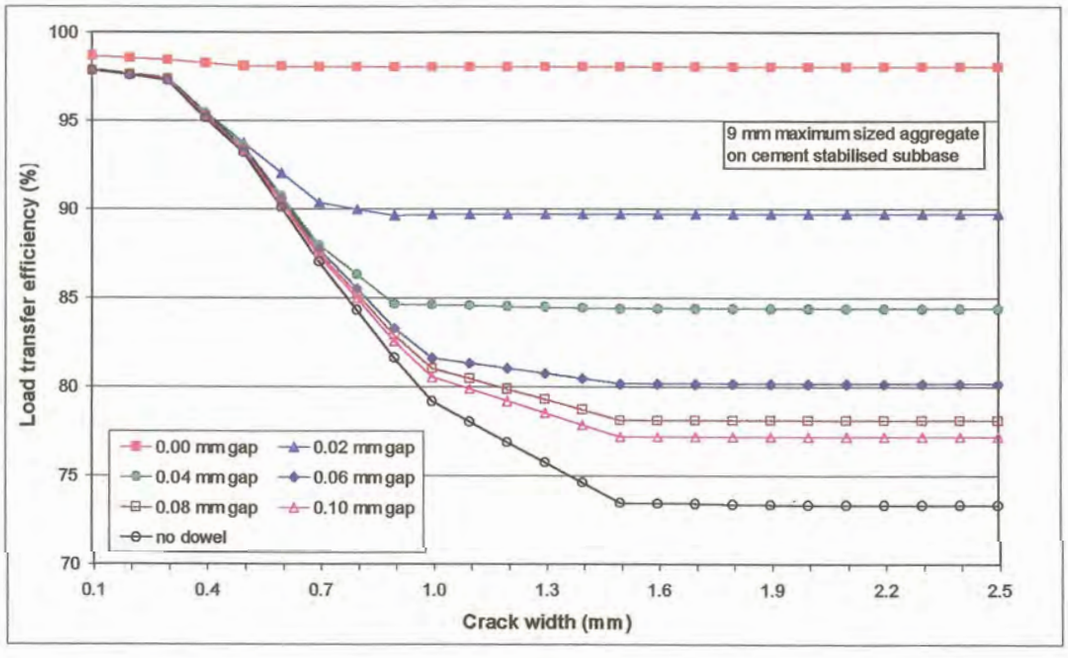

Figure 2.28: Deflection LTE in the wheel path – 9 mm maximum sized aggregate – combined affect of aggregate interlock and dowels (gap around dowel)

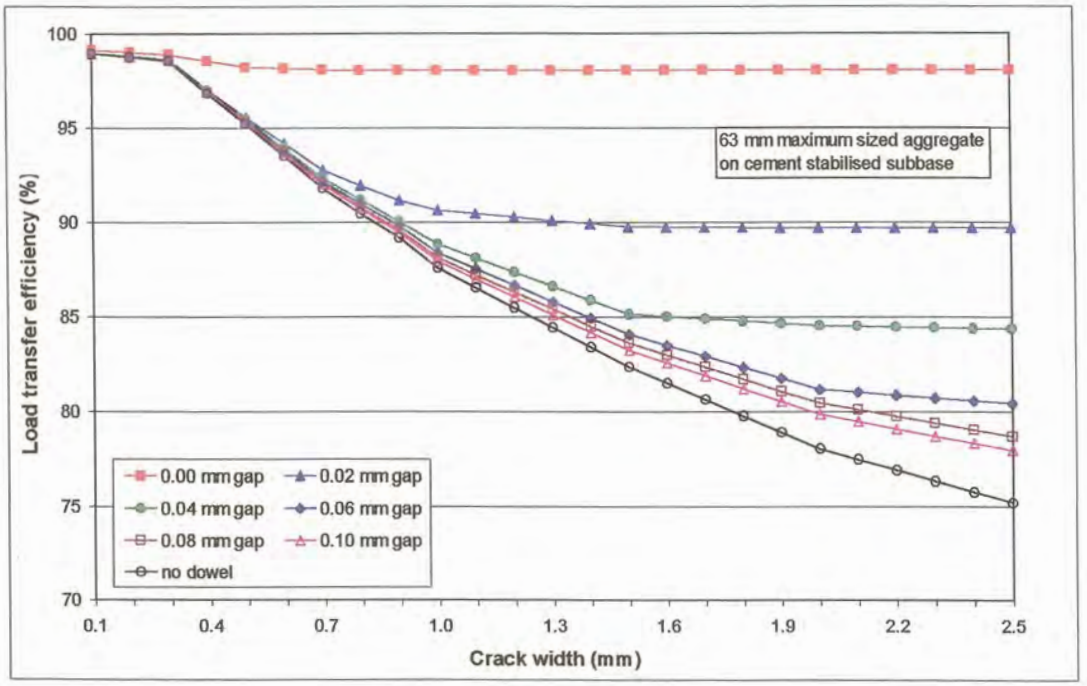

Figure 2.29: Deflection LTE in the wheel path – 63 mm maximum sized aggregate – combined affect of aggregate interlock and dowels (gap around dowel)

Jeong and Zollinger (2001) also conducted a study where the combined effect of aggregate interlock and dowel action was characterised in terms of a mechanistic process to address faulting and punch-out development. They used the work conducted by Ioannides and Korovesis during 1990 and 1992 (Ioannides and Korovesis, 1990; Ioannides and Korovesis, 1992) as the basis for this characterisation.

It was stated that shear capacity (s_0) is a parameter that represents the maximum shear stress that a slab joint or crack is capable of carrying for a given crack or joint opening. In combination the dimensionless joint stiffness ratios for aggregate interlock ($Agg/kl = J_{AI}$) and for dowel action ($D/skl = J_D$) represent a total stiffness ratio, $J = J_{AI} + J_D$ which in effect can be related to load transfer (in percent) as follows (Ioannides and Hammons, 1996):

$$LTE = \frac{100}{1+\log^{-1}\left[\frac{0{,}214 - 0{,}183\left(\frac{a}{l}\right) - \log(J)}{1{,}18}\right]} \qquad (2.48)$$

Where:

LTE = Load transfer efficiency;

a = Radius of applied load;

l = Radius of relative stiffness of the slab-foundation; and

J = Total stiffness ratio.

The aggregate interlock joint stiffness ($f = Agg/kl$) in Equation (B.44) is replaced by the total stiffness ratio (J) in Equation (2.48).

By combining Equation (2.48) with Equation (2.29) the effect of stiffness due to dowels or aggregate interlock can be taken into account. This study confirmed that the degree to which dowels can transfer load is limited. A greater load transfer capability can be achieved only through aggregate interlock and small crack opening. In other words, as stated above, high load transfer can be achieved through aggregate interlock. Even though dowels make a significant contribution to the transfer of load from one slab to another, crack width is critical to achieving and maintaining a high load transfer condition.

2.5.5 Summary of dowel modelling

Probably the most important aspect when modelling load transfer in concrete pavements due to dowel action, is the effect of dowel looseness. Dowel looseness has an important effect on the structural performance of the dowel; since it can function at full efficiency only after this looseness is taken up by load deflection. This is true for both initial looseness and that which develops during repetitive loading. Teller and Cashell (1958) made the statement that *tests that do not include repetitive loading and complete stress reversal, provide no information on dowel looseness and no measure of its effects.* An exponential relation was found to exist between dowel diameter and load transfer capacity, other conditions being constant (Teller and Cashell, 1958).

Most attempts to predict the initial shear stiffness of the dowels across a crack in reinforced concrete modelled the dowel as a beam on elastic foundation (Friberg, 1940; Millard and Johnson, 1984). In their follow-up study Millard and Johnson (1985) investigated the combined effect of aggregate interlock and dowel action. They found that large initial crack width; low concrete strength or the use of large-diameter bars all had an adverse effect upon the anchorage stiffness of the reinforcement and consequently upon the aggregate interlock shear stiffness and strength. Guo et al. (1995) used the same model as Millard and Johnson (1984), calling it the component dowel bar model. They verified through a comparison between experimental and analytical (ILLI-SLAB) results that this model could be used to reasonably predict responses of a dowel bar load transfer system.

Buch and Zollinger (1996) presented an in-depth study of factors affecting dowel looseness in an attempt to develop a dowel looseness prediction model. They found that dowel looseness and deflection were reduced considerably when the dowel diameter was increased. As far as the dowel looseness is concerned, this is contrary to the findings by Millard and Johnson (1985) where the larger-diameter dowels had lower anchorage stiffness than smaller-diameter dowel bars.

Hammons and Ioannides (1996) demonstrated the usefulness of using the concept of dimensionless joint stiffness for developing a mechanistic-based design approach for doweled joints, in that the experimental data they used, confirmed the usefulness of the dimensionless joint stiffness as a means of modelling the response of the doweled joint.

Most important though of the research done by Ioannides et al. (1990) and by Ioannides and Korovesis (1992) was to emphasise the fact that accurate theoretical equations for dowel modelling have been in place since the 1930's. It was pointed out that the so-called Friberg (1940) equations, based on the original Westergaard (1926) theory, are still applicable. Using the principles of dimensional analysis, combined with a number of executions of the ILLI-SLAB FE code Ioannides and Korovesis (1992) demonstrated the direct correspondence between aggregate interlock shear transfer (*AGG/kl*) and dowel shear transfer (*D/skl*) across a crack in a concrete pavement. The *D/skl* shear-only data plotted exactly on the previously determined *AGG/kl* curve.

The results of studies on the combined effect of aggregate interlock and dowel modelling have also been investigated. These studies emphasised that high load transfer is achieved through aggregate interlock and small crack widths.

The computer software programme, EverFE (Davids et al., 1998a, 1998b) was used for FE modelling of load transfer between concrete pavement slabs via dowel action (see Appendix D).

2.6 GUIDANCE FOR LABORATORY MODELLING

Bearing all these facts in mind, the essence of the literature review presented in this chapter had to be extracted to lend a meaningful input in order to compile the experimental programme for the current thesis.

The effectiveness of aggregate interlock load transfer at a joint in a concrete pavement depends on load magnitude, number of load repetitions, slab thickness, joint opening, subbase characteristics, subgrade bearing value, and aggregate angularity.

As the texture of the crack face is a function of the coarse aggregate type, size, and gradation, with the surface texture of the crack directly influencing the aggregate interlock and load transfer capacity of the joint (Buch, 1998) it was decided to perform a 2-level, 2-parameter experimental design. For this purpose two types of aggregates and two coarse aggregate sizes were chosen. The aggregate types chosen were Granite with an E-modulus of 27 GPa, and Dolomite with an E-modulus of 40 GPa, representing the range in modulus of crushed aggregates used in the construction industry in South Africa. The coarse aggregate sizes chosen were 19 mm and 37.5 mm.

In order to minimise the number of variables tested, it was recognised that some parameters had to be kept constant during the experiments. These were:

a) Concrete design strength – 35 MPa (standard strength used in the construction of concrete pavements in South Africa).
b) Concrete slab thickness – 230 mm (average slab thickness of jointed concrete pavements in South Africa).
c) Sand grading - had to be kept constant to ensure that the volume of coarse aggregate would be the same for different aggregate types.
d) Subbase support – construct the concrete slabs on a re-usable rubber (approximating a Winkler) subbase (The three primary response parameters in the analysis of a slab-on-grade pavement system are deflection (Δ), bending stress (σ), and subgrade stress (q). When the dense liquid foundation model is adopted, the latter may be eliminated because $q = k\Delta$ (Ioannides and Korovesis, 1990)).
e) Constant temperature during testing – by testing inside a laboratory facility temperature variation could be controlled eliminating curling of the concrete.
f) Angle of the fracture face – by inducing the crack in the slab within 24 hours after casting the concrete it was ensured that the angle of the fracture face would be as vertical as possible.
g) Dynamic loading frequency – apply the dynamic loading at a constant frequency of 3 Hz, with the interval between the maximum loading of the dynamic loading actuators, simulating a vehicle crossing the joint at 80 km/h (Colley and Humphrey, 1967).

Factors that were controlled during the testing, were:

a) Crack width, in order to determine the crack width up to which LTE is affected through aggregate interlock caused by specific sized aggregates.
b) The foundation support, which were either a continuous (top rubber layer intact) or a discontinuous (top rubber layer cut through) foundation.

The literature review indicated that there could be a difference between the performance of the laboratory models, and the results of field investigations, due to the following reasons:

a) Larger deflections could be measured in the laboratory due to a smaller resisting cross-section.
b) The effective height of the roughened interface would be less than in the field due to the crack inducer that has to be placed in the bottom of the slab.
c) To be able to test at a constant crack width, the crack width will have to be kept constant, whereas in the field temperature cycles cause opening and closing of the crack.

It was also decided to measure the VST of the experimental beams and compare the results with those published by Vandenbossche (1999).

Little research has been done on the subject of aggregate interlock shear load transfer at joints in concrete pavements in South Africa, and therefore the literature published on the subject is scarce. The main concern is that the accepted analysis models have been developed in the Northern hemisphere with environmental conditions quite different to the conditions encountered in Southern Africa. Modelling of aggregate interlock joints, using South African aggregates, and investigation into the efficiency of aggregate interlock joints in in-service pavements was therefore required.